2017

Fli1 Expression Levels During Megakaryopoiesis Affect Thrombopoiesis And Platelet Biology

Karen Vo
University of Pennsylvania, Karenvo@mail.med.upenn.edu

Fli1 Expression Levels During Megakaryopoiesis Affect Thrombopoiesis And Platelet Biology

Abstract

Friend Leukemia Virus Integration 1 (FLI1) is a critical transcription factor (TF) in terminal megakaryocyte differentiation. It is amongst the genes missing from an inherited hemizygous deletion on chromosome 11q termed Jacobsen syndrome and often results in a dysmegakaryopoiesis and macrothrombocytopenia termed Paris Trousseau syndrome (PTSx) described as being due to FLI1 allelic exclusion. It has also been reported that heterozygote FLI1 mutations in its DNA-binding domain region cause thrombocytopenia in patients suspected to have inherited platelet defects. To date, there are no reports containing comprehensive in vitro or in vivo characterization of platelet defects due to heterozygous FLI1 deletion or mutations, or that of platelets expressing increased levels of FLI1. We used induced pluripotent stem cell (iPSC)- derived megakaryocytes (iMegs) to determine if the platelet disorder observed in PTSx could be replicated, either with iPSCs generated from a PTSx patient or from a targeted heterozygous knockout of FLI1 (FLI1+/-) in control iPSCs. These studies indicate that PTSx and FLI1+/- iMegs replicate many of the clinical features described in PTSx and showed more in vitro injury to the resulting iMegs with fewer platelets released in vivo. These platelets had shortened half-lives and were functionally defective. We then examined whether increased levels of FLI1 would affect megakaryopoiesis and thrombopoiesis, and found an increased number of iMegs with less in vitro injury compared to control iMegs. FLI1-overexpressing iMegs also released more platelets in recipient mice with increased half-life and functionality. These studies confirm FLI1 heterozygosity results in defects in megakaryopoiesis and thrombopoiesis similar to that noted with other megakaryocyte-specific TFs, but unlike those TFs, FLI1 overexpression is not associated with quality or quantitative platelet deficiencies, but improved yield and functionality that may have clinical applicability.

Degree Type

Dissertation

Degree Name

Doctor of Philosophy (PhD)

Graduate Group

Pharmacology

First Advisor

Mortimer Poncz

Keywords

Gene editing, Induced pluripotent stem cells, Megakaryopoiesis, Transcription factors

Subject Categories

Pharmacology

FLI1 EXPRESSION LEVELS DURING MEGAKARYOPOIESIS AFFECT THROMBOPOIESIS AND PLATELET BIOLOGY

Karen K. Vo

A DISSERTATION

in

Pharmacology

Presented to the Faculties of the University of Pennsylvania

in

Partial Fulfillment of the Requirements for the

Degree of Doctor of Philosophy

2017

Supervisor of Dissertation

_____

Mortimer Poncz, M.D., Professor of Pharmacology and Pediatrics

Graduate Group Chairperson

_____

Julie A. Blendy, Ph.D., Professor of Pharmacology

Dissertation Committee

Rodney M. Camire, Ph.D., Associate Professor of Pediatrics (Chair)

Lawrence F. Brass, M.D., Ph.D., Professor of Pharmacology and Medicine

Stella T. Chou, M.D., Assistant Professor of Pediatrics

Deborah L. French, Ph.D., Research Associate Professor of Pathology and Laboratory Medicine

DEDICATION

To my parents, who made so many sacrifices so that I could pursue my dreams.

ACKNOWLEDGMENT

This work was completed with the help of every member of the Poncz lab. I would like to extend a special thanks to Randolph Lyde and Dr. Danuta Jarocha for their camaraderie, strong work ethic, entertaining my compulsive organizational needs, and for being my lab and life sounding boards.

I thank Dr. Mortimer Poncz for his mentorship, from whom I learned not just good science but lessons that will carry me through life.

I thank Steve for being an immeasurable source of support and motivation.

ABSTRACT

FLI1 EXPRESSION LEVELS DURING MEGAKARYOPOIESIS AFFECT THROMBOPOIESIS AND PLATELET BIOLOGY

Karen K. Vo

Mortimer Poncz, M.D.

Friend Leukemia Virus Integration 1 (FLI1) is a critical transcription factor (TF) in terminal megakaryocyte differentiation. It is amongst the genes missing from an inherited hemizygous deletion on chromosome 11q termed Jacobsen syndrome and often results in a dysmegakaryopoiesis and macrothrombocytopenia termed Paris Trousseau syndrome (PTSx) described as being due to FLI1 allelic exclusion. It has also been reported that heterozygote *FLI1* mutations in its DNA-binding domain region cause thrombocytopenia in patients suspected to have inherited platelet defects. To date, there are no reports containing comprehensive *in vitro* or *in vivo* characterization of platelet defects due to heterozygous *FLI1* deletion or mutations, or that of platelets expressing increased levels of FLI1. We used induced pluripotent stem cell (iPSC)-derived megakaryocytes (iMegs) to determine if the platelet disorder observed in PTSx could be replicated, either with iPSCs generated from a PTSx patient or from a targeted heterozygous knockout of *FLI1* ($FLI1^{+/-}$) in control iPSCs. These studies indicate that PTSx and $FLI1^{+/-}$ iMegs replicate many of the clinical features described in PTSx and showed more *in vitro* injury to the resulting iMegs with fewer platelets released in vivo. These platelets had shortened half-lives and were functionally defective. We then examined whether increased levels of FLI1 would affect megakaryopoiesis and thrombopoiesis, and found an increased number of iMegs with less *in vitro* injury compared to control iMegs. FLI1-overexpressing iMegs also released more platelets in recipient mice with increased half-life and functionality. These studies confirm *FLI1* heterozygosity results in defects in megakaryopoiesis and thrombopoiesis similar to that noted with other megakaryocyte-specific TFs, but unlike those TFs, FLI1 overexpression is not associated with

quality or quantitative platelet deficiencies, but improved yield and functionality that may have clinical applicability.

TABLE OF CONTENTS

LIST OF TABLES

LIST OF ILLUSTRATIONS

CHAPTER 1 – Introduction

Overview of hematopoiesis

Hematopoiesis is a complex process involving simultaneous regulation of multiple genes by multiple cytokines and transcription factors (TF) to differentiate cells successfully from a progenitor state to a mature blood cell. In the adult, the pluripotent hematopoietic stem cells (HSC) reside primarily in the bone marrow[1] and are responsible throughout one's extra-uterine lifetime for maintaining and replenishing all blood cell lineages[2]: red, white and platelet. Additional discussion of hematopoiesis can be found in the section entitled "Primitive versus definitive hematopoiesis." Erythroid cells are the biconcave discoid red blood cells that make up the bulk of total blood cells[3]. These hemoglobin-laden red cells are responsible for delivering O_2 to all tissues while at the same time transporting CO_2 away to be exchanged for O_2 again in the lungs[4]. White blood cells are the mainstays of the immune system[5]. Various white cell lineages provide specific components of our immune response to our environment, including pathogens like bacteria and viruses, either immediately via phagocytosis by macrophages[6] and leukocytes[7] or via a more long-term strategy with cellular response by T cells[5] and antibody production by B cells[8]. Finally, platelets are small cell fragments released from large megakaryocytes[9]. Platelets are highly organized with specific surface receptors and granules containing clotting factors and many other bioactive molecules[10]. In response to vascular injury, platelets become activated and release their granule contents as they take part in hemostasis[10]. Overall, HSCs would not be able to effectively and reliably undergo balanced differentiation into these specialized blood cell types without proper and finely tuned positive and negative regulation.

HSC differentiation via cytokine and TF regulation

The fate of the HSCs is determined by both extracellular cytokines and intracellular TFs. Cytokines are small proteins that act as a ligand to their corresponding extracellular receptors, that when bound, leads to intracellular signal transduction, ending in transcriptional changes[11]. The cytokine erythropoietin (EPO) is responsible for erythroid maturation, where binding of EPO to its receptor EPOR causes receptor conformational changes followed by a signal transduction pathway involving Jak/STAT family members that ultimately ends in upregulation of erythroid-specific genes[12]. For myeloid cells and lymphocytes, the interleukin (IL) family of cytokines is the major driver of differentiation from the pluripotent HSCs[13]. Similarly, thrombopoietin (TPO) binding to its receptor Myeloproliferative Leukemia Protein (MPL) is the primary extracellular driver of megakaryocyte maturation, also known as megakaryopoiesis[13].

Downstream of these cytokines, TFs play a pivotal and direct role in activating and inactivating lineage-specific genes. For example, GATA-binding Protein 1 (*GATA1*)[14] determines the fate of the erythroid cells while *NOTCH1* is responsible for T cell commitment[15]. Specifically focusing on transcriptional regulation of megakaryopoiesis, there are several TFs that contribute to this unique hematopoietic commitment pathway. Amongst these are also *GATA1*[16]; its coactivator Friend of GATA1 (*FOG1*)[17]; Runt-Related Transcription Factor 1 (*RUNX1*)[18,19]; Nuclear Factor, Erythroid 2 (*NFE2*)[19]; ETS Proto-Oncogene 1, Transcription Factor (*ETS1*)[20] and Friend Leukemia Virus Integration 1 (*FLI1*)[19,21]. The importance and influence of the TF *FLI1* on megakaryopoiesis will be discussed in greater detail.

Megakaryopoiesis is driven by transcriptional regulation

At the heart of HSC lineage commitment are TFs that drive expression or repression of genes responsible for the eventual morphology and functions of a blood cell. These intrinsic regulatory TFs are either expressed continuously or at specific stages during the HSC differentiation process. HSCs reside at the apex of the blood cell lineage commitment pathway and are classically described as first driven towards either the common lymphoid progenitor (CLP) fate by the TFs IKAROS Family Zinc Finger 1 (*IKZF1*), Spi-1 Proto-Oncogene (*SPI1*) and *GATA3*[22] or to the common myeloid progenitor (CMP) fate by simultaneous expression of *SPI1* and *GATA1*[23]. The CLPs ultimately give rise to T cells, B cells and natural killer cells, whereas CMPs go on to become granulocytes, monocytes and the bipotent megakaryocyte-erythroid progenitors (MEP)[23]. Specifically for megakaryocytes, several key TFs expressed in a temporally appropriate manner determine the commitment of MEPs away from the erythroid and to the megakaryocytic lineage: *GATA1*[16], *FOG1*[17], *RUNX1*[18,19], *NFE2*[19] and a few members of the ETS TF family[19-21].

While *GATA1* may be important for erythroid maturation, multiple studies have also shown a role for *GATA1* in megakaryopoiesis. Indirectly, its megakaryopoiesis influence was shown via ectopic expression of Gata1, where avian myeloblasts could be reprogramed to other blood lineages, including thrombocytes (the avian equivalent of megakaryocytes)[24]. More concrete evidence was presented in a study where loss of murine *Gata1* in the megakaryocyte lineage severely impaired megakaryocyte proliferation and maturation; thereby causing reduced platelet counts[16]. Moreover, a mouse embryonic stem (ES) cell line lacking *Gata1* had blocked early erythroid and

megakaryocyte maturation, but this phenotype was abrogated when *Gata1* was restored[25]. These studies suggest that *GATA1* plays a role in early MEP cell commitment from the CMPs.

The TF *FOG1* is highly expressed in the megakaryocyte lineage[26]. This TF was confirmed to be important for megakaryopoiesis when embryonic lethal *Fog1*$^{-/-}$ mice were reported to have a complete absence of megakaryocyte colonies when yolk sac and fetal liver cells were harvested and cultured in vitro[27]. It was also shown to complex with GATA1 during erythroid and megakaryocytic differentiation[26,28], suggesting an influence on the differentiation of MEPs to erythrocytes and megakaryocytes. Furthermore, the prevention of GATA1/FOG1 binding led to defective megakaryopoiesis[29].

RUNX1 is another TF that physically cooperates with GATA1 to drive transcription of megakaryocyte-specific genes[18]. Inducible deletion of Runx1 in mice inhibited megakaryocyte maturation, resulting in the presence of small, immature micromegakaryocytes in the bone marrow[30]. A study suggested *RUNX1* may be an important early stage TF for promoting megakaryocyte proliferation, showing that siRNA-mediated suppression of *RUNX1* in a megakaryoblastic leukemia cell line blocked proliferation and decreased megakaryocyte maturation markers[31].

NFE2, another TF originally discovered as important for erythroid differentiation, exists as a heterodimer with a hematopoietic tissue specific p45 subunit and a ubiquitous maf subunit[32]. It was later found to also be involved in megakaryopoiesis when overexpression of the p45 subunit enhanced late stage megakaryopoiesis and pro-platelet formation and release[33]. Additionally, mice that lack any NFE2 p45 had a

mild red cell phenotype but were unable to produce any platelets resulting from a block in late megakaryocyte maturation[34].

The ETS TF family and megakaryopoiesis

The ETS family is among the largest group of TFs that are linked to a plethora of functions, including but not limited to cellular differentiation and proliferation[35]. All members of this TF family share a highly conserved DNA-binding domain – the ETS domain – that recognizes an 11-base pair (bp) DNA sequence containing a purine-rich 5'-GGA-3' central motif[36,37]. The 5' and 3' ends of this 11-bp region govern the DNA-binding specificity of each ETS member[37]. It has been suggested that ETS DNA-binding could have two modes of action: a promiscuous binding for regulation of housekeeping genes and a more specific binding for specialized genes[38]. In addition to their activity at the ETS domain, this family of TFs has the ability to undergo protein-protein interactions with other ETS family members and with other proteins for more enhanced and specific transcriptional regulation of many proliferation and differentiation events, including megakaryopoiesis[35].

The founding member of this TF family, *ETS1*[39], has been shown to be upregulated during megakaryocytic differentiation from cord blood[40] and its expression maintained throughout megakaryopoiesis[20]. Furthermore, when ETS1 is overexpressed in erythroid cells, a maturation block coupled with decreased red cell-specific proteins was observed. Conversely, overexpression of ETS1 in megakaryocytes increased cell proliferation and upregulated megakaryocytic markers[20]. Interestingly, ETS1 and GATA1 can either independently or synergistically transactivate the promoter of the

megakaryocyte surface glycoprotein (GP) IIb, also known as αIIb, in HeLa cells[41]. The GA Binding Protein Transcription Factor Alpha Subunit (*GABPA*) ETS TF controls expression of early megakaryocyte genes like *ITGA2B* and *MPL*[21]. *SPI1* is another member of this family that is involved in megakaryopoiesis. Binding of GATA1 and SPI1 on a regulatory element of *FLI1*, another ETS TF, may function as transcription regulation of this TF[42]. *ERG* and *ETS2* are other ETS members involved in positive regulation of megakaryocyte development[43,44], whereas ETS variant 6 (*ETV6*) and Erythroid Kruppel-Like Factor (*EKLF*) were shown to act negatively on megakaryopoiesis via inhibition of *FLI1* activity and enhancing erythroid differentiation[45,46].

Perhaps the best-characterized ETS TF family member involved in positive stimulation of megakaryopoiesis is *FLI1*. This TF has been shown, in studies of cell lines and mouse models, to be essential for MEP commitment to the megakaryocyte lineage[47,48] and is highly expressed during megakaryocyte maturation[49]. Overexpression of FLI1 in the erythroleukemia cell line K562 was able to alter cell size, morphology and gene expression to a megakaryocytic phenotype[47]. This same group later reported that FLI1 could even block erythroid differentiation via the inhibition of GATA1[48], which is crucial for the differentiation of MEPs[25,50] as well as red cell maturation[51]. Mouse models have also confirmed the role of *FLI1* in megakaryopoiesis. *Fli1*$^{-/-}$ embryos die from brain hemorrhages at E11.5 due in part to dysmegakaryopoiesis and in part from vasculature defects. When the E11.5 fetal liver progenitors were evaluated in an in vitro colony formation assay, this group found an increase in the number of micromegakaryocytes with abnormal ultrastructures[52]. Another model with a milder disruption of mouse *Fli1* expressing a truncated protein that lacks the C-terminal ETS DNA-binding domain

reported reduced viability with thrombocytopenia and platelet aggregation and activation defects observed in the homozygous mice[53]. An inducible deletion of *Fli1* in adult mice resulted in increased numbers of MEPs as well as erythroid cells while exhibiting a drastic decrease in mature megakaryocytes[54]. Overall, cell line and mouse model studies of *FLI1* suggest the indispensable role of this TF in not only MEP commitment to the megakaryocyte lineage but also in late stage maturation of those megakaryocytes.

Platelet clinical disorders related to transcription factor defects

Because the above TFs have been experimentally proven to be crucial to the megakaryocyte lineage, it is no surprise that deficiencies of those TFs can cause a multitude of symptoms in patients related to defects in developing megakaryocytes, from mild to moderate thrombocytopenia and severe platelet defects. Defects in TFs that lead to a megakaryocyte or platelet phenotype are discussed below with an emphasis placed on the defects due to disruptions in *FLI1*.

GATA1

Since *GATA1* is required at very early stages of HSC differentiation[25], it is expected that genetic mutations of *GATA1* would affect multiple blood lineages. Indeed, *GATA1* is implicated in deficiencies of the erythroid, myeloid as well as megakaryocyte cells[55]. This TF is located on the X chromosome and is associated with several X-linked disorders in which females are asymptomatic or present with milder symptoms than seen in males where mild to severe macrothrombocytopenia and/or anemia and

neutropenia are reported[55]. An inherited V205M mutation in *GATA1* that disrupts its binding to FOG1 but leaves the DNA-binding region intact was reported to cause macrothrombocytopenia and dyserythropoietic anemia[56]. The following similar clinical mutations affecting GATA1 interaction with FOG1, but not to DNA, have since been discovered: G208S[57], G208R[58] and D218G[59] causing macrothrombocytopenia and dyserythropoiesis but not always resulting in anemia; and D218Y[60] causing severe macrothrombocytopenia and anemia with early mortality. These mutations suggest that the FOG1 cofactor is essential in normal megakaryopoiesis and, to a lesser extent, erythropoiesis.

Mutations in *GATA1* that affect its DNA-binding capability can also cause a megakaryocyte defect. The R216Q[61,62] mutation causes thrombocytopenia and β-thalassemia while R216W[63], a different substitution at the same amino acid residue, results in the additional manifestation of congenital erythropoietic porphyria[63]. Splice mutations that result in loss of full-length GATA1 and resulting in expression of only a naturally-occurring, shortened version of GATA1 (termed GATA1short or GATA1s) lacking the N-terminal transcription activation domain can severely hinder erythropoiesis and cause megakaryocyte and platelet defects[55]. This GATA1s isoform also affects production of white cells and neutrophils[55]. Overall, patients harboring mutations in *GATA1* that reduces its activity either through loss of binding to its cofactor FOG1, direct binding to DNA targets, or loss of the full-length isoform presents with not only dyserythropoiesis but also macrothrombocytopenia often associated with concurrent platelet functional defect.

RUNX1

Familial platelet disorder (FPD) in a family with a presentation of thrombocytopenia, platelet aggregation defects and a high propensity to develop acute myelogenous leukemia (AML) was linked to a locus on chromosome 21q22.1-22.2 where *RUNX1* resides[64]. Haploinsufficiency of *RUNX1*, either by nonsense mutations or intragenic deletion of one allele, was later confirmed to be responsible for FPD/AML[65]. Additionally, various mutations that abrogated the DNA-binding capacity of RUNX1 were found in other families with FPD/AML[66]. In other FPD/AML mutations, the ability of RUNX1 to heterodimerize with binding partner Core Binding Factor β, known to stabilize the interaction of the complex with DNA[67,68] and to protect it from proteolytic degradation[69], was lost[66]. Because several possible binding sites for RUNX1 were found in the promoter region of *MPL*, decreased MPL surface expression at normal TPO levels is thought to be the mechanism for thrombocytopenia in the p.Thr219Argfs* *RUNX1* defect[70]. This mechanism was further elucidated when the mutated RUNX1 was shown to be unable to regulate NFE2 expression, thereby influencing platelet granule and surface protein expression[71]. Many platelet genes, including Platelet Factor 4 (PF4, CXCL4)[72] and platelet protein kinase C-θ[73], have since been reported to also be regulated by RUNX1.

FLI1

The *FLI1* gene is found on chromosome 11q22.3-24[74] and is one of many genes hemizygously lost due to chromosome 11q terminal deletions of varying sizes[75,76], resulting in Jacobsen syndrome (JSx). Many of these deletions arise de novo, with an

estimated 1 in 100,000 prevalence[77]. Because these deletions can sometimes be up to 20 Mbp in length, patients with JSx can present with a multitude of defects, including cardiac and kidney defects, cognitive impairments, psychomotor retardation, facial dysmorphism, and macrothrombocytopenia[76]. While not all patients have the same set of symptoms, over 90% have a bleeding diathesis called Paris Trousseau syndrome (PTSx)[78,79]. PTSx patients have an increase in immature micromegakaryocytes in their bone marrow and macrothrombocytopenia with 10-15% of their platelets containing fused giant α-granules and secretion defects. The perinatal thrombocytopenia can lessen with age, but platelet function may not, suggesting that the platelet defect persists even if the platelet numbers return to usually the low normal range[79]. Because *ETS1* and *FLI1* are both deleted in PTSx (Figure 1.1) and are physically only separated by ~170 kb[80], it has been suggested that the combinatorial hemizygous loss of these two genes is to blame for the PTSx macrothrombocytopenia[81]. However, mice that are heterozygous for both genes only have a 19% reduction in platelet count with no abnormal platelet morphology and show no megakaryocyte defects[81]. A study done on peripheral blood $CD34^+$ cells harvested from 2 PTSx patients concluded that hemizygous loss of *FLI1* is responsible for the thrombocytopenia after lentivirus-mediated overexpression of FLI1 in these cells restored normal megakaryopoiesis[82]. Unfortunately, this study failed to recognize the possibility that FLI1 overexpression by itself can drive progenitor cells to differentiate into the megakaryocyte lineage[47,48], thereby not necessarily correcting the dysmegakaryopoiesis but rather just tipping the scale away from erythroid or myeloid differentiation and towards megakaryocytic differentiation. Moreover, this paper claimed that FLI1 expression was controlled by allelic exclusion where half of progenitor cells would be expressing normal levels of FLI1

and the other half with zero expression. This idea that FLI1 undergoes allelic exclusion remains in the literature[82,83] in spite of the observation that no one has shown two distinct platelet populations with one defective qualitatively and quantitatively and the other normal.

Two recent reports have suggested that the large chromosomal deletions found in JSx are not needed for PTSx-like platelet defects. A next generation sequencing study of 13 unrelated families with excessive bleeding and suspected inherited platelet disorder found 3 cases of different heterozygous *FLI1* mutations[84]. There were 2 substitution mutations at R337W and Y343C and a 4-bp deletion at p.Asn331Thrfs*4. All 3 mutations were located in the ETS DNA-binding domain. *FLI1* was reported for the first time to have an autosomal recessive inheritance pattern when a family was found to have PTSx-like macrothrombocytopenia and platelet secretion defects only in the homozygous offspring but not heterozygous parents[85]. This family's R324W mutation is also located in the ETS DNA-binding domain of FLI1. No other hematological abnormalities were observed in the patients harboring *FLI1* mutations. Overall, the higher than expected prevalence of *FLI1* mutations in patients with undiagnosed platelet disorders would suggest this TF is responsible for more cases of inherited platelet disorders than previously thought.

Challenges to studying megakaryopoiesis associated with *FLI1*

Surprisingly, the current literature on the influence of *FLI1* on human megakaryopoiesis and the details of the thrombocytopenia and platelet functional

defects observed in PTSx hemizygous deletions and the newly described heterozygous mutations are underdeveloped. While there is a recent study showing *FLI1* to account for a larger than previously thought portion of inherited platelet disorder[84], there are still many challenges to clinical studies of this TF. PTSx patients with *FLI1* deletions or mutations are rare, with many dying in infancy[86]. Given the variable genotypic background of these rare PTSx individuals and those with inherited *FLI1* mutations, linking specific details of the phenotype to the *FLI1* gene can be challenging. Comprehensive in vitro studies can be done on immortalized cell lines, but these studies may not recapitulate patient phenotype. In vivo mouse models do not fully replicate the biology of this TF in humans in that the *Fli1*$^{+/-}$ mice do not have thrombocytopenia. Thus, a solution that addresses these challenges could allow for detailed analysis of the effects of FLI1 deficiency on megakaryopoiesis, thrombopoiesis and platelet biology not yet addressed. Furthermore, the question of allelic exclusion of *FLI1* and the influence of optimal FLI1 levels in these processes could also be studied.

PTSx patient clinical data and primary cells

Studies using patient clinical data and primary cells can be very limited if the patient pool is small, with many of the patients facing more pressing challenges like life-threatening organ defects. For JSx and PTSx, there are only about 200 reports of confirmed chromosome 11qter deletions. While clinical data like platelet counts and platelet aggregation defects serve to confirm the PTSx macrothrombocytopenia phenotype, more work still needs to be done at the molecular level to study and deconstruct the disease mechanism. Most reports of PTSx patients contain clinical

analysis, but not all of them contain molecular analysis, like gene expression profiling, of megakaryocytes and platelets. The disease itself manifests as a problem, since it is hard to justify extracting bone marrow or enough whole blood on which to perform detailed in vitro studies when the patient has a bleeding diathesis. To date, there has been one mechanistic study on PTSx that used primary $CD34^+$ cells extracted from patients[82]. Even so, this group was only able to show limited in vitro data on 2 patients. Additionally, no detailed megakaryocyte or platelet biology studies have been reported on the 3 heterozygous[84] and one homozygous[85] *FLI1* mutations that have been recently described.

Immortalized cell lines

Cell lines can provide researchers with an unlimited quantity of material to study. Indeed, immortalized cell lines have been used to study the biology of *FLI1* in megakaryopoiesis, though this approach also has its limitations. For example, the myelogenous leukemia cell line K562 was transduced with a retroviral construct to overexpress FLI1, which created cells that were large, like megakaryocytes, and also expressed the megakaryocyte-specific αIIb[47]. While this study was able to identify the ability of retroviral FLI1 overexpression to cause a leukemia cell line to differentiate along the megakaryocyte lineage, there were not studies that demonstrate that these cells can undergo thrombopoiesis and release functional platelets. Immortalized cell lines may also have a different phenotype than their origin tissue sources would suggest, having gone through significant mutations during the immortalization process[87].

Mouse/animal models

For almost any human disease that has been studied, at least one animal model has been created to evaluate the pathology at an organismal level. Most of these animal models are created using mice due to their size, ease of breeding and cost. Unfortunately in the case of *FLI1*, multiple mouse models proved that mice are not men. In humans, haploinsufficiency of *FLI1* results in the megakaryocyte and platelet defects described above. In mice, however, only the homozygotes had a defective phenotype, and heterozygotes display normal platelet counts and function[52-54]. One study even reported a normal megakaryocyte/platelet phenotype in mice homozygous for a severely mutated Fli1 expressing only its first 10 amino acids[88]. Of course, these mouse models provide important insights into the in vivo biology of *FLI1* on megakaryocyte development, yet the incongruent inheritance pattern raises the question of how far we can translate mouse studies to the clinical setting. No other species have been used to create a *FLI1*-deficient model to study megakaryopoiesis.

Induced pluripotent stem cells and their applications in hematopoietic studies

To pursue additional insights into the role of FLI1 and its level in megakaryopoiesis, thrombopoiesis and platelet biology in patients, we turn to an alternative model using induced pluripotent stem cells (iPSC) for analysis. iPSCs are cell lines that have been created by transducing somatic cells with a set of stem-cell specific TFs, thereby reverting them back to a pluripotent state. This methodology was first described in 2006 by Takahashi and Yamanaka, detailing the successful reprogramming

of adult mouse fibroblasts to iPSCs after viral transduction of the TFs Oct3/4, Sox2, c-Myc and Klf4[89]. This group later showed the same could be done for human fibroblasts[90]. These iPSCs proved to have ES cell morphology and gene expression profile. Furthermore, when injected subcutaneously into mice, the tumors that develop exhibits all three germ layers: endoderm, mesoderm and ectoderm[89,90]. Due to their ES-like qualities, iPSCs have a wide variety of applications, especially in disease modeling.

The pluripotency of iPSCs proved very useful for researchers studying diseases that are found in any tissue. It is now possible to collect a small sample of cells using noninvasive procedures like a blood draw or skin biopsy from patients to create disease-specific cell lines. iPSC lines have since been created from cells of patients with type 1 diabetes[91], spinal muscular atrophy[92], thalassemia and sickle cell anemia[93] and many other diseases. These iPSC lines can then be differentiated into the relevant tissues to study specific disease pathology.

iPSCs are also self-renewing cell lines, meaning they can be cultured indefinitely. This unique property provides a virtually unlimited amount of material with which studies can be done. No longer do researchers studying rare diseases need to worry about procuring a vast quantity of primary cells from patients. Even at smaller or remote institutions where there may not necessarily be opportunities to obtain patient samples to create iPSCs, numerous commercial and institutional cell banks have been set up around the country and the world where one could send for very specific iPSC lines. The pluripotent and self-renewing properties of iPSCs can provide an unparalleled access to disease models not available otherwise.

Disease modeling of hematopoietic disorders using iPSCs

In vitro modeling of hematological diseases using iPSCs has been well-documented[94,95]. These lines, generated from patient fibroblasts or various blood cells, retain the original genomic aberrations and could recapitulate the disease pathology once differentiated in vitro. It is even possible to correct the genetic defect, as shown in Fanconi anemia[96], before iPSCs were generated and obtain disease-free hematopoietic progenitor cells (HPC) that are more lineage-committed than the HSCs[97].

Primitive versus definitive hematopoiesis

While iPSC technology is undeniably useful in studying the pathogenesis of diseases, they do have limitations. This is especially concerning for hematopoietic studies, where differentiation of iPSCs to the various blood cells may undergo either or both primitive and definitive hematopoiesis. During mammalian hematopoiesis, different blood progenitor cells are produced based on both spatial and temporal factors. The first blood cells emerge in the yolk sac before circulation begins and then migrate to the aorta-gonad-mesophrenos region as organs start to develop[98]. Later in fetal maturation, hematopoiesis occurs mainly in the liver. The final region where hematopoiesis occurs, shortly before birth and into adulthood, is the bone marrow[98].

The first blood cells that arise from the yolk sac are primitive erythrocytes, megakaryocytes and macrophages[99]. This first wave of hematopoietic progenitors includes primitive or embryonic erythroid lineage[100]. These progenitor cells become large nucleated erythroid cells expressing fetal ε and ζ globin genes, which are then switched to γ globin in the fetal liver and β globin in the bone marrow for definitive

erythrocytes[101,102]. The primitive megakaryocytes and macrophages, however, are virtually indistinguishable from their definitive equivalents[103]. This presents a challenge in identifying and characterizing primitive versus definitive megakaryocytes for in vitro differentiation protocols where there are no spatial or temporal queues to establish their status. Ideally, in vitro differentiation of ES cells and iPSCs to definitive multilineage progenitors that have the ability to become other myeloid cells would allow for clinical applications such as bone marrow transplantation.

The differentiation of iPSCs into HPCs was adapted and developed from the already established ES differentiation protocol[104]. Like ES cell differentiation, the in vitro iPSC differentiation program directs cells along the primitive streak[105,106]. This primitive HPC differentiation is a challenge for translating this research into clinical use. Regarding this issue, strides have been made with the overexpression of various single[107] or combinatorial TFs[108] that favor definitive differentiation. The area of research for directed iPSC differentiation towards definitive hematopoiesis is ongoing. Meanwhile, the currently established protocol allows for comprehensive disease modeling and mechanistic studies of hematopoietic disorders with the limitations of these iPSC lines taken into account.

Summary

While *FLI1* has been established as an important TF regulator of megakaryopoiesis, either through cell line or mouse model analyses, key questions in studying *FLI1*-associated megakaryocyte and platelet defects as it pertains to human

biology remains. I approach these questions using human iPSCs that express varying levels of FLI1 during megakaryopoiesis, with iPSCs from a normal control line that has then been gene-edited to establish isogenic sublines that were either *FLI1* heterozygous or that overexpressed FLI1. I also studied megakaryopoiesis with iPSCs established from a patient with PTSx which we gene edited to overexpress FLI1. I hypothesize that the expression level of FLI1 during megakaryopoiesis has a direct, correlative influence on megakaryocyte maturation, subsequent thrombopoiesis and in vivo-released platelet quality. The scope of this thesis encompasses the creation of relevant iPSCs to study *FLI1*-associated megakaryopoiesis as well as detailed in vitro and in vivo characterization of megakaryocytes and platelets. Chapter 2 outlines the generation of iPSCs and their genome editing to effectively study *FLI1* influence on megakaryopoiesis and thrombopoiesis. Chapter 3 details the in vitro effects of *FLI1* on megakaryocytes and platelets. In vivo analyses of thrombopoiesis and released platelet quality are described in Chapter 4. Finally, in Chapter 5, I will discuss the relevant findings and potential clinical implications from these studies.

Figures

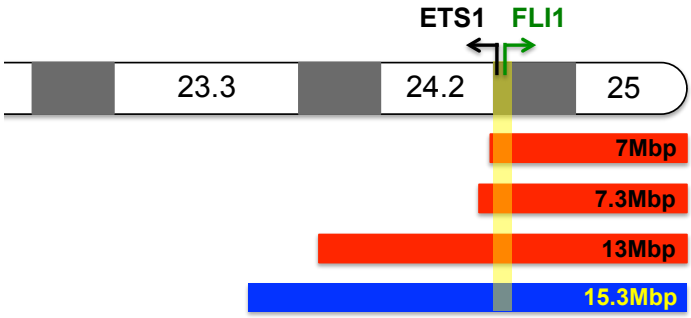

Figure 1.1. Schematic of 4 PTSx 11qter deletions.

Schematic illustrating 4 PTSx 11qter chromosomal deletions of various sizes, all containing *FLI1* and *ETS1*[109]. The PTSx patient studied in this thesis is visualized by the blue box. Deletion was determined by chromosomal microarray by CHOP's Genomic Diagnostics Laboratory (Philadelphia, PA).

CHAPTER 2 – Creation of FLI1-iPSC lines using gene-editing strategies

Abstract

I describe in this Chapter the generation of human iPSCs from a normal control wildtype (WT) and a PTSx patient, the use of zinc-finger nuclease (ZFN) technology to transgenically express FLI1 in tissues of interest and the use of transcription activator like effector nuclease (TALEN) to mutate *FLI1* on these iPSC lines. First, using a ZFN-mediated protocol previously developed by our group, I generated megakaryocyte-specific FLI1-overexpressed control (WT-OE) and PTSx (PTSx-OE) iPSCs. The WT line was used to create a heterozygous *FLI1*$^{+/-}$ iPSC line with the TALEN gene targeting methodology. ZFN, TALEN, and more recently, clustered regularly interspaced short palindromic repeats (CRISPR)/CRISPR-associated protein (Cas)9 technologies are relatively novel technologies that have facilitated sequence-specific mutagenesis. The experimental protocols for these powerful new tools are relatively easy to learn and carry out, allowing for fast and efficient in vitro-generation of gene-edited cell lines or primary cells and makes possible in vivo gene editing when used in combination with novel in vivo-nanoparticle delivery methods. Coupled with iPSC technology, gene editing allows for normal control lines to be mutated to recapitulate patient-specific phenotypes and patient lines can be returned to normal via the insertion of either a missing or corrected DNA sequence. Other cell line generation techniques used during the course of this thesis are also described in this Chapter.

Introduction

The study of rare disorders that do not have a suitable cell line or animal model that can faithfully reiterate the human phenotype can be a challenging undertaking. However, with the successful reprogramming of somatic cells into pluripotent stem cells of mice in 2006[89] and humans in 2007[90], many of these challenges have since been addressed. With this technology, a pluripotent and self-renewing iPSC line could be made directly from a small sample of blood or skin tissue of relevant patients and controls. The pluripotency property gives researchers the flexibility of studying diseases affecting one or multiple tissue types by differentiating these cell lines into those specific tissues. The self-renewing capability of these iPSCs allows for a virtually unlimited source of material for experimentation. Moreover, since these are cell lines, further manipulation employing the use of targeted introduction of transgenes and gene-editing techniques enables generation of properly controlled lines, including a normal control (WT) line and lines with a specific mutation that can be theoretically studied on the same genotype background.

The pluripotency capability of iPSCs generated from humans, mice or other organisms has been capitalized on for various studies. Directed in vitro differentiation of these cells into multiple tissues; including neuronal, cardiac and hematopoietic cells; has been reported[110,111]. One of the first reports of an iPSC line generated for disease modeling was for spinal muscular dystrophy, where motor neurons differentiated from those iPSCs exhibited degeneration characteristics seen in the patients' neurons[92]. Similarly, cardiomyocytes differentiated from iPSCs generated from patients with long QT syndrome had the same typical cardiac phenotypes associated with the disease[112].

Early iPSC models of hematological disorders include Fanconi anemia[96], thalassemia[93], sickle cell anemia[93] and myeloproliferative disorders[113]. Platelet disorders that have been successfully modeled and corrected in the iPSC system include congenital amegakaryocytic thrombocytopenia[114] and Glanzmann thrombasthenia[115].

Another advantage of using iPSCs to model diseases is the ability to modify the genome of these cell lines for further and more thorough examination of patient-specific genetic pathogenesis. Our laboratory has previously reported megakaryocyte lineage-specific expression of transgenes using ZFNs at the adeno-associated virus integration 1 (AAVS1) locus[115]. More recently, advances in alternative technologies such as TALENs and CRISPR/Cas9 have allowed for faster development of gene-editing strategies for in vitro as well as in vivo applications. The basic principle behind these three technologies is similar: there is a sequence-specific DNA-recognition portion along with a catalytic portion for DNA cleavage that takes advantage of the endogenous DNA repair mechanism to effect genomic changes.

ZFNs contain a modular portion that has been designed to bind to a specific DNA sequence called a zinc finger domain and is bound to a catalytic restriction endonuclease domain. In 1996, the first report of the fusion of the modular zinc finger domain to the cleavage domain of type IIS endonuclease FokI characterized the DNA cutting patterns of this fusion protein[116]. Each modular zinc finger motif binds a 2- to 4-bp DNA sequence, with a typical ZFN containing a sequence of 3 to 6 different zinc finger modules to confer up to an 18-bp sequence-specific binding[117,118]. Because the FokI endonuclease activity requires dimerization[119], a pair of ZFNs binding to opposite sides on the DNA target site is required for double-strand breaks, which increases the specificity of the ZFN. Gene correction using ZFNs was first demonstrated in 2003,

where a green fluorescent protein (GFP) mutation was successfully corrected[120]. Clinical applications of ZFNs are being developed for HIV resistance in T cells[121,122]. While the basic and translational benefits of ZFNs have been established, their modular DNA-binding motifs have limitations. Specificity can be limited as the zinc finger modules can sometimes only recognize 2 of 3 bases, thereby increasing the chances of off-target recognition[123,124].

A more recent discovery in the sequence-specific targeting of DNA is TALEN technology. Similar to ZFNs, TALENs are fusion proteins consisting of a sequence-programmable TALE DNA-binding domain and the same FokI endonuclease used in ZFNs. The TALE portion is derived from bacteria[125] and each domain contains a conserved 33-35 amino acid repeat with repeat variable diresidues (RVD) at positions 12 and 13 conferring nucleotide specificity[126]. TALEs could then be designed to bind with high affinity to specific DNA sequences by using different RVDs that correspond to the four nucleotides adenine, guanine, thymine and cytosine[127]. Another advantage other than high specificity is that TALEN construction is much simpler than ZFN construction[128], with high-throughput TALEN assembly[129] aiding in the creation of a library spanning the human genome[130]. Like ZFNs, however, complicated and limited construct design as well as relatively limited efficacy and partial off-target concerns[131] need to be addressed with the use of TALENs in gene editing.

Lastly, the development of CRISPR/Cas9 for specific DNA targeting in the past few years has provided an even more simplified protocol for gene editing. CRISPR were discovered to be used by bacteria and archaea in conjunction with the Cas endonuclease as an adaptive immunity response to destroy foreign DNA[132,133]. The most commonly used system for eukaryotic genome targeting is the Type II CRISPR

containing the Cas9 endonuclease and the guide RNA (gRNA) consisting of the CRISPR RNA (crRNA) that confers sequence specificity and the transactivating crRNA (tracrRNA) that complexes with the Cas[134]. When all components of the CRISPR/Cas9 are delivered to the cell, the gRNA directs the Cas9 to the target sequence and DNA cleavage occurs three base pairs upstream of the NGG protospacer-associated motif (PAM) on the target DNA strand[135]. Variants of the Cas9 endonuclease have since been discovered that can provide higher efficiency or specificity of this system[136].

The goal of all three described technologies is to induce double-strand DNA breaks at very specific, targeted sites in the genome then taking advantage of cell's own DNA repair mechanisms to create site-specific mutagenesis. The DNA breaks can be repaired either through the homology-directed repair (HDR) or the error-prone non-homologous end joining (NHEJ) pathways[137]. In the HDR pathway, the cellular DNA repair relies on a template to introduce single nucleotides or transgenes at the DNA break[138]. The NHEJ repair mechanism detects a double-strand break and simply ligates the ends back together. Because this method does not use a template for repair, it often causes the introduction, at the repair site, of small insertions or deletions that can cause a single amino acid or a frameshift mutation[139]. These two endogenous DNA repair mechanisms facilitate the efficiency of gene-editing tools described.

This Chapter provides detailed descriptions of the generation of iPSCs from a control wildtype (WT) and a PTSx patient with subsequent gene editing techniques used on these lines. Overexpression of FLI1 was performed using the ZFN technique on WT (WT-OE) and PTSx (PTSx-OE) lines. A *FLI1*$^{+/-}$ line (FLI1$^{+/-}$) was created using the TALEN method. I will also describe the CRISPR/Cas9 gRNAs generated in the attempt to create *FLI1*$^{-/-}$ and *ETS1*$^{-/-}$ iPSCs.

Methods

Plasmids used for reprogramming and gene editing

The WT iPSC line was generated as described previously[140]. Co-transfection of a tetracycline-inducible expression cassette pHAGE-Tet-hSTEMCCA (Figure 2.1A) containing the four reprogramming factors OCT4, SOX2, KLF4 and MYC and the reverse tetracycline transactivator protein (rTTA) containing vector pHAGE2-CMV-rTTA resulted in cell reprogramming in the presence of doxycycline.

The PTSx iPSC line was generated using a humanized, floxed single excisable lentiviral stem cell cassette hSTEMCCA-loxP (Figure 2.2A) described previously[141]. This polycistronic vector contains the four reprogramming factors OCT4, SOX2, KLF4 and MYC. The resulting integration of this floxed vector can be excised on exposure to Cre recombinase with the transient transfection of pHAGE2-Cre-IRES-PuroR (Figure 2.2B).

The megakaryocyte-specific transgene expression strategy was previously described[115]. Two ZFN plasmids under the constitutively active phosphoglycerate kinase (PGK) promoter and targeting the AAVS1 locus were used: pPGK-AAVS1-ZFNL and pPGK-AAVS1-ZFNR (Figures 2.3A and 2.3B). A third plasmid carrying the donor *FLI1* cDNA, AAVS1-Gp1ba-hFLI1 (Figures 2.3C and 2.4), contains a murine megakaryocyte-specific *Gp1ba* promoter.

Generation of the WT iPSC line

The WT iPSC used for this thesis was generated by the Children's Hospital of Philadelphia (CHOP) Human Pluripotent Stem Cell Core (Philadelphia, PA) and named WTBM1-8[115]. Bone marrow cells were purchased from the Stem Cell Core at the University of Pennsylvania (Philadelphia, PA) and approximately 1 X 10^5 $CD34^+$ cells were selected and seeded in 35-mm culture plates. Cells were co-transfected in the presence of 5 µg/ml polybrene with lentiviral vectors pHAGE-Tet-hSTEMCCA and pHAGE2-CMV-rTTA (Figure 2.1)[140]. The medium was replaced after 16 hours with iPSC medium consisting of DMEM/F12 (Gibco, Carlsbad, CA) with 20% KnockOut Serum Replacement (Invitrogen, Carlsbad, CA), 1 mM L-glutamine (Sigma-Aldrich, St. Louis, MO), 0.1 mM β-mercaptoethanol (Sigma-Aldrich), 1% nonessential amino acid solution (Invitrogen), and 10 ng/ml basic fibroblast growth factor (bFGF) (R&D Systems, Minneapolis, MN). Doxycycline at 1 µg/ml was supplemented in the iPSC medium from the first day of reprogramming and removed 2-3 weeks later after individual iPSC clones resistant to doxycycline were mechanically picked with a 10 µl pipette tip under 40X magnification. These clones were selected based on iPSC morphology and colony size spanning at least half of the magnification field (Figure 2.5).

Generation of the PTSx iPSC line

The PTSx iPSC line was generated by the CHOP Human Pluripotent Stem Cell Core with fibroblasts collected from a PTSx patient (Table 2.1 and Figure 1.1), using reprogramming methodology as described[141]. Fibroblast cells were obtained as leftover samples from the Division of Genomic Diagnostics Lab (CHOP), cultured in T75 plates and split 1:3 when 80% confluent. Reprogramming was done after 3 passages, at which

time approximately 1 X 10^5 fibroblasts were plated in DMEM with 10% FBS on a 0.01% gelatin (Sigma-Aldrich)-coated 35-mm plastic tissue culture dish. The next day polybrene was added to the media (5 µg/ml), and the cells were infected with the excisable hSTEMCCA-loxP (Figure 2.2A) single cassette lentivirus. On day 2, the medium was changed to iPSC medium. On day 6, the culture dish was trypsinized and passaged at a 1:16 split ratio onto two 0.01% gelatin-coated 10-cm culture dishes that had been plated the day before with a feeder layer of irradiated mouse embryonic fibroblasts (irMEFs). iPSC clones were picked as described above for WT iPSCs. The excision of viral sequences was performed using the Hela Monster transfection reagent (Mirus, Madison, WI) according to manufacturer's instructions. A 35-mm tissue culture well of iPSC colonies at 30% confluency and growing on puromycin-resistant MEFs (GlobalStem, Gaithersburg, MD) were transiently transfected with medium containing 2 µg of pHAGE2-Cre-IRES-PuroR (Figure 2.2B) plasmid DNA along with 6 µl of transfection reagent and 3 µl of the Monster reagent. The medium was changed the next day with iPSC supplemented with 1.2 µg/ml puromycin for selection 24 hours post transfection and lasted for 48 hours. The re-emergence of iPSC colonies was noted within 1 week, and colonies from each well were picked, as above, approximately 1-2 weeks later.

Pluripotency characterization of WT and PTSx iPSC lines

Analysis of pluripotency surface markers stage-specific embryonic antigen (SSEA) 3, SSEA4, Tumor-related Antigen (TRA)-1-60 and TRA-1-81 was performed via flow cytometry (Figure 2.6A). iPSCs were detached using Accutase (Invitrogen), washed once in fluorescence-activated cell sorting (FACS) buffer of phosphate buffered saline

(PBS, calcium chloride and magnesium chloride free, Gibco) containing 0.01% bovine serum albumin (BSA, Sigma-Aldrich). Single cell suspensions at approximately 1-2 X 10^5 cells were stained in 100 µl FACS buffer. Antibodies were used (Table 2.2) at the following dilutions: SSEA3 Alexa Fluor (AF) 488 1:200, SSEA4 AF 647 1:400, TRA-1-60 AF 488 1:50 and TRA-1-81 AF 647 1:50 (Biolegend, San Diego, CA). Cells were incubated at room temperature (RT) for 15 minutes then washed once with FACS buffer and resuspended in 200 µl of FACS buffer before data were collected using a BD FACSCanto II (BD Biosciences, San Jose, CA) and analyzed using FlowJo software (Tree Star, Ashland, OR).

For teratoma formation, approximately 6 X 10^6 iPSCs were harvested using Accutase and resuspended in 140 µl of DMEM/F12. Immediately prior to injection, 60 µl of Matrigel (BD Biosciences) was added to the cell suspension at 4°C, and the resulting mixture injected subdermally between the scapulae of each anesthetized severe combined immunodeficiency (SCID)-Beige mouse (strain 250, Charles River, Wilmington, MA). Resulting tumors were harvested at 6-8 weeks post injection, fixed in 4% paraformaldehyde, and paraffin tissue sections were prepared and stained with hematoxylin and eosin according to standard methods[142] (Figure 2.6B). Karyotyping was performed by Cell Line Genetics (Madison, WI) (Figure 2.6C).

Maintainence of iPSC lines

Maintenance of iPSCs is as previously described[143]. Reprogrammed cells were cultured in iPSC medium. Culture dishes were coated with 0.01% sterile gelatin (Millipore) before plating a feeder layer of irMEFs and were incubated at 37°C at 5% CO_2

1-2 days prior to iPSC culturing. Passaging was performed approximately every 3-4 days at a 1:6 to 1:24 split ratio. Cells were incubated with Accutase for 3-5 minutes at 37°C to detach them from the dish, and then centrifuged at 1200 rpm for 3 minutes before passaging at the appropriate split ratios in iPSC medium containing 10 μM Y-27632 dihydrochloride Rho Kinase (ROCK) inhibitor (Tocris, Bristol, UK) overnight. iPSC medium without ROCK inhibitor was changed every day except on Sundays, when cells were fed with double the medium volume the previous day. The iPSCs were maintained at 37°C at 5% O_2 in the undifferentiated state for 20-30 passages before tossing and thawing out of a fresh vial of cells.

Generation of WT-OE and PTSx-OE iPSC lines

Overexpression of FLI1 was performed by targeting the AAVS1 safe-harbor locus using a *Gp1ba*-driven *FLI1* transgene using ZFNs, as previously described for expression of *ITGA2B*[115] (Figure 2.3). WT and PTSx iPSCs were plated 24-48 hours prior to transfection on 1:3 matrigel basement membrane matrix (Corning, Corning, NY)-coated 35 mm dishes pre-seeded with drug-resistant MEFs. When cells were approximately 30% confluent, they were washed 2X with Iscove's Modified Dulbecco's Medium (IMDM, Gibco) and fed 2 ml of iPSC medium (20 ng/ml bFGF) 3 hours prior to transfection. Cells were transiently co-transfected with 0.2 μg of each of the AAVS1-targeting ZFN plasmids (pPGK-AAVS1-ZFNL and pPGK-AAVS1-ZFNR), 0.6 μg of a vector containing the *Gp1ba* promoter construct driving the primary *FLI1* transcript cDNA (AAVS1-Gp1ba-hFLI1) and 3 μl of Roche x-tremeGENE9 in 100 μl IMDM mixture added to 2 ml cell medium. The cells were washed once with IMDM the next day. iPSC medium

supplemented with 0.5 µg/ml puromycin was changed for selection 48 hours post transfection and lasted for 72 hours. The re-emergence of iPSC colonies was noted within 1 week, and colonies were picked, as above, approximately 1-2 weeks later.

Generation of the FLI1$^{+/-}$ iPSC line

The heterozygous disruption of FLI1 was achieved by using TALEN nucleases with recognition-site sequences TCCCACCACAGCAGGAGT and TCCCAGTTGCAGTTCGCCCT within exon 2 (Figure 2.7). This pair of TALENs was designed with the help of the University of Pennsylvania Gene Targeting Core (Philadelphia, PA). WT iPSCs cells plated 24-48 hours prior to transfection on 1:3 matrigel-coated 35 mm dishes pre-seeded with drug-resistant MEFs. When cells were approximately 30% confluent, they were washed 2X with Iscove's Modified Dulbecco's Medium (IMDM) and fed 2 ml of iPSC medium with 20 ng/ml bFGF 3 hours prior to transfection. Cells were co-transfected with 0.2 µg each of the two AAVS1-targeting ZFN plasmids (pPGK-AAVS1-ZFNL and pPGK-AAVS1-ZFNR), 0.6 µg of a plasmid with homology arms to the AAVS1 locus containing only the puromycin resistance gene (AAVS1-SA-2A-puro-pA donor), 0.2 µg each of the two TALEN plasmids targeting FLI1 at exon 2 (TALEN-E2-L and TALEN-E2-R, Figure 2.7) and 3 µl of Roche x-tremeGENE9 in 100 µl IMDM mixture added to 2 ml cell medium. The cells were washed once with IMDM the next day. iPSC medium supplemented with 0.5 µg/ml puromycin was changed for selection 48 hours post transfection and lasted for 72 hours. The re-emergence of iPSC colonies was noted within 1 week, and colonies were picked, as above, approximately 1-2 weeks later.

Confirmation of FLI1-modified iPSC lines

WT and PTSx iPSC clones targeted for FLI1 overexpression were confirmed to contain either 1 or 2 copies of the transgene via Southern Blot analysis[142,144] (Figure 2.8). Cells were passaged 3-4 times, then genomic DNA (gDNA) was purified using the DNeasy Blood & Tissue Kit (Qiagen, Hilden, Germany). 10-15 µg DNA was digested with 2000 U of SphI-HF (New England Biolabs, Ipswich, MA) endonuclease overnight at 37°C then electrophoresed on a 0.7 % agarose gel with 0.1 mg/ml ethidium bromide (Invitrogen) in Tris base, acetic acid and EDTA (TAE) buffer. The gel was depurinated in hydrochloride buffer for 30 minutes, washed with distilled water, and then placed in denaturing buffer for two 20-minute washes. DNA was transferred onto a Nylon Hybond –N+ membrane (GE Healthcare, Pittsburgh, PA) overnight. DNA was cross-linked onto the membrane, which was then pre-hybridized for 1-2 hours before adding probe. The radioactive ^{32}P-labeled probe was created using a portion of the AAVS1-Puro donor plasmid after digestion with BamHI that corresponds to the AAVS1 left homology arm of the plasmid, with the following sequence: GATCCTCCCCGTGTCTGGGTCCTCTCCGG-GCATCTCTCCTCCCTCACCCAACCCCATGCCGTCTTCACTCGCTGGGTTCCCTTTT CCTTCTCCTTCTGGGGCCTGTGCCATCTCTCGTTTCTTAGGATGGCCTTCTCCGAC GGATGTCTCCCTTGCGTCCCGCCTCCCCTTCTTGTAGGCCTGCATCATCACCGTTT TTCTGGACAACCCCAAAGTACCCCGTCTCCCTGGCTTTAGCCACCTCTCCATCCTC TTGCTTTCTTTGCCTGGACACCCCGTTCTCCTGTGGATTCGGGTCACCTCTCACTC CTTTCATTTGGGCAGCTCCCCTACCCCCCTTACCTCTCTAGTCTGTGCTAGCTCTTC CAGCCCCCTGTCATGGCATCTTCCAGGGGTCCGAGAGCTCAGCTAGTCTTCTTCCT

CCAACCCGGGCCCCTATGTCCACTTCAGGACAGCATGTTTGCTGCCTCCAGG. After overnight hybridization with the probe, the membrane was washed and exposed on film for visualization.

The FLI1$^{+/-}$ iPSC line was confirmed via sequencing (Figure 2.6). Selected clones were passaged 3 times before gDNA was purified using the DNeasy Blood & Tissue Kit. Primers flanking the target site at exon 2 (Forward: 5'-CGACGAGTCC-CTCTTTGACTCAG-3', Reverse: 5'-AGCCCCATCTGCTGCAAAAAC-3') were used for polymerase chain reaction (PCR). Sequencing of the isolated PCR products was performed to confirm gene editing.

CRISPR/Cas9 constructs targeting FLI1 and ETS1

While a few failed attempts at creating a FLI1$^{+/-}$ iPSC line using the same TALEN strategy were being performed, CRISPR/Cas9 technology was developed for even faster and more efficient gene editing. CRISPR gRNAs targeting either the same TALEN-targeted exon 2 of *FLI1* or exon 2 of *ETS1* were designed using the MIT CRISPR Design website (http://crispr.mit.edu). After submitting the exon 2 target sequences, gRNAs were selected (Table 2.3) based on their low off-target probability. Additionally, to decrease off-target effects, I used a strategy involving transfection of a D10A mutant version of Cas9 that only creates a single-strand break (Cas9n), requiring the presence of 2 gRNAs for 2 Cas9n proteins to nick opposite strands of DNA. All components of this CRISPR/Cas9n system are contained in a single vector that was transiently transfected into WT iPSCs (Figure 2.9).

The single CRISPR/Cas9n vector containing either 2 gRNAs targeting exon 2 of *FLI1* or 2 gRNAs targeting exon 2 of *ETS1*, the Cas9n transgene and an enhanced GFP (eGFP) transgene was transfected into WT iPSCs, adapted from the liposomal transfection protocol for AAVS1 targeting plasmids. eGFP positive cells were detected and single-cell sorted 24-48 hours post transfection. After culturing for 1-2 weeks, 12 iPSC clones each for *FLI1* or *ETS1* were mechanically picked as described above. Similar to the TALEN protocol for sequencing of clones, gDNA was purified and the sequence of interest amplified via PCR using primers flanking the targeted sequence (FLI1 Forward: 5'-CTTGCTTGGGTGAAGAGTGAC-3', FLI1 Reverse: 5'-CCTCTCTGCCTTAGCTCT-CTAG-3', ETS1 Forward: 5'- TGCCTTCTTACAGCCC-ATTTG-3', ETS1 Reverse: 5'- CAGGCAAGTTTGAGGACCAC-3') before submission for sequencing.

Study approval

Animal studies and human tissue sampling were done in accordance with CHOP's Institutional Animal Care and Use Committee and Institutional Review Board, respectively.

Results

Reprogramming of WT and PTSx primary cells into iPSCs

The WT and PTSx iPSC lines were previously created at the CHOP Human Pluripotent Stem Cell Core using two different techniques. The WT line was

reprogramed from bone marrow-derived $CD34^+$ cells of a normal control donor using a tetracycline-inducible stem cell cassette (Figure 2.1) in the presence of doxycycline[140]. The PTSx line was from a baby boy who died 4 days after birth. He was diagnosed with JSx, with a confirmed 15.3 Mbp 11qter deletion and showing other JSx clinical phenotypic features (Table 2.1). This patient also had PTSx thrombocytopenia. Fibroblasts were obtained after death and reprogrammed using a single excisable stem cell cassette carrying the 4 Yamanaka TFs, which was later excised by Cre recombinase[141].

Successful reprogramming of both cell lines was demonstrated by stem cell surface marker analysis of SSEA3, SSEA4, TRA-1-60 and TRA-1-81 by flow cytometry. These data show the reprogrammed cells were able to express all four stem cell surface markers at a high level (Figure 2.6A). Teratoma formation assays performed by injecting SCID-Beige mice with these iPSCs showed the presence of all three germ layers of endoderm, mesoderm and ectoderm in the analysis of the tumor immunohistochemistry sections (Figure 2.6B). Furthermore, karyotype analyses of at least 20 cells per line showed no chromosomal abnormalities after reprogramming (Figure 2.6C).

Generation of FLI1-OE WT and PTSx iPSC lines

The same overexpression strategy was employed for WT and PTSx iPSC, using a previously published megakaryocyte-specific method[115]. The AAVS1 safe harbor locus, at which gene insertions have been shown to be resistant to silencing in iPSCs as well as having no deleterious effects reported[145], was targeted for the insertion of either 1 or 2 copies of the AAVS1-Gp1ba-hFLI1 vector containing primary *FLI1* cDNA driven by

the mouse *Gp1ba* promoter. After successful puromycin selection of approximately 12 clones per line, Southern Blot analysis was performed to confirm presence of transgene. While there were some iPSC clones that contained off-target DNA, correct insertion of FLI1 was confirmed for both WT and PTSx lines (Figure 2.8). Henceforth, the single *FLI1* transgene insertion will be named WT-OE1 and PTSx-OE for WT and PTSx lines, respectively. The double transgene insertion will be named WT-OE2 for the WT line.

Generation of the heterozygous FLI1 iPSC line from WT iPSCs

Since the TALEN plasmids did not contain a selection gene, I co-transfected cells with the TALENs along with the ZFNs used for generation of WT-OE and PTSx-OE iPSCs. This strategy was used in order to positively select for colonies that successfully received the puromycin resistance gene, which means the probability that the TALEN plasmids also entered the cell was increased. A total of 12 puromycin-resistant colonies were selected, as described for iPSC generation above. After sequencing using primers flanking the TALEN target site at exon 2 of *FLI1*, one clone with a heterozygous deletion, 73128_73129delCA, was confirmed (Figure 2.7). Further computational analysis of this 2-bp deletion showed a frameshift mutation occurring at amino acid 60 and resulting in a premature stop codon at amino acid 69 with a hypothetical protein estimated size of 7.3 kDa[146].

CRISPR/Cas9n transfections

WT iPSCs transfected with CRISPR/Cas9n in the same manner as the AAVS1- and TALEN-targeted experiments expressed fluorescent eGFP 24-48 hours post

transfection. Single cell sorting for these eGFP positive cells was performed no more than 72 hours post transfection. These sorted cells were plated in low density on a 100-mm dish containing irMEFs and eventually lost their fluorescence, indicating no integration of vector DNA occurred. After individual clone picking and sequencing analysis, however, no mutated clones were observed for either *FLI1* or *ETS1*. This experiment was repeated three times, including once where the puromycin resistance gene was used for selection instead of eGFP.

Discussion

Generation of self-renewing and pluripotent iPSC lines from human somatic cells has opened the door to many studies not possible before. While these cell lines do not fully capture the complete physiology of in vivo cells, they do allow for in depth analysis of pathogenesis of rare or hard to model diseases. Moreover, with new gene editing technologies like TALENs and CRISPR/Cas9, it is possible to easily create additional isogenic iPSC lines, having the same genetic background that was generated from a single individual. In this study, I used a control WT and a PTSx patient iPSC created at CHOP as tools to answer key questions about *FLI1* biology in megakaryopoiesis. For further and detailed studies that ask the question of whether or how varying levels of FLI1 would impact megakaryocytes and platelets, I used ZFNs and TALENs to gene edit both WT and PTSx iPSC lines to either have increased or decreased FLI1 expression with controlled genotypic backgrounds.

Methods for the successful generation of iPSCs have been studied and developed rigorously in the past decade[140,141,147]. The ideal reprogramming technique would be either virus-free or integration free so as to not disrupt the genome, causing unintended deleterious effects. I used two iPSC lines in my thesis that were created using integrating viral constructs, but the reprogramming genes can either be induced[140] or excised[141]. These methods minimize the disruption of functional genes in these lines. Standard pluripotency analyses of these two lines were performed: stem cell markers (Figure 2.6A), teratoma formation (Figure 2.6B), karyotyping (Figure 2.6C). Flow cytometry data show normal expression of stem cell surface markers SSEA3, SSEA4, TRA-1-60 and TRA-1-81. Teratoma tumor formation assays done in SCID-Beige mice proved the ability of the iPSCs to differentiate into endoderm, mesoderm and ectoderm lineages, as seen in immunohistochemistry tissue sections. Finally, the reprogramming methods used to generate the WT and PTSx iPSC lines did not alter the genomic integrity and stability of these cells. This was shown through the normal karyotypes obtained from representative cells.

From the two WT and PTSx iPSC lines, I utilized various gene-editing strategies to create isogenic FLI1 overexpression or FLI1 heterozygous mutation lines. Starting with the WT and PTSx iPSCs, ZFNs targeting the AAVS1 safe harbor locus and a donor plasmid containing the *FLI1* transgene driven by the murine *Gp1ba* promoter were transfected to generate overexpression of FLI1 in a megakaryocyte-specific manner. This strategy has proven to be successful in our laboratory for the megakaryocyte-specific expression of both eGFP and αIIb[115]. Confirmation of the insertion was done through Southern Blot analysis of gDNA from the resulting iPSC clones (Figure 2.8). Integration of the *FLI1* donor plasmid was indeed successful for many of the selected

iPSC clones, along with clones containing off-target integration. I selected 2 WT-OE iPSC clones for further in vitro and in vivo studies: WT-OE1 and WT-OE2, containing 1 or 2 copies of transgene that was correctly integrated into the genome, respectively. The PTSx-OE clone selected for further studies contained 1 copy of correctly integrated transgene.

For the disruption of *FLI1* in WT iPSCs, I used TALEN technology in combination with the AAVS1-targeting ZFNs. At the time, the field of TALEN gene editing was still very novel and, while they are much easier to construct than ZFNs[127], their efficiency can be very low due to sensitivity to cytosine methylation, a known mechanism of DNA silencing[148]. The TALEN containing plasmids used for this study had no positive or negative selection marker, so we relied on the ZFNs used above in conjunction with a donor plasmid carrying the puromycin resistance gene. This strategy exploits the hypothesis that if the ZFN and donor plasmids were able to enter the cell and integrate into the AAVS1 locus, the TALEN plasmids more than likely have also entered the cell. Unfortunately, the efficiency of this method was low, with only one puromycin resistant WT iPSC clone containing a TALEN-mutated sequence on one allele of *FLI1*. This heterozygous clone was named FLI1$^{+/-}$ and used in our subsequent megakaryopoiesis studies.

A *FLI1*$^{-/-}$ iPSC line is of interest to our group, as there are no known reports of homozygous loss of *FLI1* in humans, although there is a single report of homozygous inheritance pattern for *FLI1* with a R324W mutation in the DNA-binding domain[85]. Multiple attempts at creating a WT-derived *FLI1*$^{-/-}$ iPSC line using the TALENs above were unsuccessful. Therefore, I employed the CRISPR/Cas9 technology that has since emerged to be a fast and efficient method for gene editing. To address the high off-

target mutations attributed to a tolerance of single base mismatches[149], I used a D10A Cas9 (Cas9n) endonuclease that only creates single-strand breaks[150]. This method reduces off-target effects by requiring a pair of gRNAs binding on opposite strands of DNA, guiding the Cas9n to nick both strands at the intended target site. Because these gRNAs are relatively easy to design, in addition to targeting FLI1, I also generated a pair of gRNAs to target exon 2 of ETS1, hoping to create either iPSCs with the following genotypes: *ETS1*$^{+/-}$, *ETS1*$^{-/-}$, or *FLI1*$^{+/-}$*ETS1*$^{+/-}$. As with TALENs, multiple attempts at gene editing using CRISPR/Cas9n yielded no mutagenesis. These negative results are perhaps due to the low efficiency of the 2 pairs of gRNAs designed. Alternatively, the *FLI1* and *ETS1* genes may be undiscovered essential genes for cellular viability. For further conclusions about efficiency or gene essentiality, more gRNAs targeting other sites on these genes need to be tested. Unfortunately, it was not possible for me to further pursue optimizing this CRISPR/Cas9n protocol as part of my thesis. Moreover, the iPSC lines that were already successfully generated allowed a complete and comprehensive testing of our overall hypothesis that FLI1 expression levels during megakaryopoiesis positively correlates with megakaryocyte maturation, subsequent in vivo thrombopoiesis and released platelet quality.

Tables

Clinical Description	PTSx patient	Reference range
Platelet count	61 – 83 X 10^3/µl	150 – 400 X 10^3/µl
Mean platelet volume	9.1 – 9.8 fl	7.4 – 10.4 fl
White blood cell count	10.7 – 18.8 X 10^3/µl	9.0 – 30.0 X 10^3/µl
Hemoglobin	16.4 – 17.6 g/dl	14.5 – 22.0 g/dl
Other clinical manifestations	Jacobsen's syndrome, hypoplastic left heart syndrome, intrauterine growth restriction and dysmorphic features	

Table 2.1. Hematologic and other data of the patient with PTSx.

Description of the patient diagnosed with PTSx. This patient was a newborn male with a 15.3 Mbp hemizygous deletion at chr11:119,574,140-134,940,416 in hg19. Data were collected prior to the patient expiring at 4 days of life, at which time fibroblasts were obtained and used to create iPSCs.

Target	Source	Reactivity	Label	Company	Catalog number	Usage
SSEA-3	Polyclonal rat	Human	AF 488	Biolegend	330306	Flow cytometry
SSEA-4	Polyclonal mouse	Human	AF 647	Biolegend	330408	Flow cytometry
TRA-1-60	Polyclonal mouse	Human	AF 488	Biolegend	330614	Flow cytometry
TRA-1-81	Polyclonal mouse	Human	AF 647	Biolegend	330706	Flow cytometry

Table 2.2. List of antibodies used for iPSC pluripotency analysis. Description of antibodies used for stem cell surface marker analysis via flow cytometry. Alexa Fluor is abbreviated as AF.

Targeted Gene	gRNA Sequence	Strand Orientation
FLI1	5'-AGGCCGACATGACTGCCTCGGGG-3'	Forward
FLI1	5'-CTCCGTACGCTGAGTCAAAGAGG-3'	Reverse
ETS1	5'-GCATTAAAAGCTACTTTCAGTGG-3'	Forward
ETS1	5'-TTGCTGCTTGGAGTTAATAGTGG-3'	Reverse

Table 2.3. gRNA pairs designed for disruption of FLI1 and ETS1.

One pair of gRNAs was designed to target either *FLI1 or ETS1*, both at exon 2 of each gene. These tandem gRNAs were used with a nickase mutant of Cas9, Cas9n.

Figures

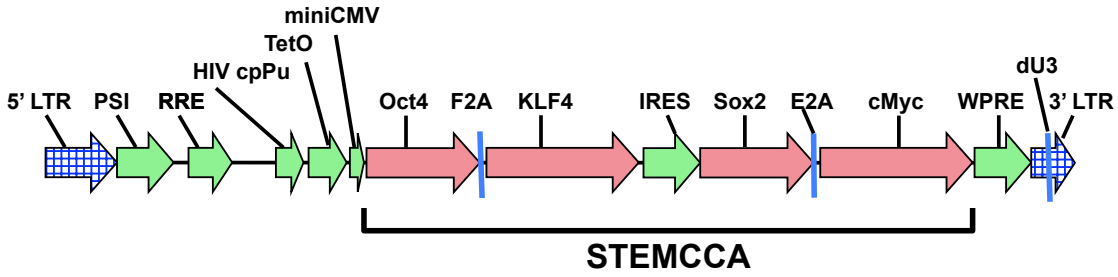

Figure 2.1. Vector schematic of the tetracycline-inducible expression cassette.

iPSC generation using an inducible stem cell cassette pHAGE-Tet-hSTEMCCA. Vector schematic illustrating the pHAGE-Tet-hSTEMCCA plasmid containing the 4 reprograming genes. This stem cell cassette consists of a single multicistronic mRNA transcribed under the control of a tetracycline-inducible TetO-miniCMV promoter. Abbreviations: cpPu, central polypuryne tract; dU3, deleted U3; HIV, human immunodeficiency virus; IRES, internal ribosome entry site; LTR, long terminal repeat; miniCMV, mini-cytomegalovirus; PSI, packaging signal; RRE, rev responsive element; STEMCCA, stem cell cassette; WPRE, woodchuck hepatitis virus post-transcriptional regulatory element.

Adapted from Sommer et al. *Stem Cells*. 2009

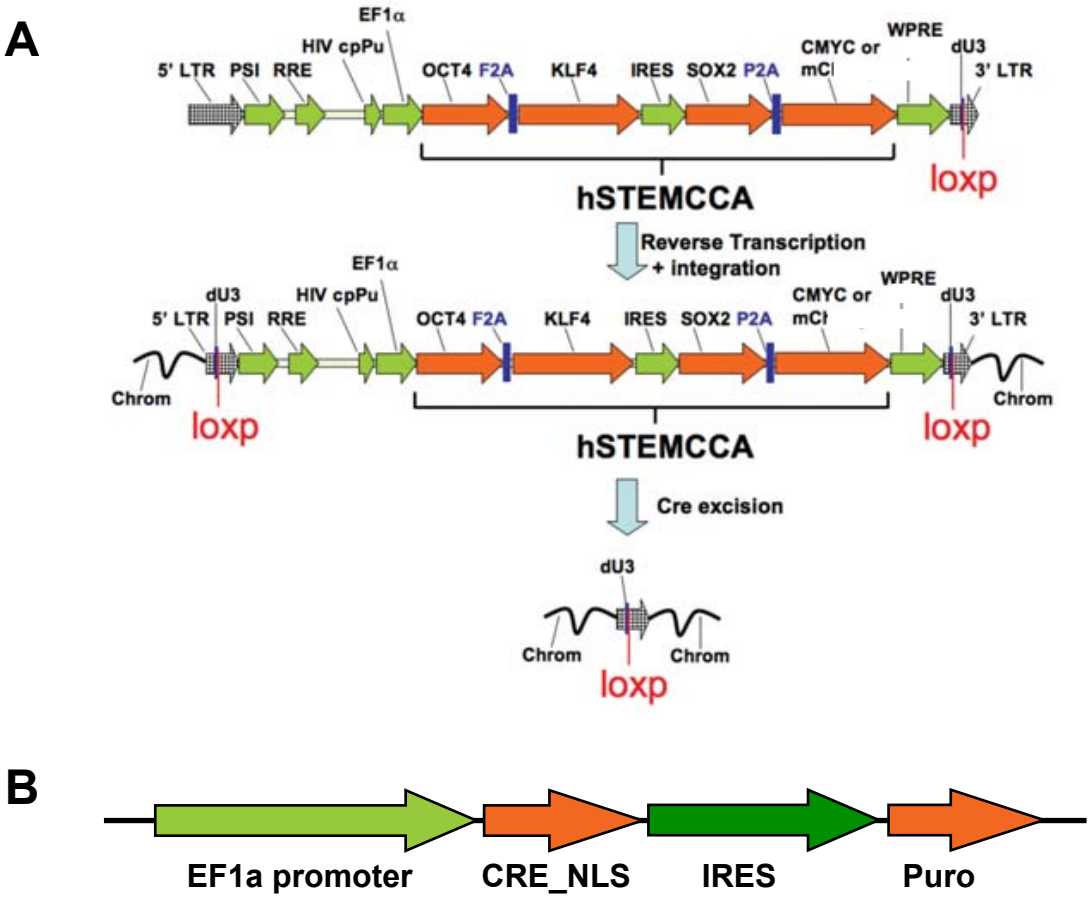

Figure 2.2. Vector schematics of the single excisable lentiviral stem cell reprogramming cassette and Cre-IRES-Puro plasmid.

iPSC generation using a single excisable lentiviral stem cell cassette (hSTEMCCA-loxP). (**A)** Vector schematic illustrating the lentiviral backbone containing human cDNA sequences of the four reprogramming factors. A loxP site inserted in the viral 3'LTR is duplicated to the 5'LTR during viral infection and reverse transcription. (**B)** Vector schematic illustrating the plasmid for transient expression of the genes for Cre recombinase and puromycin resistance. The floxed hSTEMCCA-loxP vector integrated

in the host mammalian genome can be excised on exposure to Cre recombinase Abbreviations: See Figure 2.1 and CMYC, cellular myelocytomatosis oncogene; EF1a, elongation factor 1 alpha constitutive promoter; hSTEMCCA, humanized version of the single lentiviral stem cell cassette; NLS, nuclear localization signal; PRE, post-transcriptional regulatory element; Puro, puromycin resistance gene; RT, reverse transcription.

Adapted from Somers et al. *Stem Cells*. 2010

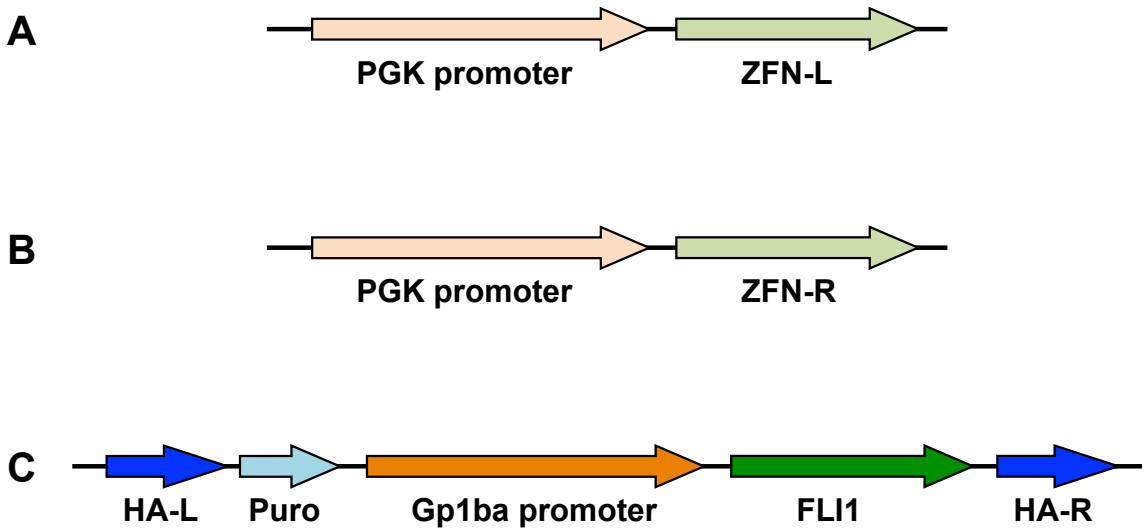

Figure 2.3. Vector schematics the AAVS1-targeting ZFN and donor plasmids for FLI1 overexpression.

Generation of FLI1 overexpression iPSCs. (**A and B)** Vector schematics illustrating the pPGK-AAVS1-ZFNL and pPGK-AAVS1-ZFNR plasmids containing the ZFNs that target the HA-L or HA-R, respectively, on the AAVS1 locus, with both being driven by the constitutive PGK promoter[144]. (**C)** Vector schematic illustrating the AAVS1-Gp1ba-hFLI1 donor plasmid containing homology arms to the AAVS1 locus, puromycin resistance gene and *FLI1* cDNA driven by the *Gp1ba* promoter. Abbreviations: HA, AAVS1 homology arm; L, left; PGK, phosphoglycerate kinase; R, right; ZFN, zinc finger nuclease.

Figure 2.4. *FLI1* cDNA sequence used for transgene overexpression.

ATGGACGGGACTATTAAGGAGGCTCTGTCGGTGGTGAGCGACGACCAGTCCCTCT
TTGACTCAGCGTACGGAGCGGCAGCCCATCTCCCCAAGGCCGACATGACTGCCTC
GGGGAGTCCTGACTACGGGCAGCCCCACAAGATCAACCCCCTCCCACCACAGCAG
GAGTGGATCAATCAGCCAGTGAGGGTCAACGTCAAGCGGGAGTATGACCACATGA
ATGGATCCAGGGAGTCTCCGGTGGACTGCAGCGTTAGCAAATGCAGCAAGCTGGT
GGGCGGAGGCGAGTCCAACCCCATGAACTACAACAGCTATATGGACGAGAAGAAT
GGCCCCCCTCCTCCCAACATGACCACCAACGAGAGGAGAGTCATCGTCCCCGCAG
ACCCCACACTGTGGACACAGGAGCATGTGAGGCAATGGCTGGAGTGGGCCATAAA
GGAGTACAGCTTGATGGAGATCGACACATCCTTTTTCCAGAACATGGATGGCAAGG
AACTGTGTAAAATGAACAAGGAGGACTTCCTCCGCGCCACCACCCTCTACAACACG
GAAGTGCTGTTGTCACACCTCAGTTACCTCAGGGAAAGTTCACTGCTGGCCTATAA
TACAACCTCCCACACCGACCAATCCTCACGATTGAGTGTCAAAGAAGACCCTTCTTA
TGACTCAGTCAGAAGAGGAGCTTGGGGCAATAACATGAATTCTGGCCTCAACAAAA
GTCCTCCCCTTGGAGGGGCACAAACGATCAGTAAGAATACAGAGCAACGGCCCCA
GCCAGATCCGTATCAGATCCTGGGCCCGACCAGCAGTCGCCTAGCCAACCCTGGA
AGCGGGCAGATCCAGCTGTGGCAATTCCTCCTGGAGCTGCTCTCCGACAGCGCCA
ACGCCAGCTGTATCACCTGGGAGGGGACCAACGGGGAGTTCAAAATGACGGACCC
CGATGAGGTGGCCAGGCGCTGGGGCGAGCGGAAAAGCAAGCCCAACATGAATTA
CGACAAGCTGAGCCGGGCCCTCCGTTATTACTATGATAAAAACATTATGACCAAAG
TGCACGGCAAAAGATATGCTTACAAATTTGACTTCCACGGCATTGCCCAGGCTCTG
CAGCCACATCCGACCGAGTCGTCCATGTACAAGTACCCTTCTGACATCTCCTACAT
GCCTTCCTACCATGCCCACCAGCAGAAGGTGAACTTTGTCCCTCCCCATCCATCCT
CCATGCCTGTCACTTCCTCCAGCTTCTTTGGAGCCGCATCACAATACTGGACCTCC
CCCACGGGGGGAATCTACCCCAACCCCAACGTCCCCCGCCATCCTAACACCCACG
TGCCTTCACACTTAGGCAGCTACTACTAG

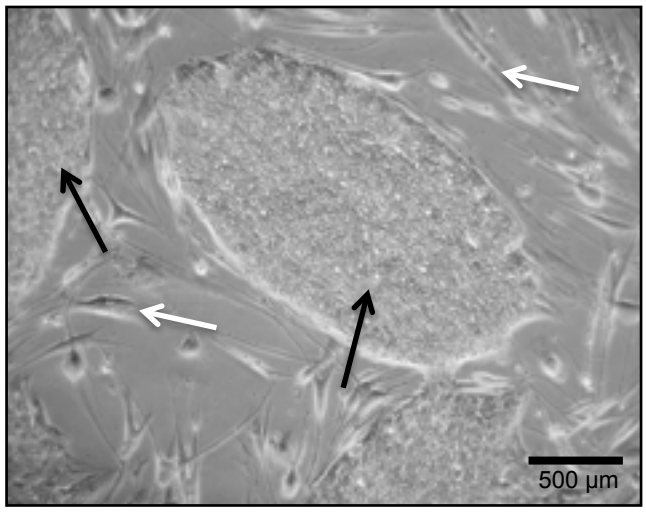

Figure 2.5. iPSC morphology.

Representative iPSC colony depicting typical morphology of the clones selected for further cell culture. Black arrows indicate iPSC colonies and white arrows indicate irradiated mouse embryonic fibroblast feeder layer. Brightfield image taken at 40X using a Zeiss Axio Observer 7.1 microscope.

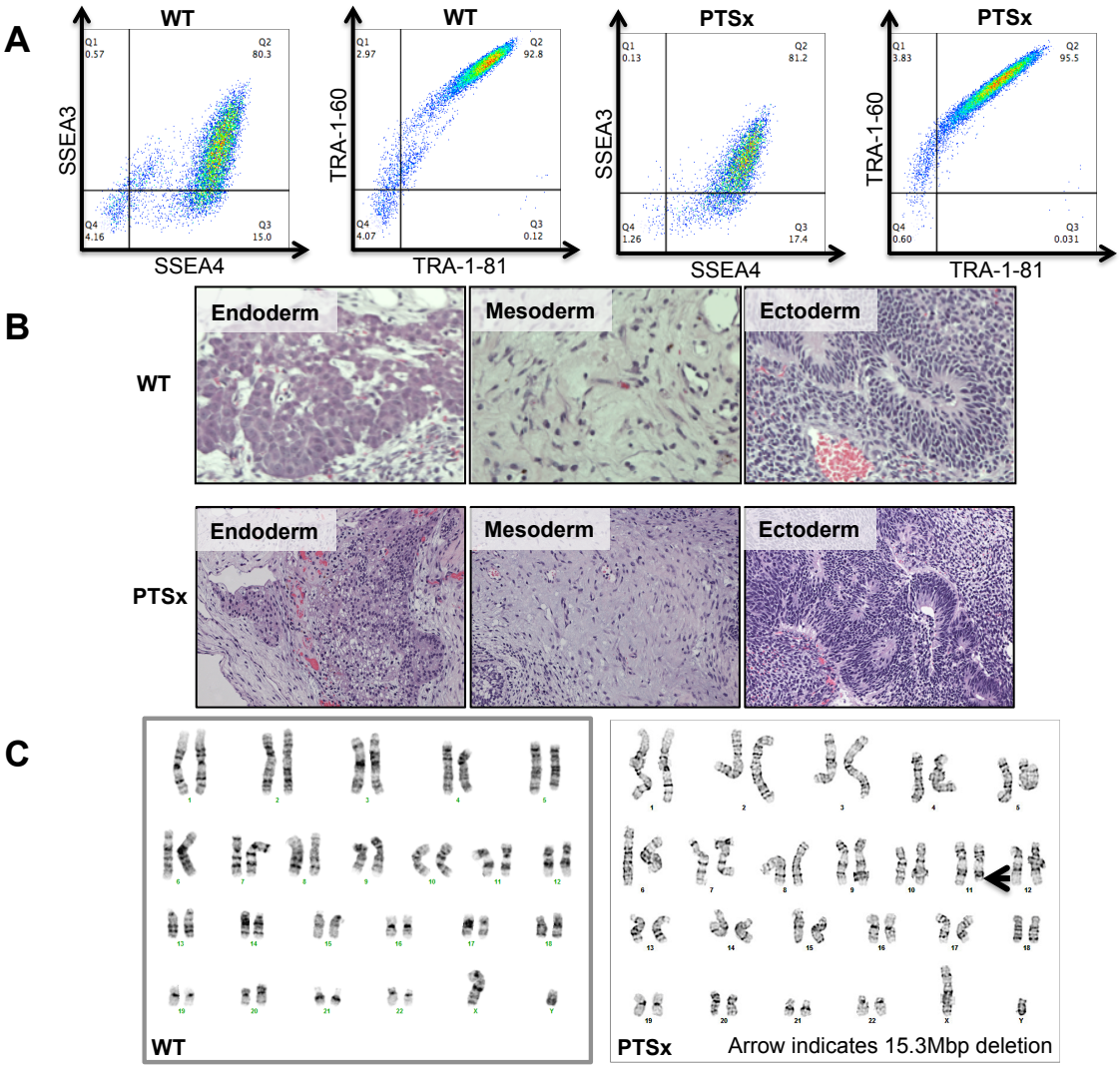

Figure 2.6. Confirmation of successful reprogramming of WT and PTSx cells.

Pluripotency analysis of the two iPSC lines generated. (**A)** Flow cytometry data show stem cell surface markers SSEA3, SSEA4, TRA-1-60 and TRA-1-81 are concurrently expressed at a high level for both WT and PTSx iPSCs. (**B)** Teratoma tumor immunohistochemistry sections show evidence of endoderm, mesoderm and ectoderm cell differentiation in SCID mice. (**C)** Karyotype analysis shows no chromosomal

abnormalities after iPSC reprogramming. Abbreviations: SSEA, stage-specific embryonic antigen; TRA, tumor-related antigen.

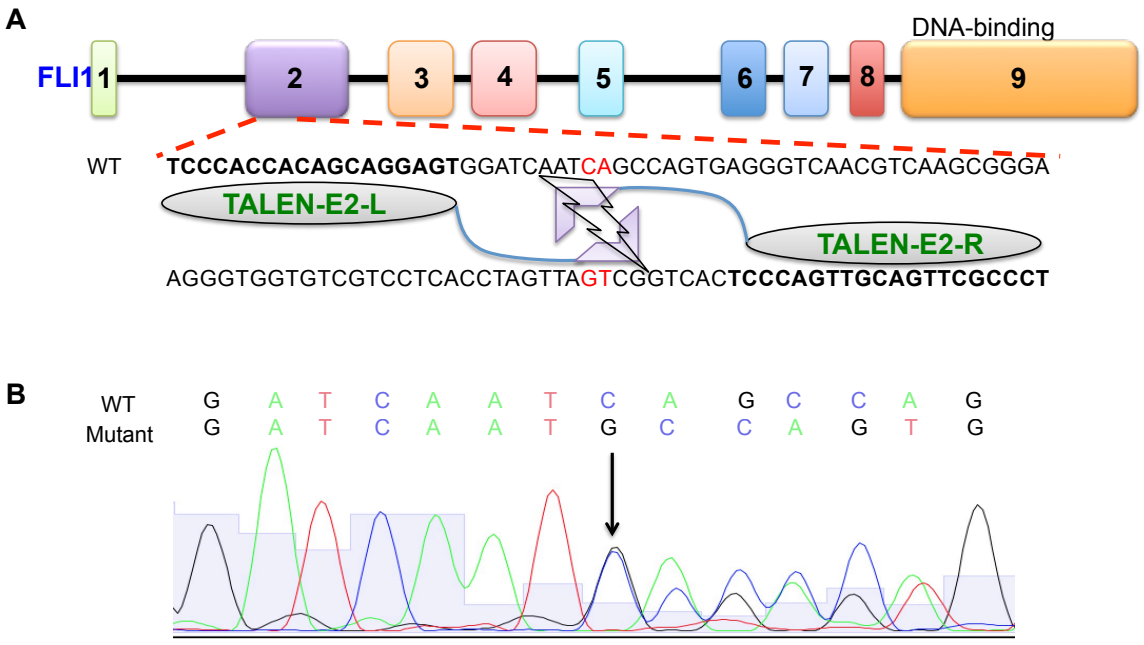

Figure 2.7. Using TALENs to mutate *FLI1*.

Generation of the FLI1$^{+/-}$ iPSC line using TALENs targeting *FLI1* exon 2. (**A)** Schematic of the TALEN pair targeting a site on exon 2 of *FLI1* (TALEN-E2-L and TALEN-E2-R). (**B)** Chromatograph depicting a heterozygous 2-nucleotide deletion (shown in red in Figure 2.6A) confirmed by sequencing. Abbreviations: FLI1, Friend Leukemia Virus Integration 1; TALEN-E2-L, transcription activator like effector nuclease targeting FLI1 exon 2, left strand; TALEN-E2-R, transcription activator like effector nuclease targeting FLI1 exon 2, right strand.

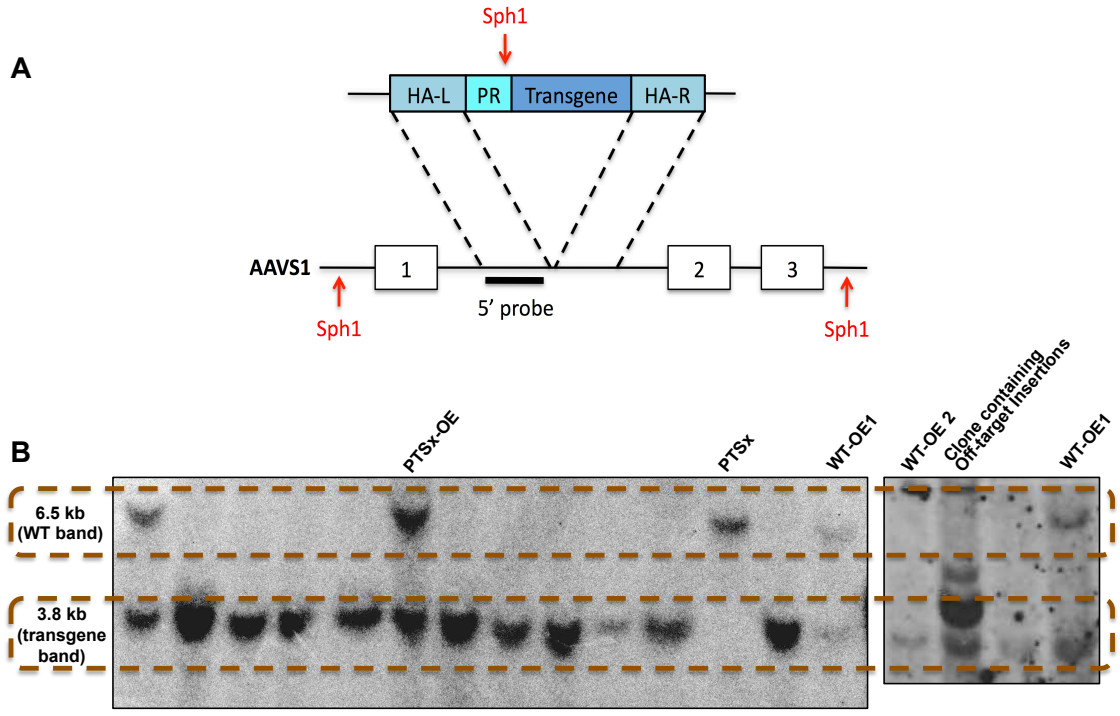

Figure 2.8. Genomic DNA analysis for the confirmation of correct *GP1ba-FLI1* transgene insertion.

Southern Blot analysis of WT and PTSx iPSC clones generated after AAVS1-targeted *FLI1* overexpression. (**A)** Schematic illustrating the Southern Blot assay experimental set up. The 5' ^{32}P probe binds to an endogenous region in the AAVS1 locus, flanked by two SphI restriction sites. When the transgene had been successfully inserted at the right position, a new SphI restriction site on the plasmid DNA will allow for a smaller DNA fragment. (**B)** Southern Blot membrane image of the various iPSC lines generated post-SphI digestion. The 6.5 kb long gDNA band is endogenous allele without targeting, and runs slower than the 3.8 kb transgene band that represents a targeted allele. Abbreviations: See Figure 2.3 and PTSx, Paris Trousseau syndrome patient iPSC line; PTSx-OE, PTSx iPSC line with one allele targeted; WT-OE1, normal control WT iPSC

line with one allele targeted; WT-OE2, normal control WT iPSC line with both alleles targeted.

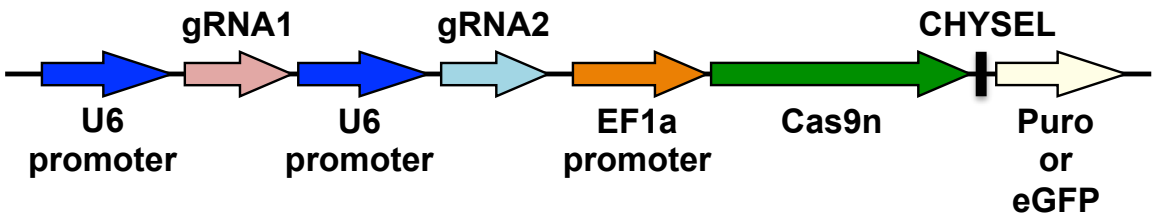

Figure 2.9. Vector schematic of CRISPR/Cas9n.

Schematic illustrating the single CRISPR/Cas9n vector containing the 2 gRNAs, the nickase Cas9n and either a puromycin resistance or eGFP selection gene. Abbreviations: Same as Figures 2.2 and 2.3 and CHYSEL, cis-acting hydrolase element; eGFP, enhanced green fluorescent protein.

CHAPTER 3 – In vitro analysis of FLI1-modified iPSC-derived megakaryocytes and platelets

Abstract

We studied induced pluripotent stem cell (iPSC)-derived megakaryocytes (iMegs) to better understand clinical PTSx and *FLI1* mutation disorders using iPSC lines generated from a PTSx patient and from a targeted heterozygous *FLI1* knockout ($FLI1^{+/-}$) in a control line. PTSx and $FLI1^{+/-}$ iMegs replicate many of the megakaryocyte and platelet features previously described with a decrease in iMeg yield, cell size and ploidy. These iMegs had lower levels of mature megakaryocyte surface marker expression as well as increased levels of markers of in vitro iMeg injury. We noted that the closely-linked ETS Proto-Oncogene 1 (ETS1) and ETS Variant 6 (ETV6) TFs have increased and decreased expression, respectively, in FLI1-deficient iMegs. The inverse *FLI1/ETS1* levels suggest that FLI1 negatively regulates ETS1 in megakaryopoiesis. Finally, we examined whether FLI1 overexpression would affect megakaryopoiesis and thrombopoiesis. We found an increased yield of non-injured in vitro iMegs as well as higher ploidy and cell size. These studies confirm *FLI1* heterozygosity results in pleiotropic defects similar to those noted with other critical megakaryocyte-specific TFs, but that its overexpression does not alter megakaryopoiesis, which differs from that seen with GATA1 overexpression in a murine setting.

Introduction

The current literature on megakaryocyte and platelet defects associated with PTSx, and also a growing number of reports of *FLI1* mutations, provide clinical descriptions to the degree of the macrothrombocytopenia, platelet ultrastructure analysis and findings of immature micromegakaryocytes either in bone marrow or cultured progenitors[78,79,151]. A next generation sequencing study done on 13 families with inherited platelet disorder that found 3 different *FLI1* mutations in the DNA-binding domain[84] included platelet aggregation analysis of one of the *FLI1*-deficient families. The single report of a homozygous *FLI1* mutation causing PTSx-like platelet features presents data on a defect in collagen-induced platelet aggregation as well as on decreased platelet protein expression of GPVI, GPIX and GPIIb (or αIIb). Both reports used the human embryonic kidney cell line HEK293 to test the TF activity of the mutated FLI1 proteins.

These studies, while informative and highlight the clinical implications of *FLI1* influence on megakaryocytes and platelets, provide only limited insights into the cellular defects and do not provide comparison analyses to a common genotypic control. To date, there had only been one report of in vitro analysis of *FLI1* biology on megakaryopoiesis: a PTSx primary $CD34^+$ cell study on 2 patients[82]. It is not surprising that there are not more detailed reports on PTSx and *FLI1* mutation megakaryocytes and platelets. These patients are rare and harvesting enough cells to experiment on is a challenge. We approached this challenge with the use of iMegs.

Our group had previously used iPSCs to study iMegs in the setting of Glanzmann Thrombasthenia (GT)[115], a rare autosomal recessive disease resulting in the lack of

functional platelet integrin αIIbβ3[152]. GT patients present with a bleeding diathesis due to the integral role of αIIbβ3 in platelet aggregation[153]. By using the described murine *Gp1ba* promoter to drive expression of the αIIb transgene, iMeg surface expression of αIIbβ3 was restored in iPSC lines generated from two GT patients with mutations in αIIb. These gene-corrected GT iPSC lines showed functional αIIbβ3 biological activity upon activation of iMegs by a known platelet activator via the collagen receptor GPVI, convulxin[154]. With this proof-of-principle study in mind, we used the same system to overexpress *FLI1* in PTSx patient-derived and WT iPSCs, and created WT iPSCs that either lack one functional copy of *FLI1* or express extra copies of *FLI1*. This strategy allows for creation of iPSC lines from the same genetic background with varying levels of FLI1 expression. This Chapter outlines the use of the described FLI1-modified iPSC lines to study megakaryopoiesis and in vitro characteristics of the resulting megakaryocytes. In vivo studies of these iMegs are described in Chapter 4.

Methods

Differentiation of iPSCs into megakaryocytes

iPSC lines were maintained in iPSC medium with an irMEF feeder layer, as described in Chapter 2. Before differentiation into HPCs, iPSCs were transitioned to a feeder-free system in mTESR-1 medium (Stem Cell Technologies, Vancouver, Canada) for at least 4 passages. Confluent cells were gently detached using 1 U dispase (Stem Cell Technologies) per 35-mm culture dish for 6-8 minutes at 37°C then washed 2X with RT DMEM/F12. They were then mechanically scraped off and centrifuged at 1200 rpm

for 3 minutes. Cells were then resuspended in RT mTESR-1 medium and plated at a 1:3 to 1:9 ratio onto plates pre-coated with Matrigel hESC-qualified matrix (Corning).

Hematopoietic differentiation of iPSCs to HPCs was performed as previously described[115,143]. Differentiation starts on Day 0 by feeding iPSCs plated the day before (Day -1) with 4 ml per 35-mm dish with Roswell Park Memorial Institute medium (RPMI, Gibco) supplemented with 1mM L-glutamine (Sigma-Aldrich), 50 µg/ml ascorbic acid (Wako Chemicals, Richmond, VA), 3 µl/ml monothiolglycerol (MTG, Sigma-Aldrich), 5 ng/ml Bone Morphogenic Protein 4 (BMP4, Stemgent, Cambridge, MA), 50 ng/ml Vascular Endothelial Growth Factor (VEGF, R&D Systems) and 1 µM Glycogen Synthase Kinase 3 inhibitor CHIR (Tocris). On Day 2, cells were washed once with RPMI and fed with 4 ml per 35-mm dish with 1:1 RPMI and StemPro-34 serum-free medium (SP34, Gibco) supplemented with 1mM L-glutamine, 50 µg/ml ascorbic acid, 3 µl/ml MTG, 5 ng/ml BMP4, 50 ng/ml VEGF and 20 ng/ml bFGF. On Day 4, cells were fed with 4 ml per 35-mm dish with SP34 supplemented with 1mM L-glutamine, 50 µg/ml ascorbic acid, 3 µl/ml MTG, 15 ng/ml VEGF and 5 ng/ml bFGF. On Day 6, cells were washed once with IMDM and fed with 3 ml per 35-mm dish with serum-free differentiation medium (SFD: 75% IMDM; 1% B-27 and 0.5% N-2 supplements, Invitrogen; 1 mM (1%) L-glutamine; 0.5% BSA; and 22% Hams F12 medium, Corning) containing 50 µg/ml ascorbic acid, 3 µl/ml MTG, 50 ng/ml VEGF, 100 ng/ml bFGF, 10 ng/ml IL-6, 50 ng/ml TPO (R&D Systems), 25 ng/ml Fms-Like Tyrosine Kinase 3 Ligand (FLT-3L, Gibco) and 25 ng/ml Stem Cell Factor (SCF, Gibco). HPCs in suspension were collected from the culture dish supernatant at Days 7 or 8.

Differentiation of HPCs into iMegs was as previously described[143]. Collected HPCs at Days 7 or 8 of differentiation were cultured in SFD medium supplemented with

50 µg/ml ascorbic acid, 3 µl/ml MTG, 25 ng/ml SCF and 100 ng/ml TPO (Day 0 of iMeg differentiation). This medium was changed on Day 3 to SFD medium supplemented with 50 µg/ml ascorbic acid, 3 µl/ml MTG, 1 ng/ml SCF and 100 ng/ml TPO, 10 ng/ml IL-6 and 13.5 ng/ml IL-9. iMegs were collected on Day 5 for in vitro analysis.

Flow cytometry analysis of iMegs and other cells

iMegs and in vitro-derived platelet particles were stained as described in Chapter 2. Data were collected with a BD FACSCanto II and analyzed using FlowJo software. Antibodies used in this study for FACS analysis and other studies are detailed in Table 3.1. Ploidy was assessed via flow cytometry after incubating live cells with Vibrant DyeCycle Green DNA dye (Thermo Fisher Scientific) at 37°C for 30 minutes.

Analysis of megakaryocyte mRNA and protein levels

iMegs were selected using the AutoMACS Pro (Miltenyi, Bergisch Gladbach, Germany) after staining with a primary phycoerythrin (PE)-labeled, anti-human CD41a antibody (BD Biosciences, Table 3.1) and secondary anti-PE microbeads (Miltenyi). RNA isolation was performed using the RNeasy isolation kit (Qiagen), after which cDNA synthesis was performed using the high capacity cDNA synthesis kit (Life Technologies, Carlsbad, CA). Taqman probes for *GAPDH* (Hs02758991_g1), *FLI1* (Hs00956711_m1), *ETS1* (Hs00428293_m1), *ETV6 (*Hs00231101_m1), *RUNX1 (*Hs02558380_s1), *ITGA2B* (Hs01116228_m1), *GP9* (Hs01040883_g1), *PF4* (Hs00427220_g1), and *MPL* (Hs00180489_m1) were used for quantitative real-time PCR (qRT-PCR) on a 7900HT

Fast Real-Time PCR System (Applied Biosystems, Foster City, CA). Data were analyzed using the $2^{-\Delta\Delta CT}$ method[155].

Western Blot analyses on CD41a-selected iMegs were performed after protein extraction using the NE-PER Nuclear and Cytoplasmic Extraction Kit (Thermo Scientific, Waltham, MA). Lysate protein concentrations were then determined using the bicinchoninic acid protein assay kit (Thermo Scientific). NuPAGE LDS Sample Buffer (Invitrogen), containing lithium dodecyl sulfate at pH 8.4 and 5% added β-mercaptoethanol (Sigma-Aldrich), was mixed with protein samples and loaded into 4-12% NuPAGE Bis-Tris precast gels (Invitrogen) under reducing conditions. Proteins were separated by gel electrophoresis and transferred onto polyvinylidene fluoride membranes with the iBlot Dry Blotting System (Invitrogen). Membranes were blocked in 5% nonfat dry milk in PBS with 0.01% Tween 20 (PBST, BioRad, Hercules, CA) for 1 hour at RT, followed by primary antibody incubation in 1% nonfat dry milk in PBST overnight at 4°C. The next day, membranes were washed with PBST for 15 minutes 3X to remove excess antibody, then incubated with the appropriate secondary antibody conjugated to horseradish peroxidase at RT for 1 hour. After washing 3X with PBST, membranes were developed using the SuperSignal West Pico Chemiiluminescent Substrate detection system (Thermo Scientific). Antibodies shown in Table 3.1 were used at the indicated volume/volume (v/v) dilutions: FLI1 (1:2000), PF4 (1:15,000) and TATA-box binding protein (1:2000). Secondary antibodies were horseradish peroxidase-goat anti-rabbit IgG (1:10,000) and horseradish peroxidase-goat anti-mouse IgG (1:10,000).

Hematopoietic colony-forming assays and liquid expansion of HPCs to iMegs

Single cell HPCs collected from the iPSC differentiation medium were used in methylcellulose and Megacult colony assays (Stem Cell Technologies) according to manufacturer instructions. Flow cytometry for CD41a and CD235a surface markers were used to determine purity and absolute number of HPCs. Expansion to iMegs was performed by plating 5 X 10^5 HPCs per 35-mm well in SFD medium, as described above. After 5 days, the quality and absolute number of iMegs were calculated from the percentage of cells expressing surface CD41a, CD42a, CD42b and annexin V via flow cytometry.

Transmission electron microscopy (TEM) analysis of iMegs

iMeg samples for ultrastructure analysis were fixed with 2.5% glutaraldehyde, 2.0% paraformaldehyde in 0.1 M sodium cacodylate buffer, pH 7.4, overnight at 4°C. Samples were post-fixed in 2.0% osmium tetroxide for 1 hour at room temperature, and washed in the same cacodylate buffer followed by deionized H2O. After dehydration through a graded ethanol series, the tissue was infiltrated and embedded in EMbed-812 (Electron Microscopy Sciences) at the University of Pennsylvania Electron Microscopy Resource Laboratory (Philadelphia, PA). Thin sections were stained with uranyl acetate and lead citrate and examined with a JEOL 1010 electron microscope fitted with a Hamamatsu digital camera and AMT Advantage image capture software.

Statistical analysis

Statistical analysis was performed using one-way ANOVA and data was reported as mean ± 1 standard error of the mean (SEM) using the GraphPad Prism software version 6.00 for Mac (GraphPad Software, La Jolla, CA). Differences were considered significant when the *P* value was less than 0.05.

Study approval

Animal studies and human tissue sampling were done in accordance with CHOP's Institutional Animal Care and Use Committee and Institutional Review Board, respectively.

Results

Establishment and characterization of iMegs with differing levels of FLI1

To evaluate whether the megakaryocyte and platelet defects observed in patients with PTSx are specifically due to FLI1 expression levels, patient-specific and gene-edited iPSC lines were created as described in Chapter 2 and summarized in Table 3.2. Briefly, a normal control iPSC line, labeled WT, was used to create three additional isogenic lines: a single allele insertion of *FLI1* transgene at the AAVS1 locus (WT-OE1), a double allele insertion of *FLI1* transgene at the AAVS1 locus (WT-OE2) and a heterozygous *FLI1* mutation ($FLI1^{+/-}$) in exon 2 resulting in a markedly truncated protein with 53 normal N-terminal amino acids followed by the frameshift mutation containing 10 amino acids. The endogenous protein is 452 amino acids long. A PTSx patient iPSC was also used to generate a PTSx-OE line that had a single insertion of *FLI1* transgene

at the AAVS1 locus. These 6 iPSC lines were then differentiated along the hematopoietic lineage into HPCs and eventually to iMegs.

The expected differences in *FLI1* mRNA expression levels were confirmed in iMegs derived from these different lines (Figure 3.1A). During the 5-day expansion of HPCs to iMegs in the OE lines, *FLI1* mRNA expression was increased compared to their respective parental lines. Although the *Gp1ba* promoter is a late megakaryocyte promoter, we have previously shown that it is also active in the iPSC-derived progenitor cell[115]. *FLI1* mRNA expression in the PTSx and FLI1$^{+/-}$ lines started out at approximately half of WT on day 1, but gradually increased as differentiation progressed. FLI1 protein levels measured on Day 5 of differentiation in the various lines were consistent with the genotypes of these lines (Figure 3.1B).

In addition to *FLI1*, mRNA levels of TFs known to be important in megakaryopoiesis (*ETS1*, *ETV6* and *RUNX1*) (Figure 3.2) and several megakaryocyte-specific genes *(MPL, MYH10, GP9*, *ITGA2B,* and *PF4*) (Figures 3.3 and 3.4A) were also examined throughout the 5 days of iMeg expansion. After day 1, *ETS1* levels were inversely related with the level of *FLI1* in the developing megakaryocytes. *ETS1* is physically close to *FLI1*[80] and is deleted along with *FLI1* in PTSx. There has been speculation as to whether the PTSx phenotype is related to haploinsufficiency of *ETS1* as well as *FLI1*[81]. However, in spite of having only one copy of *ETS1*, PTSx megakaryocytes have an excess rather than a deficiency of *ETS1* TF. Primary megakaryocyte ChIP-Seq data[156] demonstrated a FLI1-binding site ~100 kb downstream of *ETS1 (*Figure 3.3A). Markers of active enhancers, including H3K4me1 and H3K27ac[157], also localized to this site[158]. This region was annotated by ChromHMM as 'enhancer' chromatin in several cell types[159]. Together, this pattern could indicate a

regulatory mechanism by which FLI1 binding mediates suppression of *ETS1* (Figure 3.3B).

The other TFs and megakaryocyte-specific proteins either correlated with or showed no clear relationship to *FLI1* mRNA expression levels. A correlative relationship in mRNA levels was seen for *ETV6* (Figure 3.2), another ETS family member whose haploinsufficiency also results in a quantitative platelet disorder[160]. *MPL* mRNA levels also correlated with *FLI1* mRNA levels (Figures 3.1A and 3.4A). Surface MPL protein levels in iMegs at days 2 to 5 of differentiation (Figure 3.4B) were decreased in the FLI1$^{+/-}$ and PTSX lines, consistent with reports of decreased MPL after FLI1 mutation[85] and of *MPL* as a direct target gene of FLI1[161]. *MYH10* transcript was increased during iMeg differentiation in the FLI1-low lines, reflecting reports of increased MYH10, silenced during normal megakaryocyte polyploidization and maturation[162], in PTSx patient platelets[84,85,163]. Levels of PF4 protein were comparable in all lines (Figure 3.4B). Levels of *RUNX1*, *GP9*, *ITGA2B* and *PF4* transcripts were normal. *GP9*, *ITGA2B* and *PF4* have all been reported as direct targets of FLI1[161,164], but also are increased as a result of ETS1 overexpression during megakaryopoiesis[20]. Perhaps the unexpectedly high *ETS1* levels compensate for the decreased *FLI1* levels for these genes.

Effect of FLI1 on megakaryocyte and other lineage potential

To assess the effect of *FLI1* on megakaryocyte clonogenic potential, a hematopoietic colony-forming assay in a collagen-based culture system[165] was used to analyze the yield of large and small megakaryocyte colony-forming units (CFU-MKs). In this system, large CFU-MKs were defined as colonies containing ≥50 cells and small

CFU-MKs as colonies containing <50 cells (Figure 3.5A). No large CFU-MKs were generated from PTSx and FLI1$^{+/-}$ progenitors, whereas the level of small CFU-MKs from these lines were ~10% and ~20% of WT, respectively. The WT-OE1 and WT-OE2 lines had more large CFU-MKs, and significantly more small CFU-MKs compared to WT. These findings suggest that decreased expression of FLI1 affects megakaryocyte potential, especially large CFU-MK potential. Conversely, the overexpression of FLI1 in both WT and PTSx lines either increased the number of small CFU-MKs or the numbers were comparable to the parental lines. PTSx-OE large CFU-MKs were decreased compared to WT, but small CFU-MK numbers were comparable.

The relative expansion of iMegs from HPCs in liquid culture was analyzed as another approach to quantitatively study the effect of FLI1 levels on megakaryopoiesis. The differentiation and expansion of HPCs to iMegs yielded results comparable to colony formation data (Figure 3.5B): The PTSx and FLI1$^{+/-}$ progenitors yielded fewer iMegs compared to WT. HPCs from the WT-OE1 and WT-OE2 lines yielded high expansion numbers of ~150% (P = 0.08) and ~230% (P < 0.01) per HPC, respectively, compared to WT. The PTSx-OE HPCs yielded more iMegs than parent PTSx HPCs, but to only 63% of WT. Perhaps here, the genotypic background of the PTSx patient differed from the WT individual affecting maximal iMegs per HPC.

The effect of FLI1 levels on myeloid and erythroid progenitor potential was also analyzed (Figure 3.6). Myeloid progenitor potential was comparable amongst all lines, while PTSx and FLI1$^{+/-}$ progenitors were biased toward the erythroid blast-forming unit (BFU-E) and CFU-E colonies. The BFU-E and CFU-E progenitor potential of WT-OE1, WT-OE2 and PTSx-OE HPCs was comparable or less than WT. These data support the

known role of *FLI1* driving the megakaryocyte-erythroid progenitor towards the megakaryocyte lineage[48,166].

Qualitative characterization of the effects of FLI1 on iMegs

We next examined whether the iMegs obtained from the iPSC lines differed qualitatively as well as quantitatively. Flow cytometry analyses of megakaryocyte-specific surface markers were performed for CD41a (GPIIb/IIIa or αIIbβ3), an early marker of the megakaryocyte lineage[167]; CD42a (GPIX), a marker of megakaryocyte maturation[168]; and CD42b (GPIX/GPIbα), an indicator of megakaryocyte injury due to cleavage and removal of the extracellular glycocalicin domain of GPIbα[169]. A significantly lower percentage of PTSx and FLI1$^{+/-}$ iMegs expressed CD41a, CD42a and CD42b compared to WT (Figure 3.7A). Slightly higher percentage of WT-OE1 and WT-OE2 iMegs expressed CD41a, CD42a and CD42b compared to WT, while PTSx-OE iMegs were comparable to WT. These data suggest that the maturation of PTSx and FLI1$^{+/-}$ iMegs may be impaired by FLI1 heterozygous deficiency and corrected with FLI1 overexpression.

Previous studies from our group have shown that in vitro-released platelets have poor in vitro and in vivo functionality and short in vivo half-lives due to faster clearance of CD42b^{-} particles in the mouse circulation[170]. In vitro-derived platelet particles, corresponding in size to human donor platelets, from iMeg cultures were analyzed for surface markers for CD41a, annexin V, and CD42b. Between 40-60% of the in vitro-derived platelet particles from all lines were CD41^{+}, but low percentages are viable annexin V^{-} particles (Figure 3.7B), suggesting that many of the CD41^{+} particles may be

activated or injured. The low percentage of $CD42a^{+}CD42b^{+}$ platelet particles supports that the vast majority (>85%) of in vitro platelet-like particles from all cell lines were injured, having CD42b cleaved (Figure 3.7B).

Besides expressing megakaryocyte-specific surface markers, another indication of maturing megakaryocytes is nuclear endoreduplication[171]. Overall, WT iMegs have low ploidy compared to bone marrow mobilized $CD34^{+}$-derived megakaryocytes[170]. However, we saw a trend towards a decrease in 4N and >4N nuclei in the FLI1-low iMegs and an increase in 4N and >4N in WT-OE1 and WT-OE2 iMegs relative to WT iMegs (Figure 3.8).

As previously reported, up to 15% of PTSx platelets, but not bone marrow megakaryocytes, have fused, giant alpha granules on electron micrographs[78,79,151]. Similar platelet giant granules were observed from a family with an autosomal recessive FLI1 mutation[85]. These previous reports of PTSx patient cells also show immature micromegakaryocytes present in the bone marrow. Transmission electron microscopy (TEM) images of $FLI1^{+/-}$ iMegs showed smaller cells when compared with the WT iMegs (Table 3.3). PTSx iMegs also trended towards being small compared to WT. This correlates with previous findings of increased micromegakaryocytes present in PTSx patient bone-marrow samples[78,79]. Conversely, TEM micrographs of WT-OE2 iMegs contained larger cells, while the size of PTSx-OE iMegs were comparable to WT iMegs. Granules and open canalicular systems were observed in all samples, but no observable giant granules were found in either the PTSx or $FLI1^{+/-}$ iMegs (Figure 3.9).

Discussion

These in vitro studies of iPSC-derived megakaryocyte and platelet products provide more in depth as well as novel analyses of the influences of *FLI1* on megakaryopoiesis than previously reported. While these cells do not completely replicate many of the primary $CD34^{+}$-derived megakaryocyte and platelet cellular characteristics like high ploidy and high platelet release, they do allow for generation of an unlimited amount of megakaryocytes and platelets for maturational, quantitative and qualitative analyses. Furthermore, these studies can be well-controlled by using iPSC lines of the same genetic background, as we did with the WT- and PTSx-derived iPSC lines with low or high *FLI1* expression.

With the PTSx and $FLI1^{+/-}$ iPSC lines, we can accurately model the PTSx and FLI1 mutation platelet disorders while generating enough megakaryocytes and platelets in vitro for detailed analyses. With this advantage, we show the PTSx and $FLI1^{+/-}$ iMegs and platelet particles having similar defective features found in reports of primary PTSx patient cells. HPC cells could not differentiate into megakaryocytes as effectively as normal cells (Figure 3.5), and the ones that could mature to iMegs are primarily damaged in vitro (Figure 3.7). These iMegs also have lower ploidy and are generally smaller in size. For the first time, we show that $FLI1^{+/-}$ megakaryocytes have more than normal *ETS1* mRNA levels, while PTSx have normal levels in spite of missing a copy of the *ETS1* gene. Protein analysis was not done due to time constraints and issues with antibodies targeting multiple isoforms of this protein. Further studies to evaluate the role of FLI1 on *ETS1* transcription need to be performed to draw conclusions.

Our megakaryocyte-specific approach to overexpression of *FLI1* limits the scope of this TF's influence to mainly the megakaryocyte lineage, with minimal effects on the erythroid cells due to the low activity of our murine *Gp1ba* promoter at the progenitor stage as shown previously[115]. There is one previous report of in vitro overexpression of FLI1 in PTSx patient cells[82], yet the constitutive lentiviral expression strategy may be driving already committed blood cells to transdifferentiate into megakaryocytes, not necessarily correcting the PTSx megakaryocyte defects. With our PTSx-OE iPSC line, we report rescue of PTSx cells during megakaryocyte maturation from HPCs (Figure 3.5); and restoration of megakaryocyte surface marker expression (Figure 3.7), ploidy (Figure 3.8) and size (Table 3.3) to normal levels. As expected, erythroid differentiation was slightly decreased while myeloid differentiation was unaffected by increased FLI1 (Figure 3.6). These data, along with the FLI1$^{+/-}$ iMeg data, support the conclusion that *FLI1* is the sole TF responsible for the PTSx and heterozygous dysmegakaryopoiesis. However, since the in vitro platelet particles from all lines are of poor quality, it is still unclear whether the platelets are negatively affected. This area was addressed via in vivo studies.

On the other hand, overexpression of FLI1 in the normal WT iPSC line generated megakaryocytes that exhibited improved characteristics. Both the WT-OE1 and WT-OE2 lines had iMegs that mature from the HPC stage more efficiently (Figure 3.5). They also expressed higher levels of megakaryocyte surface markers and an increased ability to retain CD42b (Figure 3.7), indicating they were less prone to in vitro injury and were healthier cells overall. DNA analysis shows a trend towards higher level of polyploidization (Figure 3.8), a sign of mature megakaryocytes[171]. Finally, TEM imaging

of individual iMegs show more cells that have larger diameters compared to WT iMegs (Table 3.3).

Because these are in vitro cultures with highly defined growing conditions and media, the results may not be replicated in an in vivo setting. Further studies to evaluate the in vivo thrombopoiesis of these gene-edited iMegs and the resulting in vivo-generated platelets (iPlts) from these iMegs could shed more light on the biology of *FLI1*. We address this issue in the next chapter by infusing immunodeficient mice with iMegs and studying in vivo thrombopoiesis over time. Functional characteristics of the resulting iPlts were also evaluated.

Tables

Target	Source	Reactivity	Label	Company	Catalog number	Usage
CD41a	Monoclonal mouse	Human	APC	BD Biosciences	559777	Flow cytometry
CD41a	Monoclonal mouse	Human	PE	BD Biosciences	555467	Flow cytometry
CD42a	Monoclonal mouse	Human	BV421	BD Biosciences	565444	Flow cytometry
CD42b	Monoclonal mouse	Human	APC	BD Biosciences	551061	Flow cytometry
CD42b	Monoclonal mouse	Human	PE	BD Biosciences	555473	Flow cytometry
CD235a	Monoclonal mouse	Human	APC	BD Biosciences	551336	Flow cytometry
Annexin V	Bacteria	Human	FITC	BD Biosciences	556420	Flow cytometry
CD110	Monoclonal mouse	Human	PE	BD Biosciences	562159	Flow cytometry
FLI1	Monoclonal mouse	Human		BD Biosciences	554266	Western Blot
PF4	Polyclonal rabbit	Human		PeproTech	500-P05	Western Blot
TBP	Monoclonal mouse	Human		Abcam	ab818	Western Blot
IgG	Polyclonal donkey	Mouse	HRP	Abcam	ab6820	Western Blot
IgG	Polyclonal goat	Rabbit	HRP	Abcam	ab6721	Western Blot
CD41 MWReg30	Rat Fab2	Mouse	AF 647	BD Biosciences	553847	Intra-vital injury

Table 3.1. List of antibodies used for iMeg analyses.

Description of antibodies used for flow cytometry and Western Blot analyses of HPCs, iMegs and iPlts. Abbreviations: AF, Alexa Fluor; APC, Allophycocyanin; BV, Brilliant Violet; FITC, fluorescein isothiocyanate; HRP, Horseradish Peroxidase; PE, R-phycoerythrin.

Name	Source	Genome Engineering Technology Used	Relative FLI1 mRNA Level of iMegs (% ± SEM, P value)	Relative FLI1 Protein Level of iMegs (% ± SEM, P value)
Control iPSC line (WT)	Bone marrow	Four-factor lentiviral reprogram	100	100
FLI1 overexpression (WT-OE1)	WT	AAVS1-targeted FLI1 transgene: 1 copy	431 ± 99 P = 0.020	686 ± 240 P = 0.088
FLI1 overexpression (WT-OE2)	WT	AAVS1-targeted FLI1 transgene: 2 copies	494 ± 147 P = 0.006	895± 209 P = 0.024
FLI1 heterozygous knockout ($FLI1^{+/-}$)	WT	TALEN	125 ± 19 P = 0.369	62 ± 8 P = 0.013
Paris Trousseau syndrome iPSC line (PTSx)	Patient fibroblasts	Four-factor lentiviral reprogram	84 ± 15 P = 0.624	17 ± 10 P < 0.0001
PTSx FLI1 overexpression (PTSx-OE)	PTSx	AAVS1-targeted FLI1 transgene: 1 copy	126 ± 12 P = 0.953	678 ± 301 P = 0.38

Table 3.2. iPSC lines and their relative iMeg mRNA and protein levels.

Summary of the iPSC lines used in this study. The various constructs were further analyzed by direct sequence analysis and by relative *FLI1* mRNA (n=4) and protein levels (n=4), confirming genome-editing strategies. WT-OE1, WT-OE2, $FLI1^{+/-}$, PTSx and PTSx-OE lines were compared to WT by one-way ANOVA.

Cell line	Size (μm) ± SEM, P value	Replicates (n)
WT	10.86 ± 0.34	11
WT-OE1	11.17 ± 0.49 P = 0.985	9
WT-OE2	16.27 ± 1.19 P < 0.0001	11
FLI1$^{+/-}$	8.65 ± 0.60 P ≤ 0.05	13
PTSx	9.88 ± 0.71 P = 0.410	8
PTSx-OE	10.83 ± 0.51 P > 0.999	9

Table 3.3. Size of iMegs measured on TEM imaging.

iMegs 5 days post differentiation from HPCs were prepped for TEM analysis and cell diameter of 8-13 images measured using a JEOL 1010 electron microscope fitted with a Hamamatsu digital camera and AMT Advantage image capture software. WT-OE1, WT-OE2, FLI1$^{+/-}$, PTSx and PTSx-OE lines were compared to WT by one-way ANOVA.

Figures

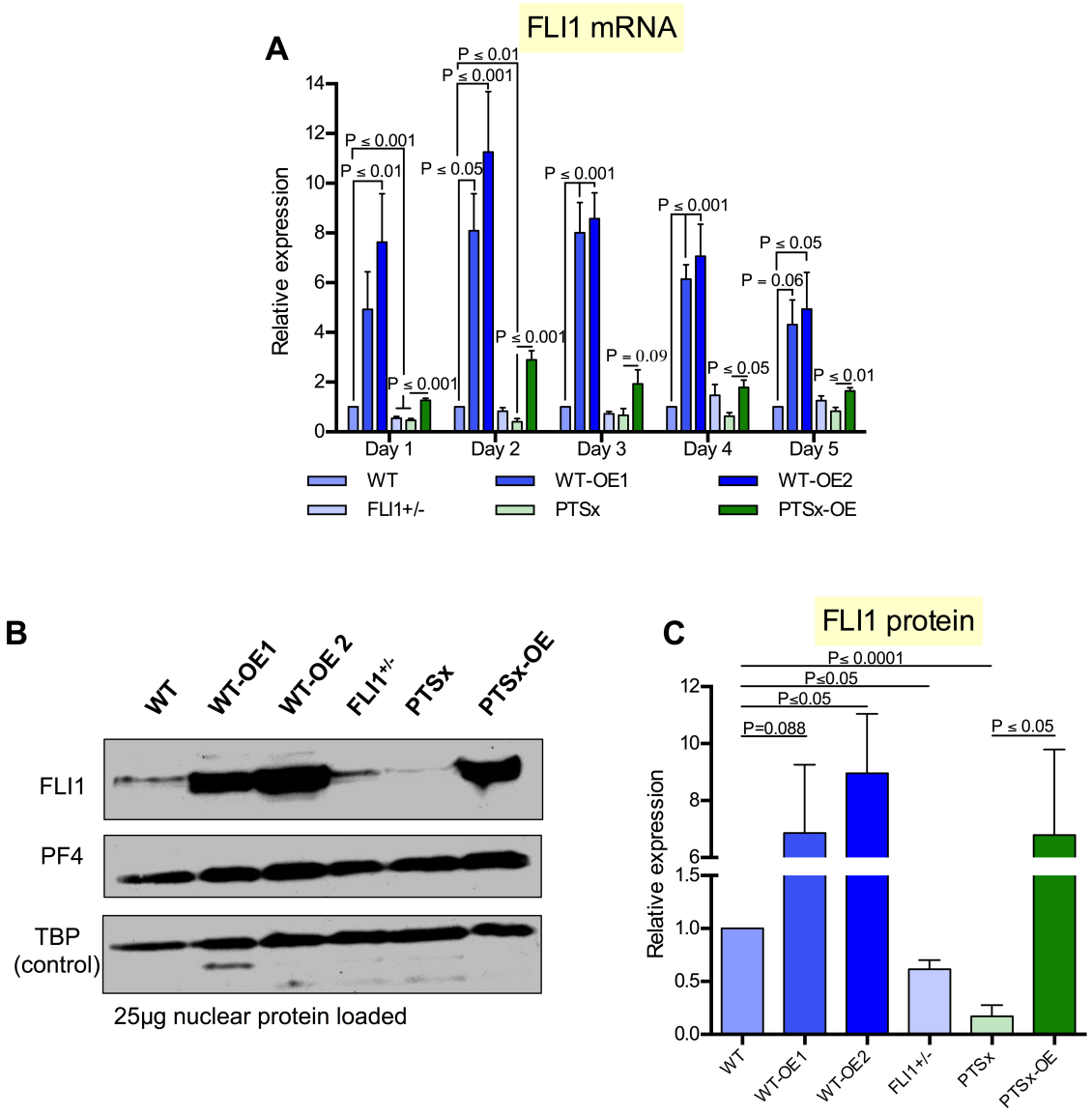

Figure 3.1 Analysis of *FLI1* mRNA and protein levels of iMegs.

iMegs were selected for CD41a and analyzed using qRT-PCR (Days 1-5) and Western blot (Day 5). (**A**) Relative expression of *FLI1* mRNA was performed using qRT-PCR

compared to WT. Mean ± 1 SEM are shown of 4 separate experiments. P values were calculated using one-way ANOVA. (**B**) Representative Western blot membrane image of FLI1, PF4 and TPB (loading control). (**C**) Quantitative analysis of FLI1, relative expression of FLI1 was compared to WT. Mean ± 1 SEM are shown for 4 separate experiments. P values were calculated using one-way ANOVA.

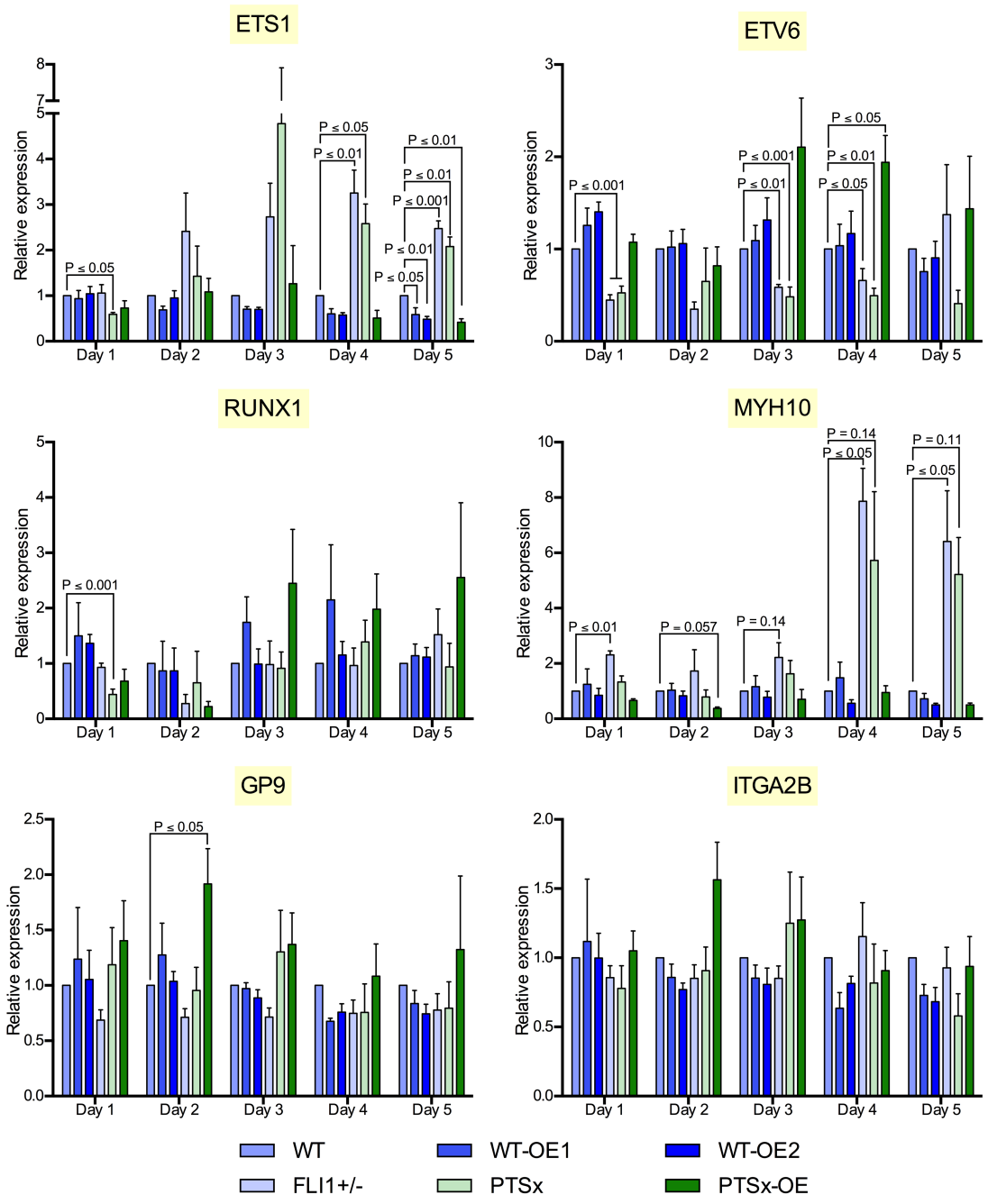

Figure 3.2. qRT-PCR analysis of iMegs for megakaryocyte-specific genes.

Same as Figure 3.1A. Mean ± 1 SEM are shown of 4 separate experiments. P values were calculated using one-way ANOVA.

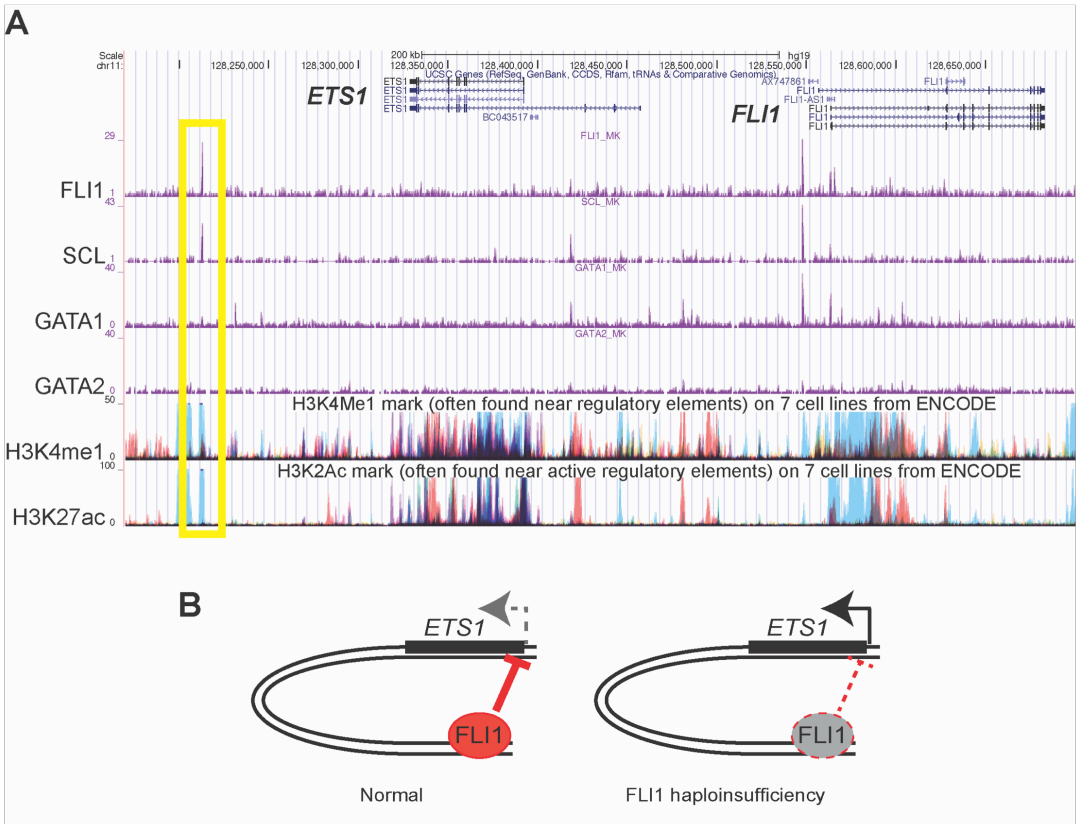

Figure 3.3. Nearby enhancer activity may disinhibit ETS1 expression in FLI1 haploinsufficiency.

(**A**) Primary megakaryocyte ChIP-Seq data, depicted in purple, with area of interest ~100 kb downstream of the *ETS1* gene body (yellow box; note that *ETS1* is transcribed right to left in this diagram). Overlying H3K4me1 and H3K27ac signals of several cell types are depicted, which were created using the UCSC Genome Browser[80]: Cyan, HUVEC; Red, GM12878; Orange, H1-hESC; Green, HSMM; Blue, K562; Lavender, NHEK; Pink, NHLF. (**B**) A schematic model by which FLI1 binding to the region in the yellow box could mediate *ETS1* repression, and result in increased *ETS1* transcription in FLI1 haploinsufficiency.

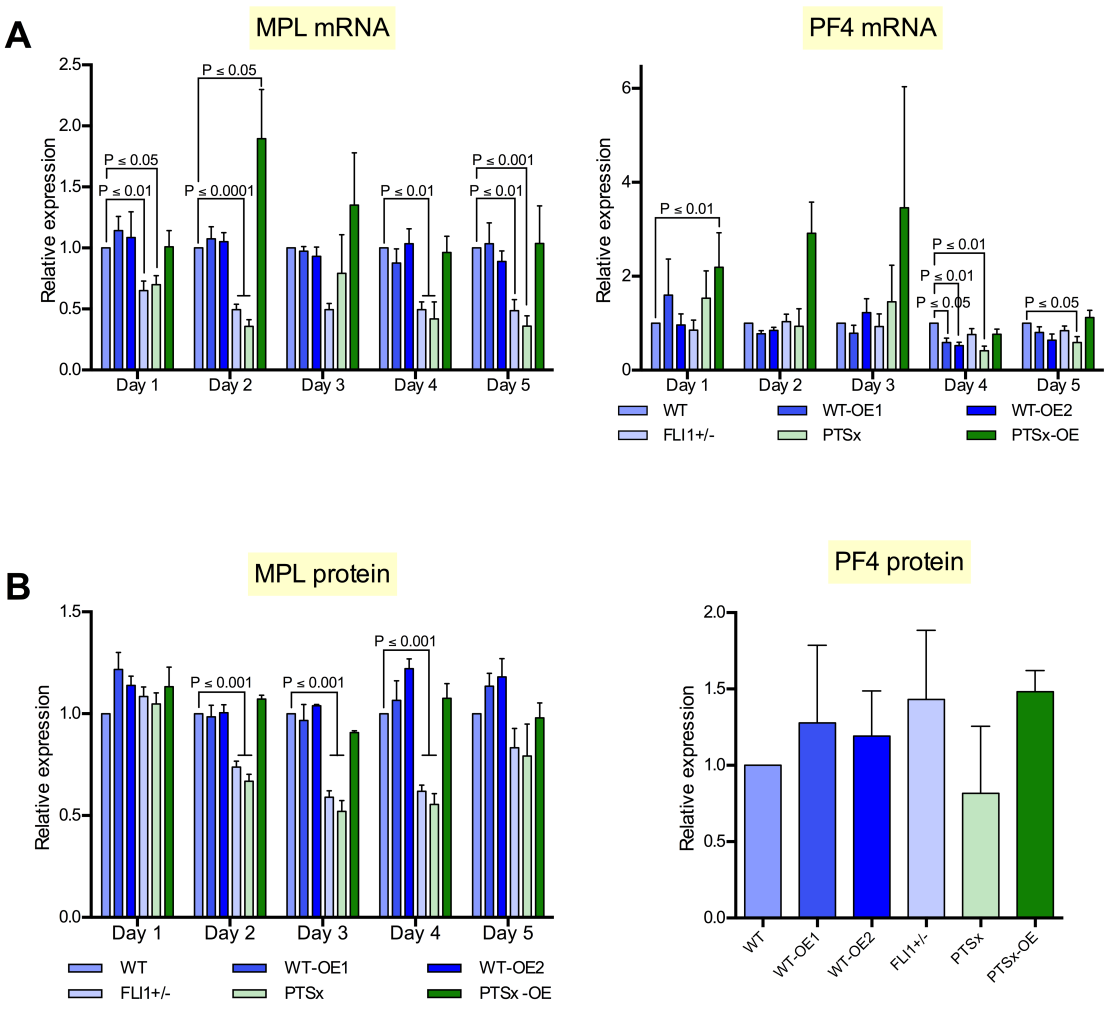

Figure 3.4. iMeg *MPL* but not *PF4* mRNA and protein levels correlate with *FLI1* mRNA and protein levels.

iMegs were selected for CD41a and analyzed using qRT-PCR (Days 1-5) and Western blot (Day 5). (**A**) Relative expression of *MPL* and *PF4* mRNA was performed using qRT-PCR compared to WT. Mean ± 1 SEM are shown of 4 separate experiments. P values were calculated using one-way ANOVA. (**B**) Relative surface MPL expression analyzed from 3 separate experiments using flow cytometry and one-way ANOVA. Western blot analysis of PF4, similar to Figure 3.1 for FLI1. Relative expression was compared to WT.

Mean ± 1 SEM are shown for 4 separate experiments. P values were calculated using one-way ANOVA.

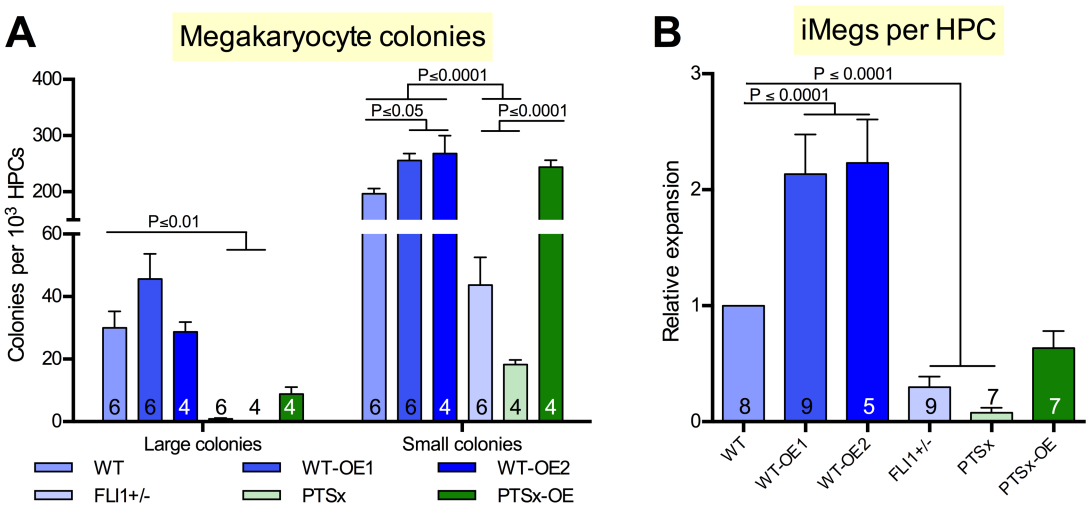

Figure 3.5. Megacult colony numbers and iMeg differentiation in liquid culture mirror FLI1 expression levels.

(**A**) HPCs were plated in a semi-solid Megacult colony system and analyzed at the end of the assay for colony count per input HPC. Mean ± 1 SEM are shown along with the number of independent experiments done. Significant P values done using one-way ANOVA are shown. (**B**) HPCs were grown in liquid culture and analyzed at the end of the assay for iMeg numbers. Relative expression to WT iPSC line is shown. Mean ± 1 SEM are shown along with the number of independent experiments done. P values were calculated using one-way ANOVA.

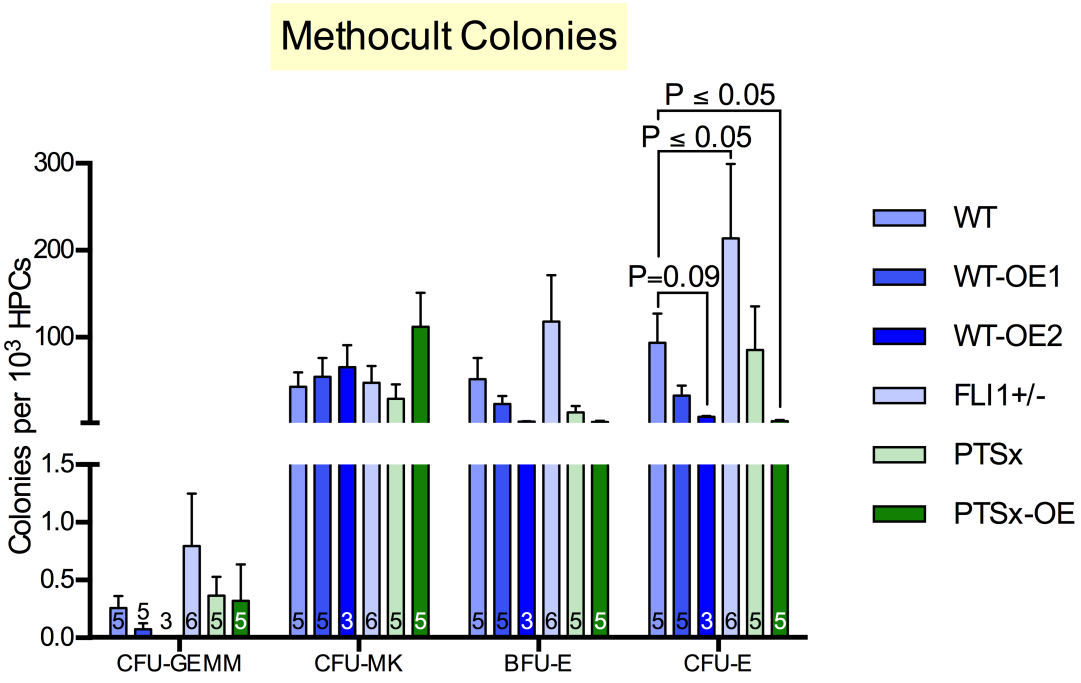

Figure 3.6. Erythroid colony numbers are changed by levels of FLI1 expression. HPCs were plated in a semi-solid methocult culture system and colonies were scored 14 days later. Results are the mean ± 1 SEM of 3-6 independent experiments, with numbers on the bar graph corresponding to number of replicates per line. P values were determined using one-way ANOVA.

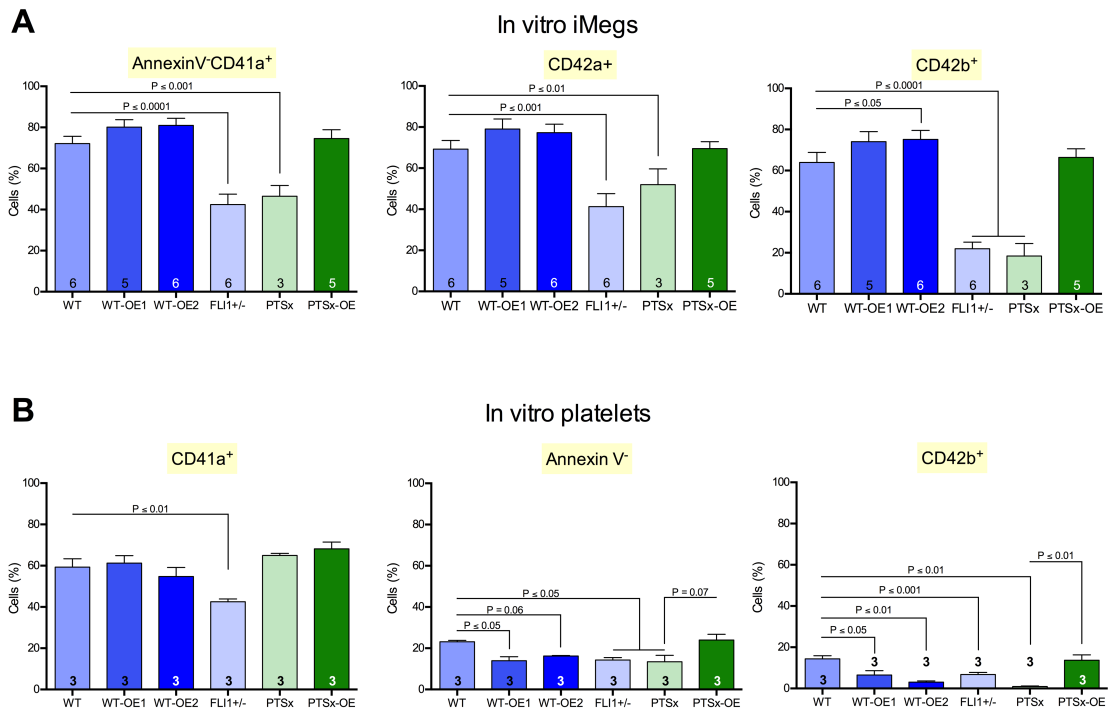

Figure 3.7. Percentage of annexinV$^-$CD41$^+$CD42a$^+$CD42b$^+$ iMegs and in vitro-released platelets.

Day 5 iMegs and released platelet-like particles were analyzed for surface markers using flow cytometry. (**A**) iMegs were negative for annexin V and positive for CD41a, CD42a, and CD42b. (**B**) In vitro platelet-like particles positive for CD41a, negative for annexin V, and positive for CD42b. Mean ± 1 SEM are shown with n=3-6 independent experiments per arm. Significant P values were determined using one-way ANOVA.

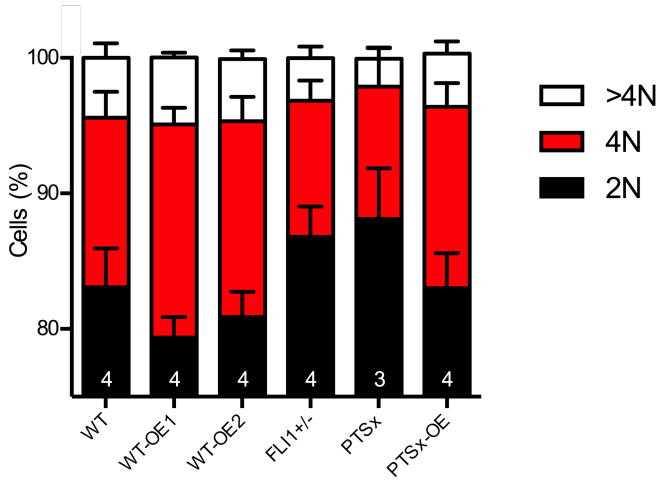

Figure 3.8. FACS analysis of iMeg DNA content.

Ploidy was determined via FACS after iMeg DNA was stained. There are no significant differences among the groups after 1-way ANOVA analysis, but the trend was similar to surface marker analyses where PTSx and FLI1$^{+/-}$ iMegs had less mature iMegs, shown here through less cells with 4N and higher ploidy, and WT-OE1 and WT-OE2 having more high ploidy cells. Results are the mean ± SEM of 3-4 independent experiments.

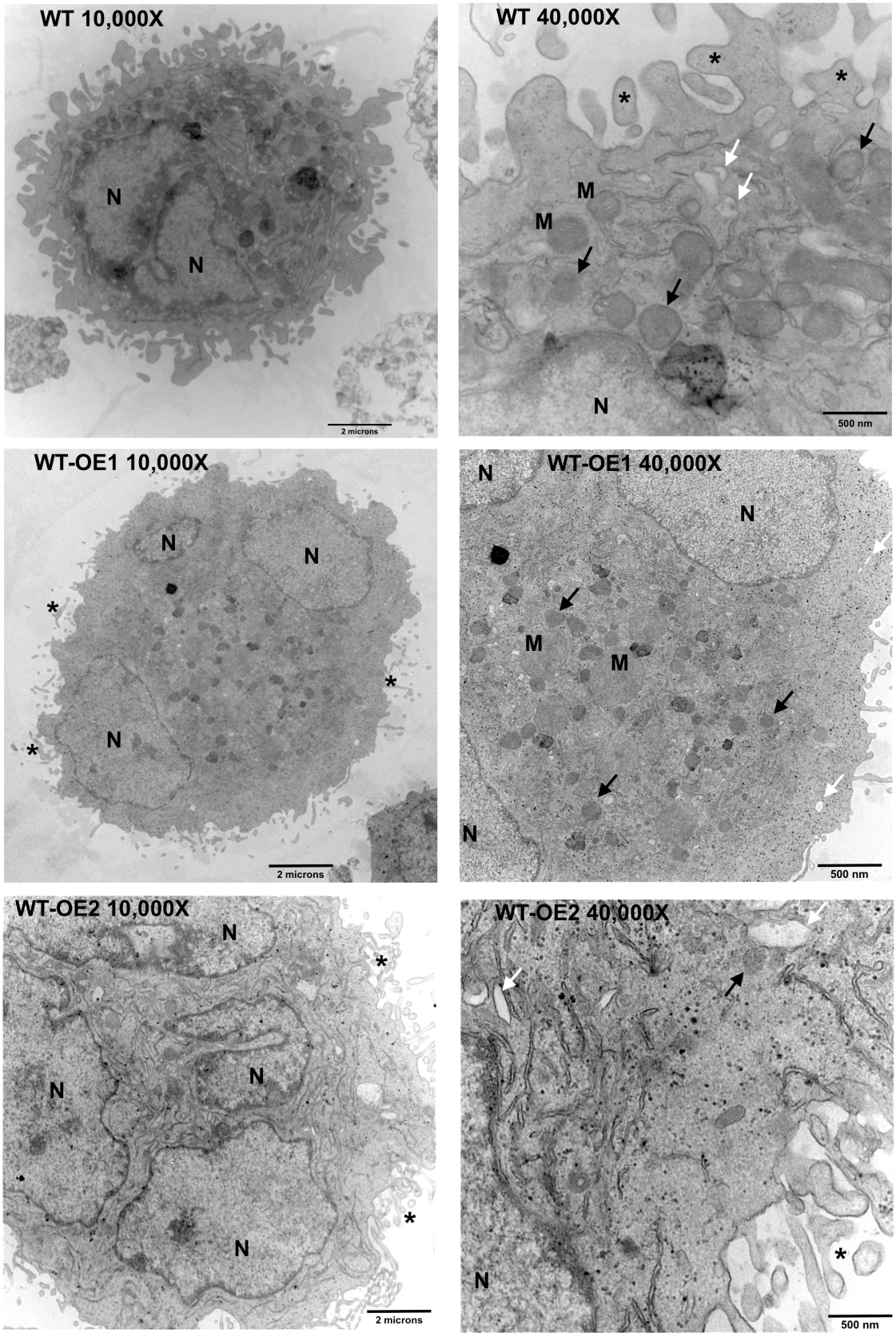

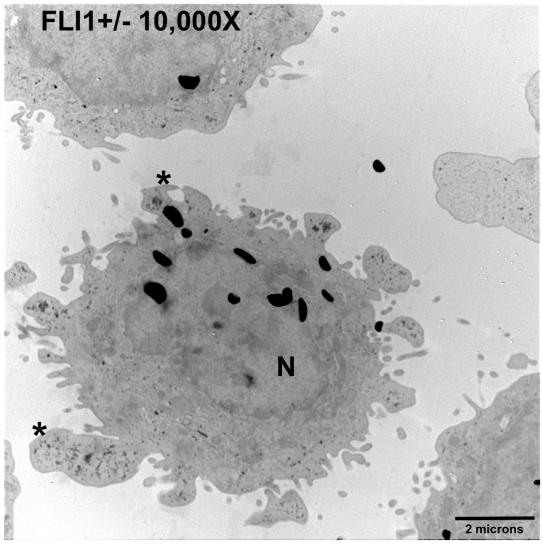

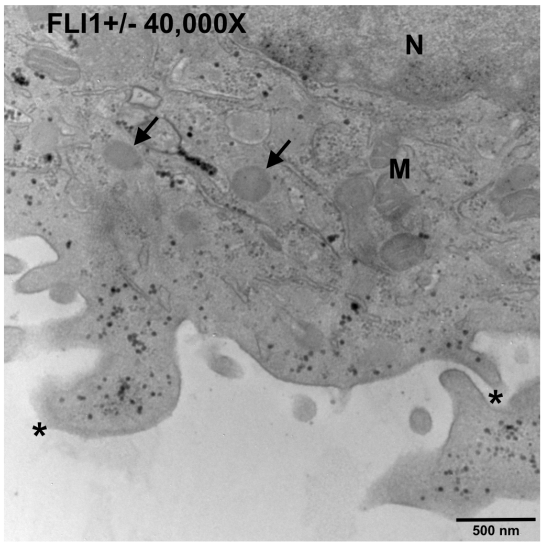

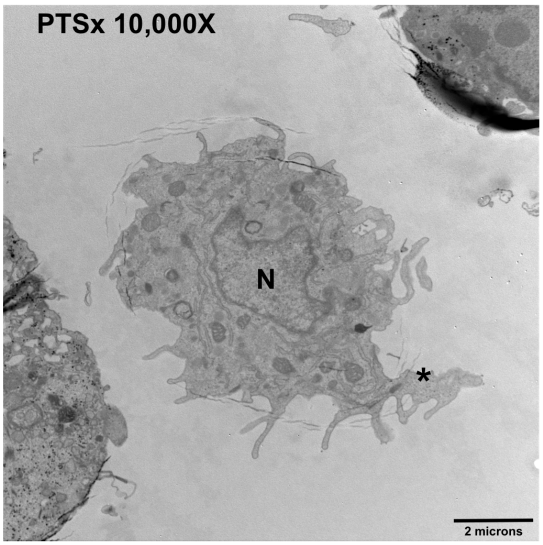

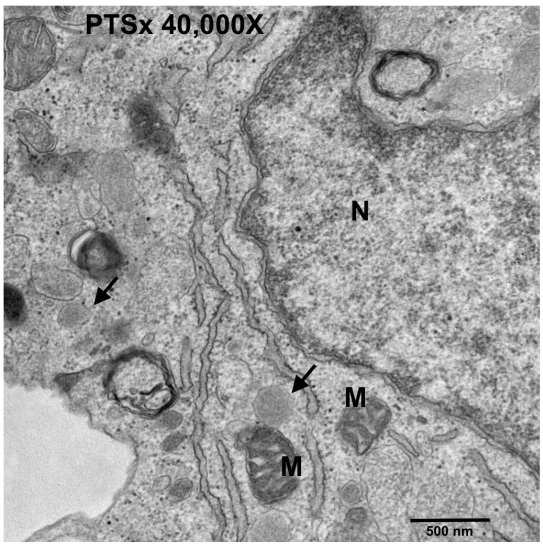

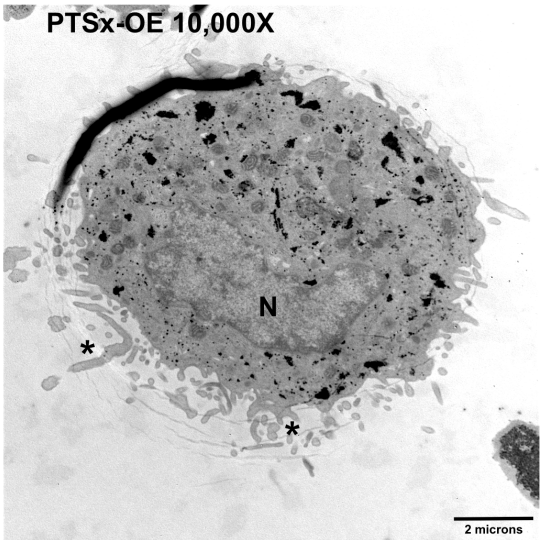

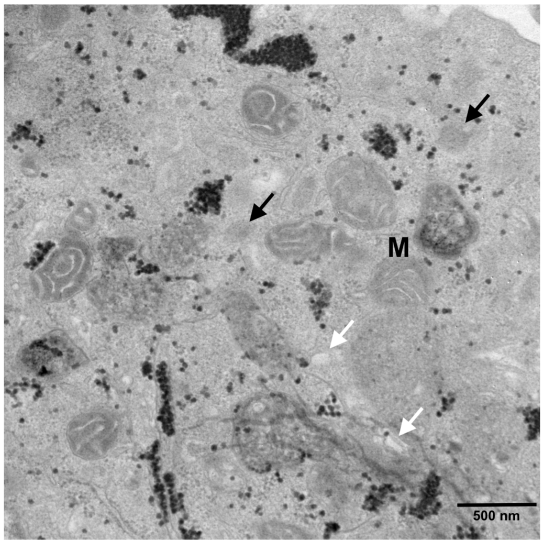

Figure 3.9. iMeg ultrastructures and pro-platelet protrusions

Representative TEM images of iMegs were analyzed at 10,000X and 40,000X for relative size and presence of pro-platelet protrusions (*), granules (black arrows) and open canalicular systems (white arrows) via TEM imaging. Nuclei are denoted with “N” and mitochondria with “M”. Micrographs taken using a JEOL 1010 electron microscope fitted with a Hamamatsu digital camera and AMT Advantage image capture software

CHAPTER 4 – In vivo analysis of infused *FLI1*-modified iPSC-derived megakaryocyte thrombopoiesis and released platelets

Abstract

We showed that iPSC-derived megakaryocytes (iMeg) are not only an unlimited source of cells, but also a viable one for studying in vitro questions of *FLI1*-related megakaryopoiesis. Having established that PTSx and FLI1$^{+/-}$ iMegs exhibit similar in vitro characteristics as primary megakaryocytes, such as small cell size and reduced numbers, we now infused immunodeficient mice to test in vivo properties of iMeg thrombopoiesis and released platelet function. We found that platelets released in vivo from infusion of these iMegs had fewer platelets released per iMeg, and the platelets that were released had poor half-lives and functionality. Finally, we found increased in vivo yield, half-life and functionality of released platelets from iMegs that overexpressed FLI1. Together, these in vivo data illustrate a novel approach to studying a critical megakaryocyte-specific TF that is hard to replicate in animal models and may be more clinically relevant.

Introduction

While the studies of PTSx and *FLI1* mutations describe clinical hematologic data and some in vitro analyses, none have shown a detailed examination of platelet biology beyond transmission electron microscopy images of ultrastructures. To fully understand the platelet defects attributable to FLI1 deficiency, comprehensive investigations need to be performed comparing affected platelets to those that are derived from the same genetic background aside from the expression of *FLI1*. I address in this Chapter platelet biology from infused iPSC-derived megakaryocytes with different expression levels, confirming the utility of this approach to studies of thrombopoiesis and released platelet biology beginning with iPSCs.

In Chapters 2 and 3, I outlined the need for a better model to study megakaryopoiesis associated with the *FLI1* TF, detailed the creation of isogenic iPSC lines from the same genetic background that had increased or decreased FLI1 expression levels, and presented in vitro analyses of the resulting *FLI1*-modified iMegs that recapitulated the PTSx and *FLI1* mutation patient defects and provided a megakaryopoiesis "correction" or improvement strategy with overexpression lines. This Chapter highlights a novel approach at studying in vivo thrombopoiesis of gene-edited iMegs and in vivo-released platelet biology.

Methods

Characterization of in vivo-generated platelets from infused iMegs

Non-obese diabetic (NOD)/SCID/interferon receptor 2γ-deficient (NSG) mice (Jackson Laboratory, Bar Harbor, ME) are severely immunodeficient and lack mature T cells, B cells, functional NK cells, and are also deficient in cytokine signaling[172]. We used this mouse strain to study in vivo thrombopoiesis of our human iMegs. Male NSG mice were infused at 8-12 weeks of age via tail vein with 1-2 X 10^7 iMegs suspended in 200 µl of PBS and 1% BSA. Isolated human platelets from healthy donors were similarly infused as a positive control. Retro-orbital blood collection was performed at various intervals post-infusion, and the human platelets and platelet-like particles from iMegs (iPlt) were stained with anti-human CD41a antibody to distinguish them from the native murine platelets[170]. Loss of the glycocalicin, an indicator of megakaryocyte injury[173], was measured using anti-human CD42a versus anti-human CD42b antibodies in addition to annexin V staining (Antibodies used for experiments in this Chapter are described in Table 3.1).

Functional analysis of iPlts via measurement of response to thrombin activation

Baseline human platelet activation and responsiveness to agonist in isolated murine blood were assessed by surface P-selectin levels in the absence and presence of thrombin. NSG mice were infused as above and ~1 ml of whole blood was collected 4 hours later from the inferior vena cava. Washed platelets were isolated and resuspended into Tyrode's buffer at pH 7.2, as described previously[174]. Platelet activation with 1 U/ml thrombin (Sigma-Aldrich) was performed for 30 minutes at 37°C then analyzed by flow cytometry.

Functional analysis of iPlts via measurement of incorporation into active thrombi

Human platelet function was assessed using the intra-vital arteriole laser injury model as described[175]. iMegs were pre-labeled with 2 mM calcein AM (Invitrogen) for 30 minutes at 37°C, washed once with PBS, then resuspended in 200 µl PBS and 1% BSA before infusion via the tail vein of male NSG mice. To label mouse platelets, Alexa Fluor 647-labeled rat monoclonal anti-mouse CD41 Fab fragments (BD) were injected intravenously shortly before injury. Laser-induced injuries of cremaster arterioles were performed 4 hours after iMeg infusion. Human platelet incorporation was recorded by confocal microscopy and compared to the concurrent circulating percent of human platelets in mouse blood[176].

Statistical analysis

Statistical analysis was performed using one-way ANOVA and data was reported as mean ± 1 standard error of the mean (SEM) using the GraphPad Prism software version 6.00 for Mac (GraphPad Software). Differences were considered significant when the *P* value was less than 0.05.

Study approval

Animal studies and human tissue sampling were done in accordance with CHOP's Institutional Animal Care and Use Committee and Institutional Review Board, respectively.

Results

In vivo-released iPlts from infused iMegs in NSG mice

Since in vitro-generated platelet-like particles were only ~50% platelets with most of these platelets being injured (Figure 4.1), platelet analyses in our studies focus on in vivo-released platelet biology from iMegs. We have previously shown that infused human megakaryocytes, including iMegs, into immunodeficient NSG mice release iPlts intrapulmonarily beginning almost immediately[170]. These platelets have comparable size-distribution, half-life and functionality as donor-derived platelets, in contrast to in vitro-released platelet-like particles[170]. iMegs of the various FLI1 lineages were infused into NSG mice, and the number and functionality of the released iPlts measured. Released iPlts over 24 hours were calculated as a percentage of human $CD42b^+$ that, on forward scatter analysis, had a size range similar to that of infused human donor platelets. This value was normalized to the number of $CD42b^+$ iMegs infused (Figure 4.1A) and separately to the number of HPCs needed to generate those iMegs (Figure 4.1B). Area under the curve (AUC) was calculated from these values. AUC of FLI1-low (PTSx and $FLI1^{+/-}$) iPlts released was significantly less than WT per iMeg and per HPC, while PTSx-OE released the same number of platelets per iMeg and per HPC as WT (Figures 4.1C and 4.1D, respectively). WT-OE1 and WT-OE2 released the same number of platelets per iMeg (Figure 4.1C), but an ~50% increase per HPC (Figure 4.1D) consistent with the higher yield of iMegs per HPC seen in these two lines in Figure 3.5B.

Calculated WT iPlt in vivo half-life was ~4 hours, comparable to our previously published value[170] (Figure 4.2). For the PTSx and $FLI1^{+/-}$ lines, iPlt half-lives were decreased to ~1 and ~2 hours compared to WT, respectively. PTSx-OE iPlts had a half-

life of ~3 hours, comparable to WT-released platelets, while WT-OE1 and WT-OE2 iPlt half-lives were increased to ~7 and ~11 hours, respectively (Figure 4.2).

Released iPlt function

PTSx platelets have been reported to be dysfunctional as well as reduced in number[78,79,151]. We asked what the effect was of FLI1 expression levels on platelet functionality in the released iPlts from the various *FLI1*-iMeg lines. Whole blood was drawn from NSG mice 4 hours after iMegs were infused and washed platelets isolated. These platelets were analyzed via flow cytometry for surface P-selectin, a marker of platelet alpha-granule degranulation as an indicator of platelet activation[177], pre- and post-activation with thrombin (Figure 4.3). Pre-activation levels of P-selectin on $CD41^+$ and $CD41^+CD42b^+$ iPlts were comparable across all lines, indicating that all iPlts were equally quiescent (Figures 4.3A and 4.3B, respectively). Post thrombin activation, both FLI1-low $CD41^+$ iPlt lines were hyporesponsive compared with WT iPlts, likely because a significant number of these iPlts were pre-injured as megakaryocytes (Figure 3.7). The FLI1-low $CD41^+CD42b^+$ iPlts showed normal responsiveness indicating that uninjured FLI1-low iPlts retained responsiveness. The overexpressing lines all showed increased responsiveness to thrombin relative to WT iPlts.

We also assessed iPlt function in vivo by visualizing human platelet incorporation into laser-induced cremaster arteriolar injuries as previously described[175]. We compared iPlts from 3 lines: WT, WT-OE1 and $FLI1^{+/-}$ (Figure 4.4). Data were consistent with the thrombin stimulation studies: active platelet incorporation into thrombi of WT-OE1 iPlts

had comparable active incorporation as WT, while the incorporation FLI1$^{+/-}$ iPlts was decreased in comparison.

Discussion

In the previous Chapter, I presented flow cytometry data of in vitro-generated platelet particles, showing that the majority of CD41^{+} platelet-like particles were already activated or injured (Figure 3.7B). This phenomenon has been reported before by our group[170], and suggests the platelets present in the tissue culture dish at the end of megakaryocyte differentiation are old and functionally limited. We have previously shown that infused human megakaryocytes, including iMegs, into immunodeficient NSG mice release iPlts intrapulmonarily beginning almost immediately[170] similar to that seen endogenously in mice where ~50% of platelets are released from megakaryocytes entrapped in the lungs[178]. Therefore, we instead used an alternative strategy by infusing iMegs into NSG mice as an in vivo method of generating young platelets[176]. We did not treat these mice with clodronate liposomes that deplete macrophages from the mouse circulation, so that the mice were sufficiently immunocompetent to remove injured and pre-activated platelets that accompanied the infused iMegs. This allowed us to assess characteristics of only quiescent platelets that were not immediately cleared by mouse macrophages[170]. Infusing iMegs into NSG mice and tracking iPlt generation over time, we saw a biphasic iPlt generation curve (Figure 4.1). A peak occurred between the 5- and 30-minute time points that indicate the platelet-like particles that had already been

released in culture. Between 4- and 6-hours post infusion, $CD42b^+$ iPlts were released from entrapped iMegs in the pulmonary beds of the recipient mice.

Comparatively, both PTSx and $FLI1^{+/-}$ iPlt generation are decreased per iMeg, and the PTSx-OE generation curve returned to normal. These calculations have already been normalized to account for only the uninjured $CD42b^+$ iMegs, indicating that while there may be healthy in vitro FLI1-deficient iMegs, they underwent diminished thrombopoiesis in an in vivo setting either calculated per iMeg or initial HPC. The WT-OE1 and WT-OE2 lines released as many iPlts per iMeg as the parent WT iMegs. However, considering the higher number of iMegs differentiated from HPCs (Figure 3.5), an ~50% increase in iPlt release was observed per HPC. The FLI1-low iPlts had shortened half-lives compared to WT iPlts, perhaps related to a higher level of baseline injury or decreased surface levels of important receptors system (Figure 3.7A) or to some additional pathway that affects platelet half-life such as the described Bcl-x_L programmed cell death pathway[179]. The shortened half-life could also be due to increased platelet desialylation, prompting removal via the hepatic Ashwell-Morell receptor[180,181]. Conversely, the WT-OE1 and WT-OE2 iPlts appeared to survive longer (Figure 4.2), approaching the half-life we described for donor-derived infused platelets[170]. Whether this is related to decreased in vitro injury, increased surface receptor levels shown in Figure 3.7A, altered cell death pathways or decreased platelet desialylation needs further study.

We confirmed iPlt functional robustness by performing an ex vivo-activation study. Whole blood containing in vivo-released iPlts was isolated at 4 hours, which corresponds to the time point where circulating levels of the $CD42b^+$ iPlts was highest (Figure 4.1). These iPlts with different FLI1 levels were indistinguishably quiescent

before activation (Figure 4.3). Once activated with thrombin, surface P-selectin levels did not increase as much on total $CD41^+$ particles derived from infused PTSx and $FLI1^{+/-}$ iMegs (Figure 4.3A); however, the few $CD42b^+$ iPlts present were normal (Figure 4.3B) suggesting that injury of FLI1-low iPlts is an important component of their decreased functionality. In comparison, all iPlts generated from FLI1 overexpressing line were more responsive relative to WT iPlts and coincidentally were derived from iMegs with less injury as indicated by loss of surface CD42b (Figure 3.7A). Whether the two observations are related will need to be tested. Finally, we compared the ability of these iPlts to be incorporated into growing mouse thrombi, using WT, WT-OE1 and $FLI1^{+/-}$ lines (Figure 4.4). These studies support that released FLI1-low iPlts are qualitatively defective and that overexpressing FLI1 did not decrease iPlt functionality.

By studying in vivo thrombopoiesis of iMegs coming from various *FLI1*-modified iPSC lines, we present novel insights into *FLI1* influence on this cellular process and shed light on the pathogenesis of PTSx and other FLI1-deficient platelet defects. We confirmed that the defect occurred at all stages of megakaryocyte and platelet maturation. Furthermore, injury at one stage can affect biology downstream. Starting at the HPC differentiation into iMeg stage, FLI1-low lines already exhibited a defect. Then, the defect extended into the stage of in vitro iMegs releasing in vivo iPlts. Additionally, these iPlts were functionally inferior to normal iPlts, not being able to respond to thrombin or participate in clotting as well as normal cells. On the other hand, FLI1 overexpression driven by the *Gp1ba* promoter was not deleterious. In fact, this strategy may enhance iMeg yield per HPC while limiting in vitro injury to developing megakaryocytes. FLI1 overexpression was also not deleterious to thrombopoiesis, with WT-OE iMegs releasing iPlts that were actually as good or better than WT iPlts in half-

life and agonist responsiveness. These data may have implications for future clinical applications.

Figures

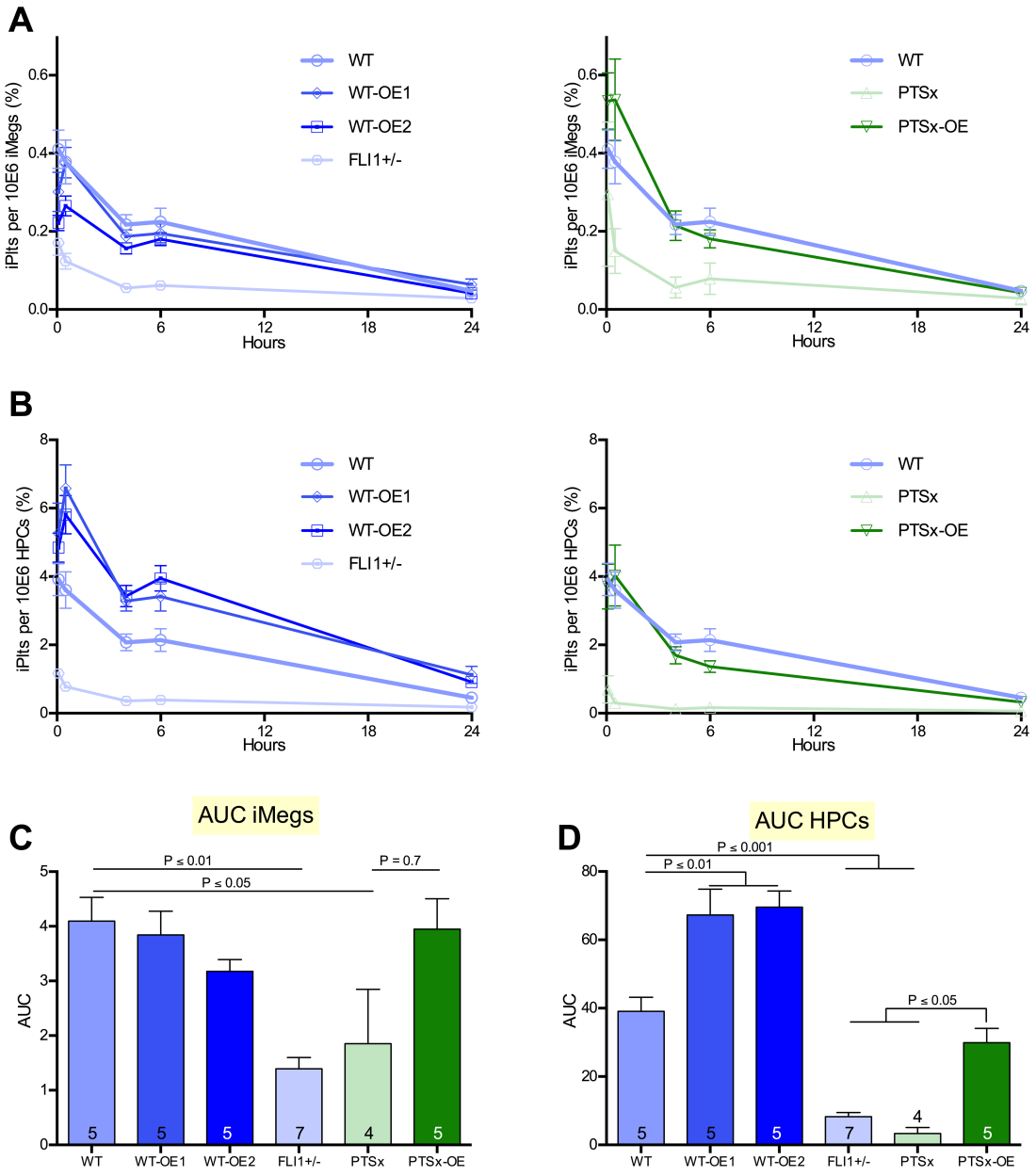

Figure 4.1. In vivo iPlt generation is decreased for FLI1-low and increased for FLI1-high lines.

In (**A**) and (**B**), NSG mice were infused with iMegs, and percent of human platelets were determined at various time points up to 24 hours. Mean ± 1 SEM are shown with 4-7 independent experiments per arm. (A) Left: Data analyzed per infused iMegs generated from isogenic genome-edited iPSC lines. Right: Data analyzed per infused iMegs WT iPSCs and the two PTSx lines. (B) Same as in (A), but analyzed per initial HPCs from which the iMegs were prepared. (**C** and **D**) AUC calculations for iPlt generation either from iMegs (C) or from HPCs (D). Mean ± 1 SEM are shown with number of independent experiments per arm shown in each bar. Significant P values were determined using one-way ANOVA.

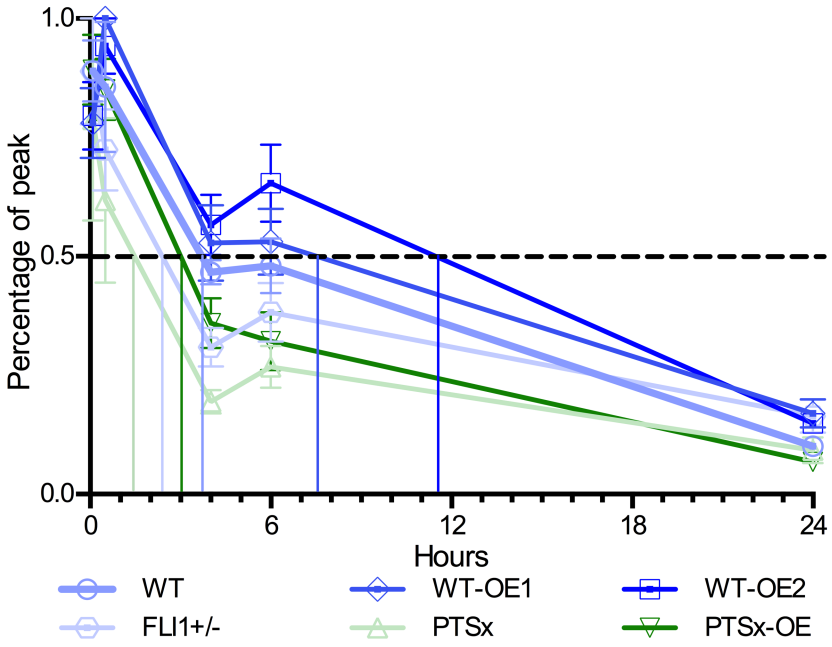

Cell line	WT	WT-OE1	WT-OE2	FLI1$^{+/-}$	PTSx
iPlt half-life (hours)	4	7	11	2	0.5

Figure 4.2. iPlt half-life is decreased for FLI1-low and increased for FLI1-high lines. Percent of peak iPlt generation up to 24 hours after iMeg infusion into NSG mice (n=4-7 independent experiments, same as Figures 4.1A and 4.1D). Half-life is determined by the time at which there is 50% of iPlts compared to peak iPlt numbers.

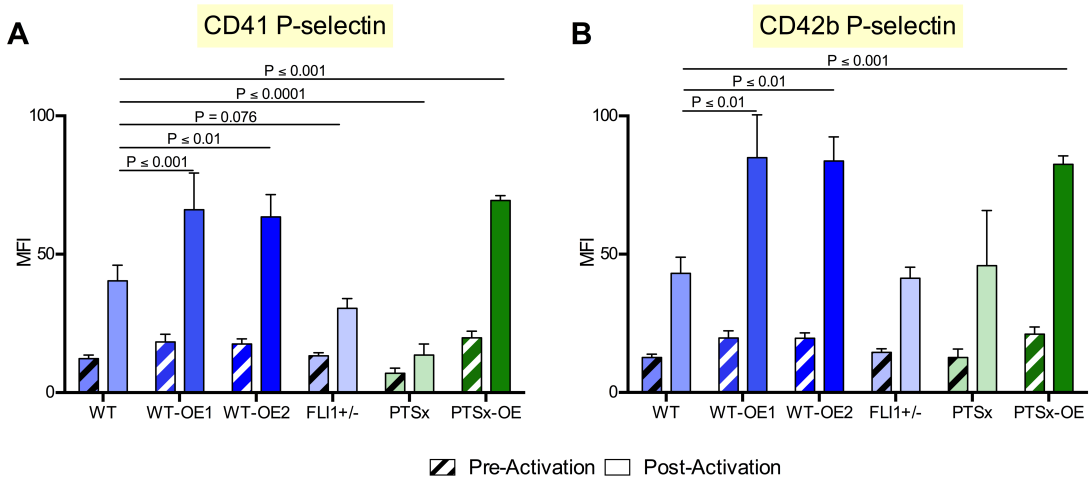

Figure 4.3. iPlt response to activation is decreased for FLI1-low and increased for FLI1-high lines.

(**A**) $CD41^+$ and (**B**) $CD41^+CD42b^+$ iPlt mean fluorescence intensity (MFI) of surface P-selectin before and after thrombin stimulation of iPlts generated at 4 hours after iMeg infusion. Mean ± 1 SEM are shown with n=6 independent experiments per arm. Significance was determined by one-way ANOVA.

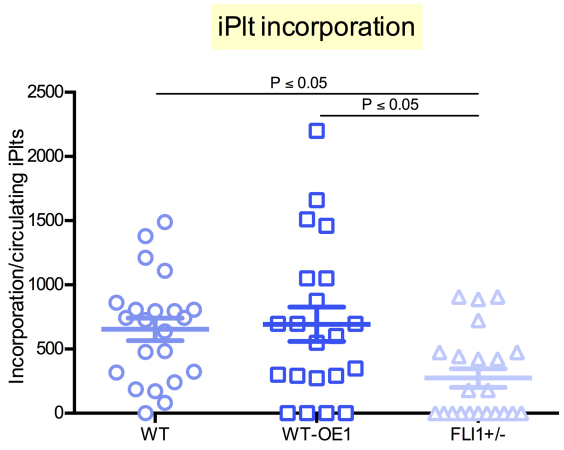

Figure 4.4. iPlt incorporation into thrombi is decreased for FLI1-low and increased for FLI1-high lines.

Intra-vital cremaster injuries were induced at 4 hours after iMeg infusion in NSG mice and fluorescent images were recorded. The numbers reported are of human particles incorporated into a growing thrombus normalized to circulating percentage of $CD42b^{+}$ iMegs in the mouse blood at the time. Shown are the individual data point and mean ± 1 SEM of experiments from four individual mice with up to six injuries per mouse. Significance was determined by one-way ANOVA.

CHAPTER 5 – Discussion and future directions

Addressing the challenges of studying *FLI1* in megakaryopoiesis

Murine models that have been established to study *FLI1* and its relation to megakaryopoiesis have provided important insights into its overall biology, like the essentiality of *FLI1* for vasculargenesis[182] and megakaryopoiesis[53,183], yet the details of its regulation of megakaryopoiesis differs from that in humans. Murine models of *Fli1*-gene targeting did not replicate the PTSx syndrome[52] or the biology in the growing number of individuals recognized with *FLI1* mutations and inherited thrombocytopenias[84]. We, therefore, turned to the relatively new iPSC technology to address key clinical questions related to the role of *FLI1* in megakaryopoiesis, thrombopoiesis and platelet biology. While in vitro-generated iMegs do not fully replicate the biology of CD34-derived or primary megakaryocytes[170], they offer the advantage of unlimited access to genetically modified iMegs that can be studied in parallel with control iPSC lines in which gene editing has been performed, and we have developed strategies in our group to specifically study questions related to megakaryopoiesis, thrombopoiesis and platelet biology.

iPSCs and gene editing

Disease modeling for rare and multigenic disorders can be a challenge, but iPSC technology has made it possible to generate a stable cell line from diseased patients that accurately reiterate the disease phenotype in vitro. Using this to our advantage, we created a PTSx iPSC line and found that the megakaryocyte and platelet defects are indeed replicated in our hematopoietic differentiation protocols. We believe the cardiac,

kidney, and other organ defects associated with these patients could also be modeled with the same iPSCs.

Another advantage of using iPSCs is the ability to use recently developed gene editing technologies to modify specific genes from the same cell line and compare differences in cells coming from the same genetic background. Consequently, we used ZFN technology to overexpress FLI1 in the hematopoietic/megakaryocyte lineages and TALEN technology to heterozygously disrupt the *FLI1* gene. The end-product cell lines could be compared to the parental cell line with the presumption that they only differ by the genetic alteration induced. Moreover, gene targeting allows one to replicate mutant iPSCs without the need to have available patients.

The FLI1-modified iMeg studies presented here provide novel insights into the role of FLI1 during megakaryopoiesis, thrombopoiesis and platelet functionality. In vivo-released iPlts from infused iMegs also allowed us additional characterization of platelets that are comparable to donor-derived platelets, which was not possible by studies of in vitro-released platelet-like particles, of which only roughly half are $CD41^+$ and of those, most are negative for CD42b and bind annexin V, indicating that they are injured and/or apoptotic[184].

Correction of the PTSx megakaryocyte and platelet phenotypes

We demonstrate that PTSx iMegs and iPlts replicated many of the known defects seen in this syndrome, beginning with a decrease in the number of iMegs derived per HPC and also decreased expression of megakaryocyte-specific markers. Moreover, we

observed a redirection of HPCs towards the erythroid lineage, limiting the number of resulting iMegs in vitro. Furthermore, these studies show a clear defect in the ability to shed iPlts relative to normal iMegs in vivo, with FLI1-low iPlts having decreased responsiveness to the thrombin agonist and a decreased ability to be incorporated into a growing thrombus. Since PTSx is part of a larger syndrome associated with significant chromosomal deletions, it was not clear that all the defined defects were related to the deletion of FLI1[76,81]. The following lines of evidence presented support that the megakaryocyte and platelet defects are predominantly or entirely due to the FLI1 deficiency: (1) Megakaryocyte-specific overexpression of FLI1 in PTSx iMegs largely corrected the defects in megakaryopoiesis, thrombopoiesis and platelet biology even with a large 15.3 Mbp deletion on chromosome 11q. (2) Similar findings were observed for both the PTSx and FLI1$^{+/-}$ iMegs. (3) The TF ETS1, which is physically linked to FLI1[80], is always deleted in PTSx[76,79], and important in megakaryopoiesis[20]; appears to be inversely regulated by FLI1. In the PTSx and FLI1$^{+/-}$ iMegs, the level of ETS1 is at least normal. There is no ETS1 TF deficiency in megakaryocytes from patients with PTSx.

FLI1 monoallelic expression

Primary megakaryocytes isolated from two patients with PTSx had been previously studied and the results were consistent with these iMeg findings. However, that study also raised the possibility that *FLI1* expression undergoes monoallelic expression based on very limited analysis of the final megakaryocytes seen[82]. This

concept that *FLI1* undergoes allelic exclusion, resulting in half of the megakaryocytes coming from the missing *FLI1* allele being affected and the other half normal, has since been echoed by others[83]. We examined whether either PTSx or FLI1$^{+/-}$ HPCs transitioning to iMegs gave rise to two distinct megakaryocytic populations consistent with monoallelic expression, but did not observe two populations. In a collagen-based culture system, PTSx HPCs gave rise to virtually no large colonies, not just half as many as allelic exclusion would predict, and this was also seen with the FLI1$^{+/-}$ line (Figure 3.5A). The vast majority of PTSx iMeg-derived iPlts also had a markedly shortened half-life after infusion of the iMegs into NSG mice (Figure 4.1). Thus, if monoallelic expression of *FLI1* had occurred, then the lower yield of iMegs per HPC, the lower yield of iPlts per iMeg and the poor half-life of the FLI1-deficient iPlts compared to WT iPlts would mean that most of the circulating iPlts in a PTSx patient would be from the normal allele, and dysfunctional macrothrombocytes would be a considerable minority in patients rather than dominating the patients' platelet presentation[52,75,79,151].

Improved megakaryopoiesis and platelet function by FLI1 overexpression

A prior study using megakaryocytes derived from the murine stem cell line G1ME suggested that continuous overexpression of TFs involved in megakaryopoiesis, such as GATA1, may harm overall megakaryocyte formation, thrombopoiesis and platelet biology[185]. We were, therefore, surprised to see that WT-OE1 and WT-OE2 lines underwent normal to enhanced megakaryopoiesis, lost less CD42b from these iMegs than WT iMegs in vitro and exhibited an extended iPlt half-life with normal platelet

functionality. The *Gp1ba* promoter is known to drive expression of a reporter gene at low levels during hematopoiesis and then at a much higher level during megakaryopoiesis[115]. Perhaps this temporal expression profile sufficiently coincides with that of FLI1 during normal human megakaryopoiesis. Alternatively, FLI1 overexpression during megakaryopoiesis may have less deleterious effects on megakaryocyte differentiation than continuous GATA1 overexpression or overexpression of TFs during murine megakaryopoiesis may be more deleterious than in human megakaryopoiesis. Indeed, human megakaryocyte progenitors constitutively overexpressing GATA1, FLI1 and TAL1 differentiated into megakaryocytes that appeared at least partially functional[186], although the in vivo biology of the released platelets was not rigorously tested, as the recipient immunodeficient mice were pretreated with clodronate liposomes, a technique that has previously been shown necessary to prolong the half-life of injured platelets[170]. Also whether in that paper, FLI1 overexpression compensated for GATA1 overexpression, which allowed for normal megakaryopoiesis. This certainly was not addressed.

FLI1 may act as a suppressor of *ETS1* transcription

Our findings of the *ETS1* transcript levels of the various *FLI1*-modified lines were quite unexpected. We had anticipated the PTSx and PTSx-OE lines to be *ETS1* deficient, since they lack one copy of *ETS1* due to the 11qter deletion. The transcript levels, however, were increased up to 4-fold in the PTSx line compared WT levels, with the PTSx-OE showing a slight increase then decrease to the level of the other FLI1

overexpressing lines. The transcript level increase of the PTSx line was also reflected in the FLI1$^{+/-}$ iMegs, which start their megakaryocyte differentiation at normal *ETS1* levels on Day 1, but then experience a sustained increase throughout the rest of differentiation. Published ChIP-Seq data revealed a FLI1-binding site near *ETS1* [156] that localized to markers of active enhancers[157-159]. These mRNA expression patterns, along with chromatin state analysis, could indicate a role of FLI1 in regulating *ETS1* transcription.

Clinical implications

Our studies contribute to the basic understanding of the biology of *FLI1* as it pertains to the megakaryocyte blood lineage, but they also have clinical implications. We show evidence with our PTSx-OE iPSC line that tissue-targeted gene editing can be a viable treatment for FLI1-deficient patients specifically, and perhaps other monogenic disorders in general. Our FLI1$^{+/-}$ iPSC line has similar megakaryocytic and platelet features as the patient cells, indicating that this line may be a genetically clean model without the other missing genes in PTSx for discovery studies of compounds that may improve FLI1 TF activity as detailed below. The WT-OE lines, with their ability to make better iMegs and iPlts could be developed into an in vitro iPSC source of cells for transfusion products. This feature may be incorporated into a final iPSC line designed for large-scale iPlt preparation to enhance uninjured iMeg yield per initial HPC with no deleterious effects on iPlt functionality. The end product would perhaps have a prolonged circulatory half-life as well, as detailed above.

Gene therapy

With the advent of technologies that allow fast and efficient sequencing of genomic DNA, we can now characterize both inherited and de novo genetic mutations that are the cause of life-threatening or debilitating symptoms. Strides have been made in the past ~20 years in the pursuit for corrections to genetic disorders. Gene therapy is no longer a dream but a reality, with over 2000 gene therapy clinical trials that are approved, ongoing or completed for cancer, cardiovascular, monogenic and other diseases[187]. We believe our studies provide an impetus for pursuing gene therapy for FLI1-deficient patients.

We show evidence that iPSCs created from a PTSx patient make poor megakaryocytes and platelets with quantitative and qualitative defects, but can undergo normal megakaryopoiesis and thrombopoiesis and have functional platelets after a single copy *FLI1* cDNA driven by the *GP1ba* promoter was inserted into the genome at the AAVS1 safe harbor locus. We observed that all parameters tested showed a rescued phenotype: number of healthy, uninjured iMegs per HPC, number of iPlts released in vivo, and half-life and function of released iPlts. Based on these results, we propose potential avenues for gene therapy for correction of the platelet defects associated with FLI1 deficiency.

Unfortunately, PTSx is part of JSx, a larger disease that is more often than not life-threatening to afflicted patients due to the large hemizygous deletions involving many genes. While we were able to abrogate the megakaryocyte and platelet pathology in our PTSx iPSC line, these patients are frequently in need of more pressing treatments for their life-threatening complications present to other targeted organs. Because of this, it is probably highly unlikely PTSx patients will be suitable candidates to undergo a *FLI1*-

centric gene therapy treatment to fix their platelets. However, recent evidence suggests that a significant portion of patients with inherited platelet disorders are heterozygous for inactivating mutations on *FLI1*[84,85]. By targeting these specific mutations and replacing them with the correct coding sequence, the bleeding diathesis of these patient will more than likely permanently resolve due to better transcriptional regulation of megakaryocyte and platelet genes by the corrected *FLI1.* Alternatively, gene therapy with the strategy described here, involving a vector driving FLI1 expression using the *Gp1ba* promoter might be useful in correcting the bleeding diathesis in such patients, with little concern of FLI1 over correction. In these patients, the drive for gene therapy intervention will depend on the degree of thrombocytopenia and bleeding diathesis seen and its impact on an individual.

Drug screening

A potential application for the FLI1$^{+/-}$ iPSC line may lie in drug discovery. Since this line has the single *FLI1* genetic mutation, it would be a useful tool to screen for compounds that specifically help to increase FLI1 TF expression level or enhance its activity. With an increasing number of inherited platelet disorders being identified with *FLI1* mutations, perhaps the discovery of a drug that specifically targets FLI1 activity will abrogate the platelet defects. Such an approach by using a PKCδ agonist that enhances FLI1 phosphorylation and activity has already been described to drive cells lines towards megakaryocytes and suppresses leukemogenesis due to heterozygous acquired loss of FLI1[188]. We believe that our FLI1-low iPSC lines may be useful to confirm these findings and/or screen for additional drugs that may be clinically useful, perhaps by beginning

with a library of drugs already approved for clinical application (Selleckchem, Houston, TX).

Developing iMegs for in vivo platelet release

Many groups have pursued an in vitro-derived platelet product to replace the reliance on donor platelets that have many issues relating to storage, immunity and contamination[189]. Some have proposed an in vitro source of platelets that has the properties of being both renewal and reliable for patients who need near constant transfusions for their disorder[190-192]. None have succeeded thus far to provide a comparable or better product than donor-derived platelets. We show in our WT-OE iMegs and iPlts a viable solution for an enhanced source of in vitro-grown megakaryocytes derived from iPSC-derived HPCs that also release a longer-lived, less injured and functional in vivo-released iPlt product. This feature can be incorporated in a final "platelet" iPSC line for large-scale platelet production with other features that can include being less immunogenic with loss of surface HLA markers[193] or delivering a protein of interest stored in its α–granules[194],

Conclusions

In summary, to gain a better understand of the role of *FLI1* in megakaryocyte and platelet biology, we have studied iMegs derived from iPSCs generated from a patient with PTSx as well as those of a WT iPSC line that has been *FLI1* heterozygously-disrupted. We have also genome-modified the WT and PTSx iPSC lines to overexpress

FLI1 in a megakaryocyte-specific fashion. With the two FLI1-deficient lines, we confirm the central role of heterozygous FLI1 loss in the megakaryocyte and platelet defects observed in PTSx and in patients with FLI1 heterozygous mutations, as well as detail their qualitative and quantitative defects. We also show that ETS1 deficiency does not contribute to the PTSx platelet phenotype and that monoallelic expression of *FLI1* does not occur. Using iPSC lines that overexpress FLI1 in HPCs and in iMegs, we did not find any deleterious effects. FLI1 overexpression instead enhanced megakaryopoiesis, thrombopoiesis and platelet functionality. Whether overexpression of FLI1 in in vitro-grown megakaryocytes can improve yield and functionality of platelets for clinical usage remains to be tested.

BIBLIOGRAPHY

1. Wilson A, Trumpp A. Bone-marrow haematopoietic-stem-cell niches. *Nat Rev Immunol.* 2006;6(2):93-106.

2. Weissman IL. Stem cells: units of development, units of regeneration, and units in evolution. *Cell.* 2000;100(1):157-168.

3. Dean L. Blood and the cells it contains. 2005; https://www.ncbi.nlm.nih.gov/books/NBK2263/. Accessed March 1, 2017.

4. Pittman RN. Oxygen transport and exchange in the microcirculation. *Microcirculation.* 2005;12(1):59-70.

5. McNutt DR. Immunity. I. Review of basic immunology. *Rev Bras Pesqui Med Biol.* 1974;7(1):71-80.

6. Binns WH, Jr. The macrophage--phagocytosis and pinocytosis: a review. *Bull Phila Cty Dent Soc.* 1967;32(8):10-13.

7. Nicolas-Avila JA, Adrover JM, Hidalgo A. Neutrophils in Homeostasis, Immunity, and Cancer. *Immunity.* 2017;46(1):15-28.

8. Fillatreau S. Regulatory roles of B cells in infectious diseases. *Clin Exp Rheumatol.* 2016;34(4 Suppl 98):1-5.

9. Machlus KR, Italiano JE, Jr. The incredible journey: From megakaryocyte development to platelet formation. *J Cell Biol.* 2013;201(6):785-796.

10. Golebiewska EM, Poole AW. Platelet secretion: From haemostasis to wound healing and beyond. *Blood Rev.* 2015;29(3):153-162.

11. Baker SJ, Rane SG, Reddy EP. Hematopoietic cytokine receptor signaling. *Oncogene.* 2007;26(47):6724-6737.

12. Watowich SS. The erythropoietin receptor: molecular structure and hematopoietic signaling pathways. *J Investig Med.* 2011;59(7):1067-1072.

13. Robb L. Cytokine receptors and hematopoietic differentiation. *Oncogene.* 2007;26(47):6715-6723.

14. Kapur R, Zhang L. A novel mechanism of cooperation between c-Kit and erythropoietin receptor. Stem cell factor induces the expression of Stat5 and erythropoietin receptor, resulting in efficient proliferation and survival by erythropoietin. *J Biol Chem.* 2001;276(2):1099-1106.

15. Radtke F, Wilson A, Stark G, et al. Deficient T cell fate specification in mice with an induced inactivation of Notch1. *Immunity.* 1999;10(5):547-558.

16. Shivdasani RA, Fujiwara Y, McDevitt MA, Orkin SH. A lineage-selective knockout establishes the critical role of transcription factor GATA-1 in megakaryocyte growth and platelet development. *EMBO J.* 1997;16(13):3965-3973.

17. Wang X, Crispino JD, Letting DL, Nakazawa M, Poncz M, Blobel GA. Control of megakaryocyte-specific gene expression by GATA-1 and FOG-1: role of Ets transcription factors. *EMBO J.* 2002;21(19):5225-5234.

18. Elagib KE, Racke FK, Mogass M, Khetawat R, Delehanty LL, Goldfarb AN. RUNX1 and GATA-1 coexpression and cooperation in megakaryocytic differentiation. *Blood.* 2003;101(11):4333-4341.

19. Zang C, Luyten A, Chen J, Liu XS, Shivdasani RA. NF-E2, FLI1 and RUNX1 collaborate at areas of dynamic chromatin to activate transcription in mature mouse megakaryocytes. *Sci Rep.* 2016;6:30255.

20. Lulli V, Romania P, Morsilli O, et al. Overexpression of Ets-1 in human hematopoietic progenitor cells blocks erythroid and promotes megakaryocytic differentiation. *Cell Death Differ.* 2006;13(7):1064-1074.

21. Pang L, Xue HH, Szalai G, et al. Maturation stage-specific regulation of megakaryopoiesis by pointed-domain Ets proteins. *Blood.* 2006;108(7):2198-2206.

22. Georgopoulos K. Transcription factors required for lymphoid lineage commitment. *Curr Opin Immunol.* 1997;9(2):222-227.

23. Zhu J, Emerson SG. Hematopoietic cytokines, transcription factors and lineage commitment. *Oncogene.* 2002;21(21):3295-3313.

24. Kulessa H, Frampton J, Graf T. GATA-1 reprograms avian myelomonocytic cell lines into eosinophils, thromboblasts, and erythroblasts. *Genes Dev.* 1995;9(10):1250-1262.

25. Stachura DL, Chou ST, Weiss MJ. Early block to erythromegakaryocytic development conferred by loss of transcription factor GATA-1. *Blood.* 2006;107(1):87-97.

26. Tsang AP, Visvader JE, Turner CA, et al. FOG, a multitype zinc finger protein, acts as a cofactor for transcription factor GATA-1 in erythroid and megakaryocytic differentiation. *Cell.* 1997;90(1):109-119.

27. Tsang AP, Fujiwara Y, Hom DB, Orkin SH. Failure of megakaryopoiesis and arrested erythropoiesis in mice lacking the GATA-1 transcriptional cofactor FOG. *Genes Dev.* 1998;12(8):1176-1188.

28. Crispino JD, Lodish MB, MacKay JP, Orkin SH. Use of altered specificity mutants to probe a specific protein-protein interaction in differentiation: the GATA-1:FOG complex. *Mol Cell.* 1999;3(2):219-228.

29. Chang AN, Cantor AB, Fujiwara Y, et al. GATA-factor dependence of the multitype zinc-finger protein FOG-1 for its essential role in megakaryopoiesis. *Proc Natl Acad Sci U S A.* 2002;99(14):9237-9242.

30. Ichikawa M, Asai T, Saito T, et al. AML-1 is required for megakaryocytic maturation and lymphocytic differentiation, but not for maintenance of hematopoietic stem cells in adult hematopoiesis. *Nat Med.* 2004;10(3):299-304.

31. Nagai R, Matsuura E, Hoshika Y, et al. RUNX1 suppression induces megakaryocytic differentiation of UT-7/GM cells. *Biochem Biophys Res Commun.* 2006;345(1):78-84.

32. Andrews NC. The NF-E2 transcription factor. *Int J Biochem Cell Biol.* 1998;30(4):429-432.

33. Fock EL, Yan F, Pan S, Chong BH. NF-E2-mediated enhancement of megakaryocytic differentiation and platelet production in vitro and in vivo. *Exp Hematol.* 2008;36(1):78-92.

34. Shivdasani RA, Rosenblatt MF, Zucker-Franklin D, et al. Transcription factor NF-E2 is required for platelet formation independent of the actions of thrombopoietin/MGDF in megakaryocyte development. *Cell.* 1995;81(5):695-704.

35. Sharrocks AD. The ETS-domain transcription factor family. *Nat Rev Mol Cell Biol.* 2001;2(11):827-837.

36. Karim FD, Urness LD, Thummel CS, et al. The ETS-domain: a new DNA-binding motif that recognizes a purine-rich core DNA sequence. *Genes Dev.* 1990;4(9):1451-1453.

37. Graves BJ, Petersen JM. Specificity within the ets family of transcription factors. *Adv Cancer Res.* 1998;75:1-55.

38. Hollenhorst PC, Shah AA, Hopkins C, Graves BJ. Genome-wide analyses reveal properties of redundant and specific promoter occupancy within the ETS gene family. *Genes Dev.* 2007;21(15):1882-1894.

39. Nunn MF, Seeburg PH, Moscovici C, Duesberg PH. Tripartite structure of the avian erythroblastosis virus E26 transforming gene. *Nature.* 1983;306(5941):391-395.

40. Terui K, Takahashi Y, Kitazawa J, Toki T, Yokoyama M, Ito E. Expression of transcription factors during megakaryocytic differentiation of CD34+ cells from human cord blood induced by thrombopoietin. *Tohoku J Exp Med.* 2000;192(4):259-273.

41. Lemarchandel V, Ghysdael J, Mignotte V, Rahuel C, Romeo PH. GATA and Ets cis-acting sequences mediate megakaryocyte-specific expression. *Mol Cell Biol.* 1993;13(1):668-676.

42. Barbeau B, Barat C, Bergeron D, Rassart E. The GATA-1 and Spi-1 transcriptional factors bind to a GATA/EBS dual element in the Fli-1 exon 1. *Oncogene.* 1999;18(40):5535-5545.

43. Rainis L, Toki T, Pimanda JE, et al. The proto-oncogene ERG in megakaryoblastic leukemias. *Cancer Res.* 2005;65(17):7596-7602.

44. Ge Y, LaFiura KM, Dombkowski AA, et al. The role of the proto-oncogene ETS2 in acute megakaryocytic leukemia biology and therapy. *Leukemia.* 2008;22(3):521-529.

45. Kwiatkowski BA, Bastian LS, Bauer TR, Jr., Tsai S, Zielinska-Kwiatkowska AG, Hickstein DD. The ets family member Tel binds to the Fli-1 oncoprotein and inhibits its transcriptional activity. *J Biol Chem.* 1998;273(28):17525-17530.

46. Bouilloux F, Juban G, Cohet N, et al. EKLF restricts megakaryocytic differentiation at the benefit of erythrocytic differentiation. *Blood.* 2008;112(3):576-584.

47. Athanasiou M, Clausen PA, Mavrothalassitis GJ, Zhang XK, Watson DK, Blair DG. Increased expression of the ETS-related transcription factor FLI-1/ERGB correlates with and can induce the megakaryocytic phenotype. *Cell Growth Differ.* 1996;7(11):1525-1534.

48. Athanasiou M, Mavrothalassitis G, Sun-Hoffman L, Blair DG. FLI-1 is a suppressor of erythroid differentiation in human hematopoietic cells. *Leukemia.* 2000;14(3):439-445.

49. Okada Y, Nobori H, Shimizu M, et al. Multiple ETS family proteins regulate PF4 gene expression by binding to the same ETS binding site. *PLoS One.* 2011;6(9):e24837.

50. Pevny L, Lin CS, D'Agati V, Simon MC, Orkin SH, Costantini F. Development of hematopoietic cells lacking transcription factor GATA-1. *Development.* 1995;121(1):163-172.

51. Pevny L, Simon MC, Robertson E, et al. Erythroid differentiation in chimaeric mice blocked by a targeted mutation in the gene for transcription factor GATA-1. *Nature.* 1991;349(6306):257-260.

52. Hart A, Melet F, Grossfeld P, et al. Fli-1 is required for murine vascular and megakaryocytic development and is hemizygously deleted in patients with thrombocytopenia. *Immunity.* 2000;13(2):167-177.

53. Moussa O, LaRue AC, Abangan RS, Jr., et al. Thrombocytopenia in mice lacking the carboxy-terminal regulatory domain of the Ets transcription factor Fli1. *Mol Cell Biol.* 2010;30(21):5194-5206.

54. Starck J, Weiss-Gayet M, Gonnet C, Guyot B, Vicat JM, Morle F. Inducible Fli-1 gene deletion in adult mice modifies several myeloid lineage commitment decisions and accelerates proliferation arrest and terminal erythrocytic differentiation. *Blood.* 2010;116(23):4795-4805.

55. Hollanda LM, Lima CS, Cunha AF, et al. An inherited mutation leading to production of only the short isoform of GATA-1 is associated with impaired erythropoiesis. *Nat Genet.* 2006;38(7):807-812.

56. Nichols KE, Crispino JD, Poncz M, et al. Familial dyserythropoietic anaemia and thrombocytopenia due to an inherited mutation in GATA1. *Nat Genet.* 2000;24(3):266-270.

57. Mehaffey MG, Newton AL, Gandhi MJ, Crossley M, Drachman JG. X-linked thrombocytopenia caused by a novel mutation of GATA-1. *Blood.* 2001;98(9):2681-2688.

58. Del Vecchio GC, Giordani L, De Santis A, De Mattia D. Dyserythropoietic anemia and thrombocytopenia due to a novel mutation in GATA-1. *Acta Haematol.* 2005;114(2):113-116.

59. Freson K, Devriendt K, Matthijs G, et al. Platelet characteristics in patients with X-linked macrothrombocytopenia because of a novel GATA1 mutation. *Blood.* 2001;98(1):85-92.

60. Freson K, Matthijs G, Thys C, et al. Different substitutions at residue D218 of the X-linked transcription factor GATA1 lead to altered clinical severity of macrothrombocytopenia and anemia and are associated with variable skewed X inactivation. *Hum Mol Genet.* 2002;11(2):147-152.

61. Yu C, Niakan KK, Matsushita M, Stamatoyannopoulos G, Orkin SH, Raskind WH. X-linked thrombocytopenia with thalassemia from a mutation in the amino finger of GATA-1 affecting DNA binding rather than FOG-1 interaction. *Blood.* 2002;100(6):2040-2045.

62. Balduini CL, Pecci A, Loffredo G, et al. Effects of the R216Q mutation of GATA-1 on erythropoiesis and megakaryocytopoiesis. *Thromb Haemost.* 2004;91(1):129-140.

63. Phillips JD, Steensma DP, Pulsipher MA, Spangrude GJ, Kushner JP. Congenital erythropoietic porphyria due to a mutation in GATA1: the first trans-acting mutation causative for a human porphyria. *Blood.* 2007;109(6):2618-2621.

64. Ho CY, Otterud B, Legare RD, et al. Linkage of a familial platelet disorder with a propensity to develop myeloid malignancies to human chromosome 21q22.1-22.2. *Blood.* 1996;87(12):5218-5224.

65. Song WJ, Sullivan MG, Legare RD, et al. Haploinsufficiency of CBFA2 causes familial thrombocytopenia with propensity to develop acute myelogenous leukaemia. *Nat Genet.* 1999;23(2):166-175.

66. Michaud J, Wu F, Osato M, et al. In vitro analyses of known and novel RUNX1/AML1 mutations in dominant familial platelet disorder with predisposition to acute myelogenous leukemia: implications for mechanisms of pathogenesis. *Blood.* 2002;99(4):1364-1372.

67. Ogawa E, Inuzuka M, Maruyama M, et al. Molecular cloning and characterization of PEBP2 beta, the heterodimeric partner of a novel Drosophila runt-related DNA binding protein PEBP2 alpha. *Virology.* 1993;194(1):314-331.

68. Wang S, Wang Q, Crute BE, Melnikova IN, Keller SR, Speck NA. Cloning and characterization of subunits of the T-cell receptor and murine leukemia virus enhancer core-binding factor. *Mol Cell Biol.* 1993;13(6):3324-3339.

69. Huang G, Shigesada K, Ito K, Wee HJ, Yokomizo T, Ito Y. Dimerization with PEBP2beta protects RUNX1/AML1 from ubiquitin-proteasome-mediated degradation. *EMBO J.* 2001;20(4):723-733.

70. Heller PG, Glembotsky AC, Gandhi MJ, et al. Low Mpl receptor expression in a pedigree with familial platelet disorder with predisposition to acute myelogenous leukemia and a novel AML1 mutation. *Blood.* 2005;105(12):4664-4670.

71. Glembotsky AC, Bluteau D, Espasandin YR, et al. Mechanisms underlying platelet function defect in a pedigree with familial platelet disorder with a predisposition to acute myelogenous leukemia: potential role for candidate RUNX1 targets. *J Thromb Haemost.* 2014;12(5):761-772.

72. Aneja K, Jalagadugula G, Mao G, Singh A, Rao AK. Mechanism of platelet factor 4 (PF4) deficiency with RUNX1 haplodeficiency: RUNX1 is a transcriptional regulator of PF4. *J Thromb Haemost.* 2011;9(2):383-391.

73. Jalagadugula G, Mao G, Kaur G, Dhanasekaran DN, Rao AK. Platelet protein kinase C-theta deficiency with human RUNX1 mutation: PRKCQ is a transcriptional target of RUNX1. *Arterioscler Thromb Vasc Biol.* 2011;31(4):921-927.

74. Hromas R, May W, Denny C, et al. Human FLI-1 localizes to chromosome 11Q24 and has an aberrant transcript in neuroepithelioma. *Biochim Biophys Acta.* 1993;1172(1-2):155-158.

75. Penny LA, Dell'Aquila M, Jones MC, et al. Clinical and molecular characterization of patients with distal 11q deletions. *Am J Hum Genet.* 1995;56(3):676-683.

76. Grossfeld PD, Mattina T, Lai Z, et al. The 11q terminal deletion disorder: a prospective study of 110 cases. *Am J Med Genet A.* 2004;129A(1):51-61.

77. Daly ME. Transcription factor defects causing platelet disorders. *Blood Rev.* 2016.

78. Breton-Gorius J, Favier R, Guichard J, et al. A new congenital dysmegakaryopoietic thrombocytopenia (Paris-Trousseau) associated with giant platelet alpha-granules and chromosome 11 deletion at 11q23. *Blood.* 1995;85(7):1805-1814.

79. Favier R, Jondeau K, Boutard P, et al. Paris-Trousseau syndrome : clinical, hematological, molecular data of ten new cases. *Thromb Haemost.* 2003;90(5):893-897.

80. Kent WJ, Sugnet CW, Furey TS, et al. The human genome browser at UCSC. *Genome Res.* 2002;12(6):996-1006.

81. Carpinelli MR, Kruse EA, Arhatari BD, et al. Mice Haploinsufficient for Ets1 and Fli1 Display Middle Ear Abnormalities and Model Aspects of Jacobsen Syndrome. *Am J Pathol.* 2015;185(7):1867-1876.

82. Raslova H, Komura E, Le Couedic JP, et al. FLI1 monoallelic expression combined with its hemizygous loss underlies Paris-Trousseau/Jacobsen thrombopenia. *J Clin Invest.* 2004;114(1):77-84.

83. Shivdasani RA. Lonely in Paris: when one gene copy isn't enough. *J Clin Invest.* 2004;114(1):17-19.

84. Stockley J, Morgan NV, Bem D, et al. Enrichment of FLI1 and RUNX1 mutations in families with excessive bleeding and platelet dense granule secretion defects. *Blood.* 2013;122(25):4090-4093.

85. Stevenson WS, Rabbolini DJ, Beutler L, et al. Paris-Trousseau thrombocytopenia is phenocopied by the autosomal recessive inheritance of a DNA-binding domain mutation in FLI1. *Blood.* 2015;126(17):2027-2030.

86. Mattina T, Perrotta CS, Grossfeld P. Jacobsen syndrome. *Orphanet J Rare Dis.* 2009;4:9.

87. Maqsood MI, Matin MM, Bahrami AR, Ghasroldasht MM. Immortality of cell lines: challenges and advantages of establishment. *Cell Biol Int.* 2013;37(10):1038-1045.

88. Melet F, Motro B, Rossi DJ, Zhang L, Bernstein A. Generation of a novel Fli-1 protein by gene targeting leads to a defect in thymus development and a delay in Friend virus-induced erythroleukemia. *Mol Cell Biol.* 1996;16(6):2708-2718.

89. Takahashi K, Yamanaka S. Induction of pluripotent stem cells from mouse embryonic and adult fibroblast cultures by defined factors. *Cell.* 2006;126(4):663-676.

90. Takahashi K, Tanabe K, Ohnuki M, et al. Induction of pluripotent stem cells from adult human fibroblasts by defined factors. *Cell.* 2007;131(5):861-872.

91. Maehr R, Chen S, Snitow M, et al. Generation of pluripotent stem cells from patients with type 1 diabetes. *Proc Natl Acad Sci U S A.* 2009;106(37):15768-15773.

92. Ebert AD, Yu J, Rose FF, Jr., et al. Induced pluripotent stem cells from a spinal muscular atrophy patient. *Nature.* 2009;457(7227):277-280.

93. Ye L, Chang JC, Lin C, Sun X, Yu J, Kan YW. Induced pluripotent stem cells offer new approach to therapy in thalassemia and sickle cell anemia and option in prenatal diagnosis in genetic diseases. *Proc Natl Acad Sci U S A.* 2009;106(24):9826-9830.

94. Paes BC, Moco PD, Pereira CG, et al. Ten years of iPSC: clinical potential and advances in vitro hematopoietic differentiation. *Cell Biol Toxicol.* 2016.

95. Arai S, Miyauchi M, Kurokawa M. Modeling of hematologic malignancies by iPS technology. *Exp Hematol.* 2015;43(8):654-660.

96. Raya A, Rodriguez-Piza I, Guenechea G, et al. Disease-corrected haematopoietic progenitors from Fanconi anaemia induced pluripotent stem cells. *Nature.* 2009;460(7251):53-59.

97. Fernandez KS, de Alarcon PA. Development of the hematopoietic system and disorders of hematopoiesis that present during infancy and early childhood. *Pediatr Clin North Am.* 2013;60(6):1273-1289.

98. Costa G, Kouskoff V, Lacaud G. Origin of blood cells and HSC production in the embryo. *Trends Immunol.* 2012;33(5):215-223.

99. Ferkowicz MJ, Yoder MC. Blood island formation: longstanding observations and modern interpretations. *Exp Hematol.* 2005;33(9):1041-1047.

100. Lacaud G, Robertson S, Palis J, Kennedy M, Keller G. Regulation of hemangioblast development. *Ann N Y Acad Sci.* 2001;938:96-107; discussion 108.

101. Palis J. Primitive and definitive erythropoiesis in mammals. *Front Physiol.* 2014;5:3.

102. Schechter AN. Hemoglobin research and the origins of molecular medicine. *Blood.* 2008;112(10):3927-3938.

103. Tober J, Koniski A, McGrath KE, et al. The megakaryocyte lineage originates from hemangioblast precursors and is an integral component both of primitive and of definitive hematopoiesis. *Blood.* 2007;109(4):1433-1441.

104. Lengerke C, Grauer M, Niebuhr NI, et al. Hematopoietic development from human induced pluripotent stem cells. *Ann N Y Acad Sci.* 2009;1176:219-227.

105. Kennedy M, Awong G, Sturgeon CM, et al. T lymphocyte potential marks the emergence of definitive hematopoietic progenitors in human pluripotent stem cell differentiation cultures. *Cell Rep.* 2012;2(6):1722-1735.

106. Kennedy M, D'Souza SL, Lynch-Kattman M, Schwantz S, Keller G. Development of the hemangioblast defines the onset of hematopoiesis in human ES cell differentiation cultures. *Blood.* 2007;109(7):2679-2687.

107. Ran D, Shia WJ, Lo MC, et al. RUNX1a enhances hematopoietic lineage commitment from human embryonic stem cells and inducible pluripotent stem cells. *Blood.* 2013;121(15):2882-2890.

108. Doulatov S, Vo LT, Chou SS, et al. Induction of multipotential hematopoietic progenitors from human pluripotent stem cells via respecification of lineage-restricted precursors. *Cell Stem Cell.* 2013;13(4):459-470.

109. Trkova M, Becvarova V, Hynek M, et al. SNP array and phenotype correlation shows that FLI1 deletion per se is not responsible for thrombocytopenia development in Jacobsen syndrome. *Am J Med Genet A.* 2012;158A(10):2545-2550.

110. Amabile G, Meissner A. Induced pluripotent stem cells: current progress and potential for regenerative medicine. *Trends Mol Med.* 2009;15(2):59-68.

111. Suh W. A new era of disease modeling and drug discovery using induced pluripotent stem cells. *Arch Pharm Res.* 2017;40(1):1-12.

112. Itzhaki I, Maizels L, Huber I, et al. Modelling the long QT syndrome with induced pluripotent stem cells. *Nature.* 2011;471(7337):225-229.

113. Ye Z, Zhan H, Mali P, et al. Human-induced pluripotent stem cells from blood cells of healthy donors and patients with acquired blood disorders. *Blood.* 2009;114(27):5473-5480.

114. Hirata S, Takayama N, Jono-Ohnishi R, et al. Congenital amegakaryocytic thrombocytopenia iPS cells exhibit defective MPL-mediated signaling. *J Clin Invest.* 2013;123(9):3802-3814.

115. Sullivan SK, Mills JA, Koukouritaki SB, et al. High-level transgene expression in induced pluripotent stem cell-derived megakaryocytes: correction of Glanzmann thrombasthenia. *Blood.* 2014;123(5):753-757.

116. Kim YG, Cha J, Chandrasegaran S. Hybrid restriction enzymes: zinc finger fusions to Fok I cleavage domain. *Proc Natl Acad Sci U S A.* 1996;93(3):1156-1160.

117. Segal DJ, Crotty JW, Bhakta MS, Barbas CF, 3rd, Horton NC. Structure of Aart, a designed six-finger zinc finger peptide, bound to DNA. *J Mol Biol.* 2006;363(2):405-421.

118. Durai S, Mani M, Kandavelou K, Wu J, Porteus MH, Chandrasegaran S. Zinc finger nucleases: custom-designed molecular scissors for genome engineering of plant and mammalian cells. *Nucleic Acids Res.* 2005;33(18):5978-5990.

119. Bitinaite J, Wah DA, Aggarwal AK, Schildkraut I. FokI dimerization is required for DNA cleavage. *Proc Natl Acad Sci U S A.* 1998;95(18):10570-10575.

120. Porteus MH, Baltimore D. Chimeric nucleases stimulate gene targeting in human cells. *Science.* 2003;300(5620):763.

121. DiGiusto DL, Cannon PM, Holmes MC, et al. Preclinical development and qualification of ZFN-mediated CCR5 disruption in human hematopoietic stem/progenitor cells. *Mol Ther Methods Clin Dev.* 2016;3:16067.

122. Tebas P, Stein D, Tang WW, et al. Gene editing of CCR5 in autologous CD4 T cells of persons infected with HIV. *N Engl J Med.* 2014;370(10):901-910.

123. Kim HJ, Lee HJ, Kim H, Cho SW, Kim JS. Targeted genome editing in human cells with zinc finger nucleases constructed via modular assembly. *Genome Res.* 2009;19(7):1279-1288.

124. Greisman HA, Pabo CO. A general strategy for selecting high-affinity zinc finger proteins for diverse DNA target sites. *Science.* 1997;275(5300):657-661.

125. Boch J, Bonas U. Xanthomonas AvrBs3 family-type III effectors: discovery and function. *Annu Rev Phytopathol.* 2010;48:419-436.

126. Moscou MJ, Bogdanove AJ. A simple cipher governs DNA recognition by TAL effectors. *Science.* 2009;326(5959):1501.

127. Zhang F, Cong L, Lodato S, Kosuri S, Church GM, Arlotta P. Efficient construction of sequence-specific TAL effectors for modulating mammalian transcription. *Nat Biotechnol.* 2011;29(2):149-153.

128. Briggs AW, Rios X, Chari R, et al. Iterative capped assembly: rapid and scalable synthesis of repeat-module DNA such as TAL effectors from individual monomers. *Nucleic Acids Res.* 2012;40(15):e117.

129. Schmid-Burgk JL, Schmidt T, Kaiser V, Honing K, Hornung V. A ligation-independent cloning technique for high-throughput assembly of transcription activator-like effector genes. *Nat Biotechnol.* 2013;31(1):76-81.

130. Kim Y, Kweon J, Kim A, et al. A library of TAL effector nucleases spanning the human genome. *Nat Biotechnol.* 2013;31(3):251-258.

131. Grau J, Boch J, Posch S. TALENoffer: genome-wide TALEN off-target prediction. *Bioinformatics.* 2013;29(22):2931-2932.

132. Barrangou R, Fremaux C, Deveau H, et al. CRISPR provides acquired resistance against viruses in prokaryotes. *Science.* 2007;315(5819):1709-1712.

133. Marraffini LA, Sontheimer EJ. CRISPR interference: RNA-directed adaptive immunity in bacteria and archaea. *Nat Rev Genet.* 2010;11(3):181-190.

134. Wiedenheft B, Sternberg SH, Doudna JA. RNA-guided genetic silencing systems in bacteria and archaea. *Nature.* 2012;482(7385):331-338.

135. Jinek M, East A, Cheng A, Lin S, Ma E, Doudna J. RNA-programmed genome editing in human cells. *Elife.* 2013;2:e00471.

136. Makarova KS, Zhang F, Koonin EV. SnapShot: Class 2 CRISPR-Cas Systems. *Cell.* 2017;168(1-2):328-328 e321.

137. Wyman C, Kanaar R. DNA double-strand break repair: all's well that ends well. *Annu Rev Genet.* 2006;40:363-383.

138. Brookhouser N, Raman S, Potts C, Brafman DA. May I Cut in? Gene Editing Approaches in Human Induced Pluripotent Stem Cells. *Cells.* 2017;6(1).

139. Boulton SJ, Jackson SP. Saccharomyces cerevisiae Ku70 potentiates illegitimate DNA double-strand break repair and serves as a barrier to error-prone DNA repair pathways. *EMBO J.* 1996;15(18):5093-5103.

140. Sommer CA, Stadtfeld M, Murphy GJ, Hochedlinger K, Kotton DN, Mostoslavsky G. Induced pluripotent stem cell generation using a single lentiviral stem cell cassette. *Stem Cells.* 2009;27(3):543-549.

141. Somers A, Jean JC, Sommer CA, et al. Generation of transgene-free lung disease-specific human induced pluripotent stem cells using a single excisable lentiviral stem cell cassette. *Stem Cells.* 2010;28(10):1728-1740.

142. Mills JA, Wang K, Paluru P, et al. Clonal genetic and hematopoietic heterogeneity among human-induced pluripotent stem cell lines. *Blood.* 2013;122(12):2047-2051.

143. Mills JA, Paluru P, Weiss MJ, Gadue P, French DL. Hematopoietic differentiation of pluripotent stem cells in culture. *Methods Mol Biol.* 2014;1185:181-194.

144. Hockemeyer D, Soldner F, Beard C, et al. Efficient targeting of expressed and silent genes in human ESCs and iPSCs using zinc-finger nucleases. *Nat Biotechnol.* 2009;27(9):851-857.

145. Sadelain M, Papapetrou EP, Bushman FD. Safe harbours for the integration of new DNA in the human genome. *Nat Rev Cancer.* 2011;12(1):51-58.

146. Yates A, Akanni W, Amode MR, et al. Ensembl 2016. *Nucleic Acids Res.* 2016;44(D1):D710-716.

147. Ye Z, Liu CF, Jang YY. Hematopoietic cells as sources for patient-specific iPSCs and disease modeling. *Cell Cycle.* 2011;10(17):2840-2844.

148. Valton J, Dupuy A, Daboussi F, et al. Overcoming transcription activator-like effector (TALE) DNA binding domain sensitivity to cytosine methylation. *J Biol Chem.* 2012;287(46):38427-38432.

149. Xu X, Duan D, Chen SJ. CRISPR-Cas9 cleavage efficiency correlates strongly with target-sgRNA folding stability: from physical mechanism to off-target assessment. *Sci Rep.* 2017;7(1):143.

150. Ran FA, Hsu PD, Lin CY, et al. Double nicking by RNA-guided CRISPR Cas9 for enhanced genome editing specificity. *Cell.* 2013;154(6):1380-1389.

151. Krishnamurti L, Neglia JP, Nagarajan R, et al. Paris-Trousseau syndrome platelets in a child with Jacobsen's syndrome. *Am J Hematol.* 2001;66(4):295-299.

152. Coller BS, Shattil SJ. The GPIIb/IIIa (integrin alphaIIbbeta3) odyssey: a technology-driven saga of a receptor with twists, turns, and even a bend. *Blood.* 2008;112(8):3011-3025.

153. Nurden AT, Freson K, Seligsohn U. Inherited platelet disorders. *Haemophilia.* 2012;18 Suppl 4:154-160.

154. Polgar J, Clemetson JM, Kehrel BE, et al. Platelet activation and signal transduction by convulxin, a C-type lectin from Crotalus durissus terrificus (tropical rattlesnake) venom via the p62/GPVI collagen receptor. *J Biol Chem.* 1997;272(21):13576-13583.

155. Livak KJ, Schmittgen TD. Analysis of relative gene expression data using real-time quantitative PCR and the 2(-Delta Delta C(T)) Method. *Methods.* 2001;25(4):402-408.

156. Tijssen MR, Cvejic A, Joshi A, et al. Genome-wide analysis of simultaneous GATA1/2, RUNX1, FLI1, and SCL binding in megakaryocytes identifies hematopoietic regulators. *Dev Cell.* 2011;20(5):597-609.

157. Calo E, Wysocka J. Modification of enhancer chromatin: what, how, and why? *Mol Cell.* 2013;49(5):825-837.

158. Consortium EP. An integrated encyclopedia of DNA elements in the human genome. *Nature.* 2012;489(7414):57-74.

159. Ernst J, Kheradpour P, Mikkelsen TS, et al. Mapping and analysis of chromatin state dynamics in nine human cell types. *Nature.* 2011;473(7345):43-49.

160. Noetzli L, Lo RW, Lee-Sherick AB, et al. Germline mutations in ETV6 are associated with thrombocytopenia, red cell macrocytosis and predisposition to lymphoblastic leukemia. *Nat Genet.* 2015;47(5):535-538.

161. Deveaux S, Filipe A, Lemarchandel V, Ghysdael J, Romeo PH, Mignotte V. Analysis of the thrombopoietin receptor (MPL) promoter implicates GATA and Ets proteins in the coregulation of megakaryocyte-specific genes. *Blood.* 1996;87(11):4678-4685.

162. Lordier L, Bluteau D, Jalil A, et al. RUNX1-induced silencing of non-muscle myosin heavy chain IIB contributes to megakaryocyte polyploidization. *Nat Commun.* 2012;3:717.

163. Antony-Debre I, Bluteau D, Itzykson R, et al. MYH10 protein expression in platelets as a biomarker of RUNX1 and FLI1 alterations. *Blood.* 2012;120(13):2719-2722.

164. Jackers P, Szalai G, Moussa O, Watson DK. Ets-dependent regulation of target gene expression during megakaryopoiesis. *J Biol Chem.* 2004;279(50):52183-52190.

165. Hogge D, Fanning S, Bockhold K, et al. Quantitation and characterization of human megakaryocyte colony-forming cells using a standardized serum-free agarose assay. *Br J Haematol.* 1997;96(4):790-800.

166. Kawada H, Ito T, Pharr PN, Spyropoulos DD, Watson DK, Ogawa M. Defective megakaryopoiesis and abnormal erythroid development in Fli-1 gene-targeted mice. *Int J Hematol.* 2001;73(4):463-468.

167. Mitjavila-Garcia MT, Cailleret M, Godin I, et al. Expression of CD41 on hematopoietic progenitors derived from embryonic hematopoietic cells. *Development.* 2002;129(8):2003-2013.

168. Debili N, Issaad C, Masse JM, et al. Expression of CD34 and platelet glycoproteins during human megakaryocytic differentiation. *Blood.* 1992;80(12):3022-3035.

169. Robert A, Boyer L, Pineault N. Glycoprotein Ibalpha receptor instability is associated with loss of quality in platelets produced in culture. *Stem Cells Dev.* 2011;20(3):379-390.

170. Wang Y, Hayes V, Jarocha D, et al. Comparative analysis of human ex vivo-generated platelets vs megakaryocyte-generated platelets in mice: a cautionary tale. *Blood.* 2015;125(23):3627-3636.

171. Zimmet J, Ravid K. Polyploidy: occurrence in nature, mechanisms, and significance for the megakaryocyte-platelet system. *Exp Hematol.* 2000;28(1):3-16.

172. Shultz LD, Lyons BL, Burzenski LM, et al. Human lymphoid and myeloid cell development in NOD/LtSz-scid IL2R gamma null mice engrafted with mobilized human hemopoietic stem cells. *J Immunol.* 2005;174(10):6477-6489.

173. Bergmeier W, Burger PC, Piffath CL, et al. Metalloproteinase inhibitors improve the recovery and hemostatic function of in vitro-aged or -injured mouse platelets. *Blood.* 2003;102(12):4229-4235.

174. Kowalska MA, Ratajczak MZ, Majka M, et al. Stromal cell-derived factor-1 and macrophage-derived chemokine: 2 chemokines that activate platelets. *Blood.* 2000;96(1):50-57.

175. Celi A, Merrill-Skoloff G, Gross P, et al. Thrombus formation: direct real-time observation and digital analysis of thrombus assembly in a living mouse by confocal and widefield intravital microscopy. *J Thromb Haemost.* 2003;1(1):60-68.

176. Fuentes R, Wang Y, Hirsch J, et al. Infusion of mature megakaryocytes into mice yields functional platelets. *J Clin Invest.* 2010;120(11):3917-3922.

177. Gremmel T, Koppensteiner R, Panzer S. Comparison of Aggregometry with Flow Cytometry for the Assessment of Agonists -Induced Platelet Reactivity in Patients on Dual Antiplatelet Therapy. *PLoS One.* 2015;10(6):e0129666.

178. Lefrancais E, Ortiz-Munoz G, Caudrillier A, et al. The lung is a site of platelet biogenesis and a reservoir for haematopoietic progenitors. *Nature.* 2017.

179. Qi B, Hardwick JM. A Bcl-xL timer sets platelet life span. *Cell.* 2007;128(6):1035-1036.

180. Grozovsky R, Hoffmeister KM, Falet H. Novel clearance mechanisms of platelets. *Curr Opin Hematol.* 2010;17(6):585-589.

181. Hoffmeister KM, Falet H. Platelet clearance by the hepatic Ashwell-Morrell receptor: mechanisms and biological significance. *Thromb Res.* 2016;141 Suppl 2:S68-72.

182. Asano Y, Stawski L, Hant F, et al. Endothelial Fli1 deficiency impairs vascular homeostasis: a role in scleroderma vasculopathy. *Am J Pathol.* 2010;176(4):1983-1998.

183. Spyropoulos DD, Pharr PN, Lavenburg KR, et al. Hemorrhage, impaired hematopoiesis, and lethality in mouse embryos carrying a targeted disruption of the Fli1 transcription factor. *Mol Cell Biol.* 2000;20(15):5643-5652.

184. Sim X, Poncz M, Gadue P, French DL. Understanding platelet generation from megakaryocytes: implications for in vitro-derived platelets. *Blood.* 2016;127(10):1227-1233.

185. Noh JY, Gandre-Babbe S, Wang Y, et al. Inducible Gata1 suppression expands megakaryocyte-erythroid progenitors from embryonic stem cells. *J Clin Invest.* 2015;125(6):2369-2374.

186. Moreau T, Evans AL, Vasquez L, et al. Large-scale production of megakaryocytes from human pluripotent stem cells by chemically defined forward programming. *Nat Commun.* 2016;7:11208.

187. Edelstein M. Gene Therapry Clinical Trials Worldwide. 2016; http://www.abedia.com/wiley/index.html. Accessed March, 2017.

188. Liu T, Yao Y, Zhang G, et al. A screen for Fli-1 transcriptional modulators identifies PKC agonists that induce erythroid to megakaryocytic differentiation and suppress leukemogenesis. *Oncotarget.* 2016.

189. Lambert MP, Sullivan SK, Fuentes R, French DL, Poncz M. Challenges and promises for the development of donor-independent platelet transfusions. *Blood.* 2013;121(17):3319-3324.

190. Nishimura T, Hatoya S, Kanegi R, et al. Generation of functional platelets from canine induced pluripotent stem cells. *Stem Cells Dev.* 2013;22(14):2026-2035.

191. Lu SJ, Li F, Yin H, et al. Platelets generated from human embryonic stem cells are functional in vitro and in the microcirculation of living mice. *Cell Res.* 2011;21(3):530-545.

192. Nakamura S, Takayama N, Hirata S, et al. Expandable megakaryocyte cell lines enable clinically applicable generation of platelets from human induced pluripotent stem cells. *Cell Stem Cell.* 2014;14(4):535-548.

193. Feng Q, Shabrani N, Thon JN, et al. Scalable generation of universal platelets from human induced pluripotent stem cells. *Stem Cell Reports.* 2014;3(5):817-831.

194. Yarovoi HV, Kufrin D, Eslin DE, et al. Factor VIII ectopically expressed in platelets: efficacy in hemophilia A treatment. *Blood.* 2003;102(12):4006-4013.